Chemical Engineering Science 164 (2017) 63–70

Contents lists available at ScienceDirect

Chemical Engineering Science

journal homepage: www.elsevier.com/locate/ces

Short Communication

Highlighting multiplicity in the Gilliland solution to the Maxwell-Stefan equations describing diffusion distillation

Rajamani Krishna

Van't Hoff Institute for Molecular Sciences, University of Amsterdam, Science Park 904, 1098 XH Amsterdam, The Netherlands

HIGHLIGHTS

- Alcohol/water mixtures can be separated by diffusion through inert gas.
- The efficacy of separation improves with higher molar mass of inert gas.
- The Gilliland equations yield three different solution sets, only one is realistic.
- The Prigogine minimum entropy production principle identifies the physically correct solution.
- If porous barriers are used, the pore diameter should large enough to ensure bulk diffusion.

GRAPHICAL ABSTRACT

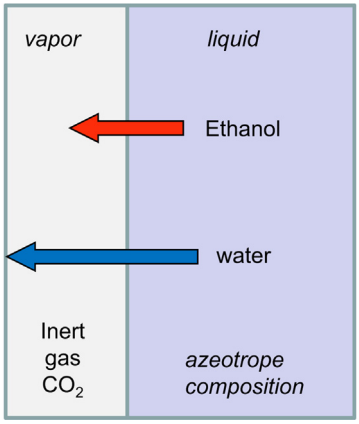

ARTICLE INFO

Article history:
Received 1 September 2016
Received in revised form 1 December 2016
Accepted 27 January 2017
Available online 7 February 2017

Keywords:
Azeotrope
Inert gas
Entropy production
Maxwell-Stefan diffusion
Multiplicity
Porous barriers

ABSTRACT

This article investigates the separation of ethanol/water, and 2-propanol/water liquid mixtures of azeotropic composition by allowing diffusion through six different inert gases: helium, nitrogen, air, argon, CO_2, and xenon. The Maxwell-Stefan (M-S) equations afford a rigorous quantification of the achievable separation. For steady-state transfer, analytic solutions to the M-S formulation were obtained in parametric form by Gilliland. For each investigated system in this study, the Gilliland approach yields three different solution sets for the transfer fluxes of alcohol and water; only one of these is physically realizable in practice. The physically realistic solution can be identified by invoking the Prigogine principle of minimum entropy production. Robust computational algorithms are essential for modeling and development of diffusion distillation technology; these are indicated.

The efficacy of diffusion distillation depends on differences in alcohol-inert and water-inert friction in the vapor phase; such differences increase with increasing molar mass of the inert component. Inert gases such as CO_2 and Xe are more effective than lighter inerts such as air, nitrogen or helium. Some of the strategies in the published literature, involve interposing porous barriers between the vapor and liquid phases; the choice of the pore diameter influences the efficacy of diffusion distillation. For alcohol/water mixtures, it is preferable to choose the pore diameter such that "bulk" diffusion, rather than Knudsen diffusion regime prevails inside the pores.

E-mail address: r.krishna@contact.uva.nl

http://dx.doi.org/10.1016/j.ces.2017.01.060
0009-2509/

Nomenclature

c_t	total molar concentration of mixture, mol m^{-3}
d_p	diameter of pore, m
$Đ_{ij}$	M-S binary pair diffusivity, m^2 s^{-1}
$D_{i,Kn}$	Knudsen diffusivity of species i, m^2 s^{-1}
$[D]$	diffusivity matrix, m^2 s^{-1}
$[I]$	identity matrix, dimensionless
M_i	molar mass of species i, kg mol^{-1}
N_i	molar flux of species i, mol m^{-2} s^{-1}
p_i	partial pressure, Pa
p_t	total pressure, Pa
P_i^0	vapor pressure, Pa
R	gas constant, 8.314 J mol^{-1} K^{-1}
t	time, s
T	absolute temperature, K
x_i	mole fraction of component i in liquid phase, dimensionless
y_i	mole fraction of component i in vapor phase, dimensionless
z	direction coordinate, m

Greek letters

γ_i	activity coefficient of component i, dimensionless
δ	film thickness, m
δ_{ij}	Kronecker delta, dimensionless
η	dimensionless distance in diffusion layer, dimensionless
λ_i	eigenvalues of $[\Phi]$, dimensionless
σ	rate of entropy production, J m^{-3} s^{-1} K^{-1}
Φ_{ij}	dimensionless mass transfer rate factors, dimensionless

Subscripts

0	referring to position, $z = 0$
δ	referring to position, $z = \delta$
1	component 1
2	component 2
3	component 3

1. Introduction

For a binary alcohol(1)/water(2) mixture, the vapor-liquid equilibrium is described by $y_i = \gamma_i x_i P_i^0/p_t$; at the azeotropic composition, we have $y_i = x_i$. Binary mixtures of azeotropic composition cannot be separated by conventional distillation because there is no driving force for transfer from liquid to vapor phase, and vice versa. The addition of an entrainer (species 3) is a common strategy employed in azeotropic and extractive distillation processes; the addition of the entrainer serves to alter the phase equilibrium thermodynamics in such a manner as to allow complete separation of species 1, and 2. Such processes are energy-intensive because of the need for solvent recovery in an additional distillation column. There is considerable research on developing energy-efficient alternatives to azeotropic and extractive distillation processes. One such alternative involves the introduction of an "inert" gas as species 3 (Fullarton and Schlünder, 1986). The separation principle is based on the differences in the interfacial mass transfer fluxes (N_1, and N_2) of components 1 and 2 in the ternary mixture (1, 2, and 3). Essentially, the separation relies on maintaining conditions such that the ratio of fluxes N_1/N_2 is significantly different from the corresponding ratio of mole fractions of the azeotrope, x_1/x_2. In the absence of the third component, we must have $N_1/N_2 = x_1/x_2 = y_1/y_2$, as there is no driving force during condensation or evaporation for each of the components of a mixture with azeotropic composition. When an inert non-condensable, is introduced into the vapor phase, this allows mixtures of azeotropic composition to be separated because the vapor compositions are altered and driving forces for component transfers are "created".

Diffusional effects have been exploited to separate alcohol/water mixtures of azeotropic composition by distillation in the presence of an inert gas such as helium, nitrogen, air, argon, and CO_2 (Fullarton and Schlünder, 1986; Singh and Prasad, 2011). Experimental verification of the efficacy of the diffusion distillation concept has been established in wetted-wall columns (Fullarton and Schlünder, 1986; Singh and Prasad, 2011, 2015; Ziobrowski et al., 2009). The same separation principle prevails in other constructs in which a porous barrier, or membrane, is interposed between the liquid and vapor/gas phases; such separations have been variously termed "sweep-gas distillation", or "frictional distillation" (Banat et al., 1999a, 1999b; Breure et al., 2008).

It must be remarked that the concept of deliberate addition of a third component to enable diffusion-selective separation was already developed in the 1950s (Cichelli et al., 1951; Keyes and Pigford, 1957). These early research activities were focused on the separation of gaseous isotopes by diffusing through a third component in the form of a condensable vapor. The following quote from Keyes and Pigford (1957) is both illuminating and instructive *partial separation of the components of a binary gas mixture can be effected by diffusion at constant total pressure through a third gas or vapor, provided there exists a difference in diffusivities of the components with respect to the vapor. The third component is commonly called the separating agent.*

Diffusion distillation, and indeed all sweep diffusion processes, place heavy reliance on the proper description of molecular diffusion phenomena in the gaseous phase. Rigorous models to describe the diffusion of three-component gas mixtures are required, and it is therefore no real surprise that the earliest practical applications of the Maxwell-Stefan (M-S) diffusion formulations are to be found in the analysis of sweep diffusion processes for separating gaseous isotopes (Cichelli et al., 1951; Keyes and Pigford, 1957).

For diffusion of a binary mixture (components 1, and 2) in the presence of an inert, non-transferring component (3), at constant pressure and temperature, the M-S equations take the form (detailed derivations are provided in the Supplementary material accompanying this publication)

$$\begin{aligned} -c_t\frac{dy_1}{dz} &= \frac{y_2N_1 - y_1N_2}{Đ_{12}} + \frac{y_3N_1}{Đ_{13}};\\ -c_t\frac{dy_2}{dz} &= \frac{y_1N_2 - y_2N_1}{Đ_{12}} + \frac{y_3N_2}{Đ_{23}} \end{aligned} \tag{1}$$

For separations operating at steady-state, we need to determine the transfer fluxes, N_1, and N_2, by solving the set of two independent Eqs. (1) together with the boundary conditions

$$\begin{aligned} z = 0; \quad (y) = (y_0)\\ z = \delta; \quad (y) = (y_\delta) \end{aligned} \tag{2}$$

At first sight, the task of determining the fluxes N_1, and N_2 seems simple and straightforward; it is neither. The earliest published solution to Maxwell-Stefan equations (1) should be credited to Edwin Richard Gilliland, one of the pioneering founders of the chemical engineering profession. Gilliland developed an analytic solution in the parametric form of Eqs. (3) and (4) below:

$$\frac{N_1}{Đ_{13}} + \frac{N_2}{Đ_{23}} = \frac{c_t}{\delta}\ln\left(\frac{y_{3\delta}}{y_{30}}\right) \tag{3}$$

and

$$\frac{N_1+N_2}{Đ_{12}}=\frac{c_t}{\delta}\ln\left(\frac{y_{1\delta}\frac{N_1+N_2}{N_1}-\frac{\left(\frac{1}{Đ_{12}}-\frac{1}{Đ_{13}}\right)}{\left(\frac{1}{Đ_{12}}-\frac{1}{Đ_{23}}\right)}\frac{N_1+N_2}{N_2}y_{2\delta}-\frac{\left(\frac{1}{Đ_{13}}-\frac{1}{Đ_{23}}\right)}{\left(\frac{1}{Đ_{12}}-\frac{1}{Đ_{23}}\right)}}{y_{10}\frac{N_1+N_2}{N_1}-\frac{\left(\frac{1}{Đ_{12}}-\frac{1}{Đ_{13}}\right)}{\left(\frac{1}{Đ_{12}}-\frac{1}{Đ_{23}}\right)}\frac{N_1+N_2}{N_2}y_{20}-\frac{\left(\frac{1}{Đ_{13}}-\frac{1}{Đ_{23}}\right)}{\left(\frac{1}{Đ_{12}}-\frac{1}{Đ_{23}}\right)}}\right) \tag{4}$$

Eqs. (3) and (4) were published in the 1st edition of *Absorption and Extraction*, authored by Thomas Kilgore Sherwood (Sherwood, 1937), another pioneer in mass transfer. Eqs. (3) and (4) are also available in the classic paper of Herbert Lawrence Toor (Toor, 1957). The fluxes N_1, and N_2 may be determined with say the Excel solver, using starting guess values. Sherwood (1937) demonstrated the utility of the Gilliland solution by means of an illustrative example for absorption of NH_3 (1) and water vapor (2) from air (3) into water. For a chosen set of conditions, three distinct sets of solutions for the fluxes N_1 and N_2 were obtained, depending on the starting guess values. On the basis of physical arguments, only one of these sets was considered to be physically realizable in practice. Later editions of the classic 1937 book of Sherwood, do not contain any discussions of Maxwell-Stefan equations, and the Gilliland solutions are omitted (Sherwood et al., 1975). Readers who do not have access to the 1937 edition of Sherwood's book, will find the discussions of the multiple solutions for NH_3(1)/H_2O (2)/Air(3) diffusion in the Supplementary material accompanying this paper; see also (Krishna, 1977). The use of the Gilliland equations for flux calculations is also illustrated by the work of Bröcker and Schulze (1991).

The objectives of the current investigation of diffusion distillation are four-fold. The first objective is to investigate the multiplicity of fluxes that result from use of Eqs. (3) and (4) when applied to diffusion distillation. We address the question of determining the physically realistic set of fluxes by invoking the Prigogine principle of minimum entropy production (Prigogine, 1961). The second objective is to elucidate the choice of the inert gas on the separation performance. Specifically, we aim to rationalize the experiments of Singh and Prasad (2011, 2015) in which the separation selectivity was found to be strongly dependent on the choice of the inert gas: helium, air, or argon. The third objective is to investigate the role of the porous barrier that is often interposed between the vapor and liquid phases. Is the porous barrier essential, and are there fundamental guidelines for choice of the pore sizes of such barriers? The fourth, and final objective is to apply the Prigogine entropy concepts in analyzing steady-state multiplicity in multicomponent diffusion with heterogeneous catalyzed reaction; the analysis is relevant in the context of reactive distillation (Higler et al., 1999; Taylor and Krishna, 2000).

The Supplementary material accompanying this publication, available for download in the online version of this article, provides detailed derivations of model equations, numerical solution methodology used, and data inputs.

2. Multiplicity of Gilliland solutions in diffusion distillation

Consider mass transfer between the liquid and vapor phase for ethanol(1)/water(2)/CO_2(3). The mass transfer resistance is assumed to be restricted to the vapor phase, and the effective film thickness of the gas phase resistance is $\delta = 1$ mm. Assume that the liquid phase is the binary mixture ethanol(1)/water(2) at T = 343.15 K. The azeotropic composition at this temperature can be calculated as x_1 = 0.87, x_2 = 0.13. Let us bring this liquid mixture in contact with an inert gas phase consisting of the CO_2 (=species 3). The vapor pressure of ethanol at 343.15 K is 71.2 kPa, and the vapor pressure of water at 343.15 K is 31.2 kPa. The total gas phase pressure p_t = 101.3 kPa. The composition of the vapor phase at the gas/liquid interface in equilibrium with the liquid mixture can be calculated from $y_i = \gamma_i x_i P_i^0/p_t$. This yields $y_{1\delta}$ = 0.6177, $y_{2\delta}$ = 0.09264, $y_{3\delta}$ = 0.2897. The bulk vapor composition is taken to be: y_{10} = 0.0, y_{20} = 0.0, y_{30} = 1.0. The driving forces are $\Delta y_1 = y_{10} - y_{1\delta} = -0.6177$, and $\Delta y_2 = y_{20} - y_{2\delta} = -0.09264$. Both driving forces are directed from liquid to the vapor phase.

The values of the vapor phase M-S diffusivities of the three binary pairs at 343.15 K, calculated using the (Fuller et al., 1966) method, are $Đ_{12} = 2.05$; $Đ_{13} = 1.27$; $Đ_{23} = 2.67 \times 10^{-5}$ m^2 s^{-1}; these diffusivities are independent of composition.

Depending on the starting guess used in any equation solver, there are three distinct sets of solutions to Eqs. (3) and (4), called Gilliland sets A, B, and C. Our solutions are based on the Given-Find solve block of MathCad 15 (PTC, 2013).

Good starting guess values for the transfer fluxes can be obtained using a simplified linearized solution to Eqs. (1), as proposed by (Krishna, 1981)

$$\begin{pmatrix}N_1\\N_2\end{pmatrix}=\frac{c_t}{\delta}[D]\begin{pmatrix}y_{10}-y_{1\delta}\\y_{20}-y_{2\delta}\end{pmatrix} \tag{5}$$

in which the diffusivity matrix

$$[D]=\begin{bmatrix}D_{11}&D_{12}\\D_{21}&D_{22}\end{bmatrix}=\frac{\begin{bmatrix}\frac{y_1}{Đ_{12}}+\frac{y_3}{Đ_{23}}&\frac{y_1}{Đ_{12}}\\\frac{y_2}{Đ_{12}}&\frac{y_2}{Đ_{12}}+\frac{y_3}{Đ_{13}}\end{bmatrix}}{\left(\frac{y_1y_3}{Đ_{12}Đ_{13}}+\frac{y_2y_3}{Đ_{12}Đ_{23}}+\frac{y_3y_3}{Đ_{13}Đ_{23}}\right)} \tag{6}$$

is evaluated at the arithmetic average vapor compositions $y_{i,av} = (y_{i0} + y_{i\delta})/2$. With this simplification, the fluxes can be evaluated explicitly as follows $N_1 = -0.446$; $N_2 = -0.11$ mol m^{-2} s^{-1}. Using these values at starting guesses, the Gilliland A solution set is obtained: $N_1 = -0.506$; $N_2 = -0.14$; both fluxes are directed from the liquid to the vapor phase. The ratio of the flux of water to that of ethanol is $N_2/N_1 = 0.225$; this ratio is higher than the ratio of the compositions in the liquid phase $x_2/x_1 = 0.15$. Diffusional evaporation leads to a relatively higher proportion of water in the vapor phase, causing separation of the azeotrope.

If the starting guess values are chosen as $N_1 = -0.3$; $N_2 = -0.27$, the Gilliland B solution set is obtained: $N_1 = -0.2476$; $N_2 = -0.6546$, yielding a flux ratio $N_2/N_1 = 2.64$. Remarkably, in this case, the flux of water is significantly higher than the flux of ethanol. There is no fundamental physical reasoning that allows us to discount, a priori, the set of fluxes obtained in the Gilliland set B.

If the starting guess values are chosen to be $N_1 = -0.3$; $N_2 = 0.1$, we obtain the Gilliland C solution set: $N_1 = -1.073$; $N_2 = 1.073$, yielding a flux ratio $N_2/N_1 = -1$. Indeed it is easy to check that $N_1 + N_2 = 0$ always satisfies Eq. (4), as also pointed out by Toor (1957).

Three different solution sets are also realized by choosing the inert gas to be helium, nitrogen, air, argon, and xenon; plots of the flux ratios N_2/N_1 for Gilliland A, B, C solution sets are presented in Fig. 1a as a function of the square root of the molar mass of the inert gas. The choice of the inert gas influences the relative values of 1–3 friction and 1–2 friction. The friction is inversely proportional to the corresponding M-S diffusivity pairs $Đ_{ij}$. The M-S diffusivity $Đ_{ij}$ is inversely proportional to the square root of the mean molar mass of the pairs $\sqrt{M_{ij}}$. We should therefore expect the ratio of fluxes to depend on the square root of the molar mass of the inert gas, $\sqrt{M_3}$. Also plotted in Fig. 1a are the flux calculations using the linearized Eq. (5); the flux ratios are above 10% higher than those of Gilliland A set of values.

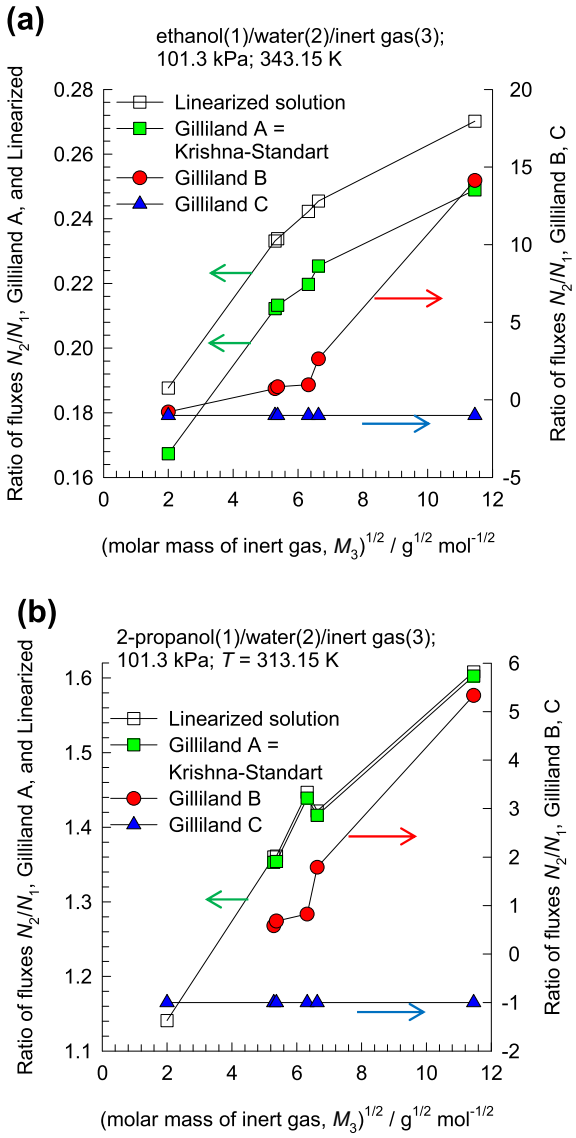

Fig. 1. Comparison of ratio of steady-state fluxes N_2/N_1 for diffusional evaporation of (a) ethanol/water, and (b) 2-propanol/water into vapor phase containing inert gas. The flux ratios are obtained using six different inert gases as component 3: helium, nitrogen, air, argon, CO_2, and xenon as inert gas. The x-axis is the square root of the molecular weight of the inert gas $\sqrt{M_3}$.

For 2-propanol(1)/water(2) mixtures the azeotrope composition at 313.15 K is $x_1 = 0.62258$, $x_2 = 0.37742$; the ratio of the mole fraction of water to that of propanol is $x_2/x_1 = 0.60624$. Let us bring this liquid mixture in contact with an inert gas phase. The vapor pressure of ethanol at 313.15 K is 13.6 kPa, and the vapor pressure of water at 313.15 K is 7.36 kPa. The total gas phase pressure $p_t = 101.3$ kPa. The composition of the vapor phase at the gas/liquid interface in equilibrium with the liquid mixture can be calculated from $y_i = \gamma_i x_i P_i^0/p_t$. This yields $y_{1\delta} = 0.09836$, $y_{2\delta} = 0.05963$, $y_{3\delta} = 0.84201$. The bulk vapor composition is taken to be: $y_{10} = 0.0$, $y_{20} = 0.0$, $y_{30} = 1.0$. The driving forces are $\Delta y_1 = y_{10} - y_{1\delta} = -0.09836$, and $\Delta y_2 = y_{20} - y_{2\delta} = -0.05963$. Both driving forces are directed from liquid to the vapor phase. Depending on the starting guess values for the fluxes, Eqs. (3) and (4) yields multiple solutions; plots of the flux ratios N_2/N_1 for Gilliland A, B, C solution sets are presented in Fig. 1b as a function of the square root of the molar mass of the inert gas.

3. The Krishna-Standart analytic solution for diffusion distillation

The solution method of Krishna and Standart (1976) will now be applied to calculate the fluxes in diffusion distillation. We define a dimensionless distance: $\eta = z/\delta$, introduce the equality $y_3 = 1 - y_1 - y_2$, and re-cast Eqs. (1) using matrix notation

$$\begin{pmatrix} \frac{dy_1}{d\eta} \\ \frac{dy_2}{d\eta} \end{pmatrix} = [\Phi]\begin{pmatrix} y_1 \\ y_2 \end{pmatrix} - \frac{\delta}{c_t}\begin{pmatrix} \frac{N_1}{\mathcal{D}_{13}} \\ \frac{N_2}{\mathcal{D}_{23}} \end{pmatrix} \tag{7}$$

where we define a two-dimensional square matrix of dimensionless fluxes, that are η-invariant

$$[\Phi] = \frac{\delta}{c_t}\begin{bmatrix} \frac{N_1}{\mathcal{D}_{13}} + \frac{N_2}{\mathcal{D}_{12}} & -N_1\left(\frac{1}{\mathcal{D}_{12}} - \frac{1}{\mathcal{D}_{13}}\right) \\ -N_2\left(\frac{1}{\mathcal{D}_{12}} - \frac{1}{\mathcal{D}_{23}}\right) & \frac{N_2}{\mathcal{D}_{23}} + \frac{N_1}{\mathcal{D}_{12}} \end{bmatrix} \tag{8}$$

Eq. (7) represents a system of coupled *ordinary* differential equations with *constant coefficients*. The system of equations can be solved analytically to obtain the mole fraction profiles within the diffusion layer

$$(y_\eta - y_0) = -[\exp[\Phi]\eta - [I]][\exp[\Phi] - [I]]^{-1}(y_0 - y_\delta) \tag{9}$$

In Eq. (9), $[I]$ is the identity matrix with Kronecker delta δ_{ik} as elements. The composition gradient at the position $\eta = z/\delta$ can be obtained by differentiation of Eq. (9); we get

$$\frac{d(y_\eta)}{d\eta} = -[\Phi][\exp[\Phi]\eta][\exp[\Phi] - [I]]^{-1}(y_0 - y_\delta) \tag{10}$$

The steady-state transfer fluxes of components 1, and 2 can be determined by combining Eqs. (1) and (10)

$$\begin{pmatrix} N_1 \\ N_2 \end{pmatrix} = -\frac{c_t}{\delta}[D_\eta]\frac{d(y_\eta)}{d\eta} = \frac{c_t}{\delta}[D_\eta][\Phi][\exp[\Phi]\eta][\exp[\Phi] - [I]]^{-1}(y_0 - y_\delta) \tag{11}$$

The diffusivity matrix $[D_\eta]$ can be evaluated from Eq. (6) using the appropriate gas phase mole fractions. Without loss of generality, we may evaluate the diffusivity $[D_\eta]$ at position $\eta = z/\delta = 0$, and obtain

$$\begin{pmatrix} N_1 \\ N_2 \end{pmatrix} = -\frac{c_t}{\delta}[D_{\eta=0}]\frac{d(y)}{d\eta}\bigg|_{\eta=0} = \frac{c_t}{\delta}[D_{\eta=0}][\Phi][\exp[\Phi] - [I]]^{-1}(y_0 - y_\delta) \tag{12}$$

The Sylvester theorem, detailed in Appendix A of Taylor and Krishna (1993) is required for explicit calculation of $[\Phi][\exp[\Phi] - [I]]^{-1}$. Though the expression (12) appears to be explicit in the fluxes, it is to be noted that the matrix $[\Phi][\exp[\Phi] - [I]]^{-1}$ is also a function of the fluxes. In the limit of vanishingly small transfer fluxes we have the limiting behavior $[\Phi][\exp[\Phi] - [I]]^{-1} \to [I]$. In this work, the set of coupled algebraic equations (12) were solved iteratively using the Given-Find solve block of MathCad 15 (PTC, 2013) using starting guesses for the fluxes. For all mixtures investigated, the final converged values of the fluxes are identical to Gilliland A set for ethanol/water/inert, and 2-propanol/water/inert, irrespective of the starting guess values; see Fig. 1a and b.

The eigenvalues λ_1, λ_2 of $[\Phi]$ provide valuable insights into the characteristics of sets A, B, and C of the Gilliland solutions. The Gilliland set A corresponds to the case in which the eigenvalues λ_1, λ_2 are both distinct, and non-zero. The Gilliland set B corresponds to the case in which the eigenvalues λ_1, λ_2 are equal to each other. The Gilliland set C corresponds to the case in which the second eigenvalue is zero, $\lambda_2 = 0$. Details of the numerical values of λ_1, λ_2

for all mixtures investigated are provided in the Supplementary material.

What fundamental principle can we employ to decide between Gilliland sets A, B, and C?

4. The Prigogine principle of minimum entropy production

The second law of thermodynamics dictates that the rate of entropy production must be positive definite, $\sigma \geqslant 0$; the situation $\sigma = 0$ manifests at thermodynamic equilibrium (Prigogine, 1961; Standart et al., 1979). For the ternary gas diffusion with $N_3 = 0$, the rate of entropy production is (detailed derivations in Supplementary material)

$$\sigma = -R\left[N_1 \frac{1}{y_1}\frac{dy_1}{dz} + N_2 \frac{1}{y_2}\frac{dy_2}{dz}\right] \geqslant 0 \qquad (13)$$

The Prigogine principle of minimum entropy production says that the steady state of an irreversible process, i.e., the state in which the thermodynamic variables are independent of the time, is characterized by a minimum value of the rate of entropy production (Prigogine, 1961).

We illustrate the application of the Prigogine principle by considering diffusional evaporation of 2-propanol(1)/water(2) into inert CO_2 (species 3).

Using the fluxes calculated from the linearized Eq. (6): $N_1 = -0.0384$; $N_2 = -0.0546$ mol m^{-2} s^{-1}, as starting guess values, Eqs. (3) and (4) yields the Gilliland A set of fluxes: $N_1 = -0.0386$; $N_2 = -0.0546$ mol m^{-2} s^{-1}, with $N_2/N_1 = 1.416$; the rate of entropy production is $\sigma = 1.55$ kJ m^{-3} s^{-1} K^{-1}.

If the starting guess values are chosen to be $N_1 = -0.03$; $N_2 = -0.05$ mol m^{-2} s^{-1}, deviating only slightly from the Gilliland A set values, we obtain the Gilliland B solution set: $N_1 = -0.0352$; $N_2 = -0.0631$ mol m^{-2} s^{-1}, yielding a flux ratio $N_2/N_1 = 1.79$; the rate of entropy production is $\sigma = 1.63$ kJ m^{-3} s^{-1} K^{-1}. A further noteworthy point is that the magnitude of the flux ratios for Gilliland sets A and B are close to one another, and neither set can be discarded by subjective hand-waving.

If the starting guess values are chosen to be $N_1 = -0.04$; $N_2 = 0.05$ mol m^{-2} s^{-1}, we obtain the Gilliland C solution set: $N_1 = -0.0997$; $N_2 = 0.0997$ mol m^{-2} s^{-1}, yielding a flux ratio $N_2/N_1 = -1$; the rate of entropy production $\sigma = 0$. A null entropy production at steady-state is not a physically acceptable situation, and we conclude that Gilliland set C is not realizable in practice; counter-diffusion of alcohol and water cannot be a physically realistic solution. On the basis of the Prigogine principle, we must conclude that Gilliland set A is the one that can be realized in practice because it produces entropy at a lower rate than for the set B.

For ethanol/water/inert gas mixtures, the rates of entropy production for the solution sets A, B, and C are plotted in Fig. 2. The rate of entropy production for set C is zero, that is only possible at thermodynamic equilibrium; this set C can be discounted on the basis that equimolar counter-diffusion of ethanol/water is not a physically realistic solution. The Gilliland set A is the one that is physically realizable because it produces entropy at a lower rate.

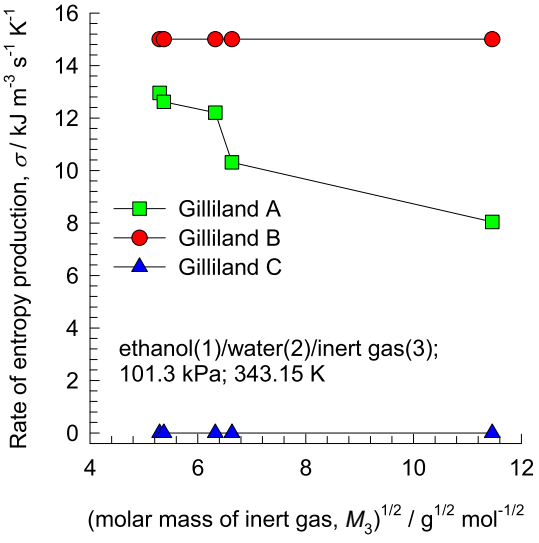

Fig. 2. Rate of entropy production, σ, for diffusional evaporation of ethanol (1)/water (2) into vapor phase containing inert gas (3).

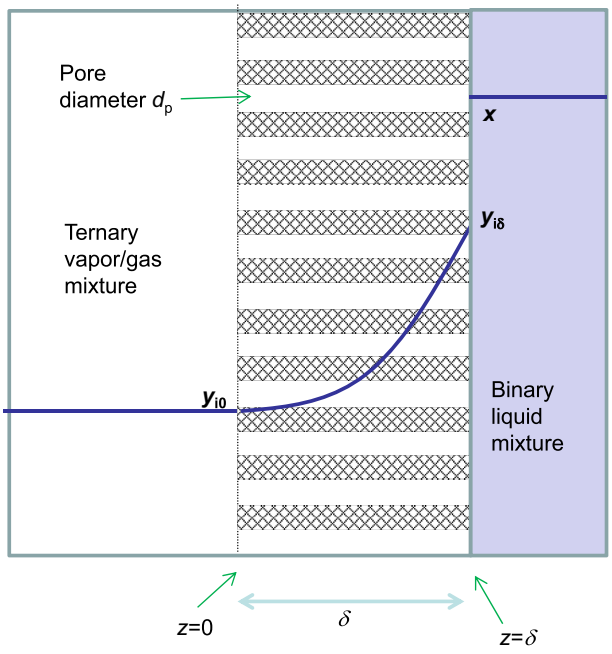

Fig. 3. Schematic showing vapor/liquid transfer across an inert porous barrier.

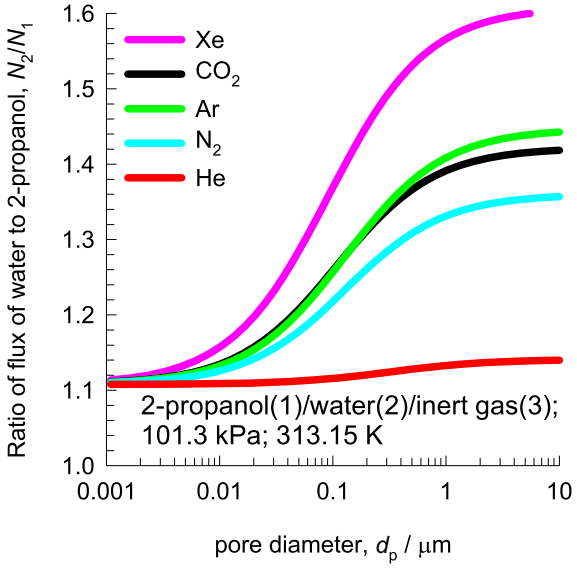

Fig. 4. Comparison of ratio of quasi-stationary fluxes N_2/N_1 for 2-propanol (1)/water (2)/inert gas (3), plotted as a function of pore diameter, d_p, of the barrier interposed between the vapor and liquid phases.

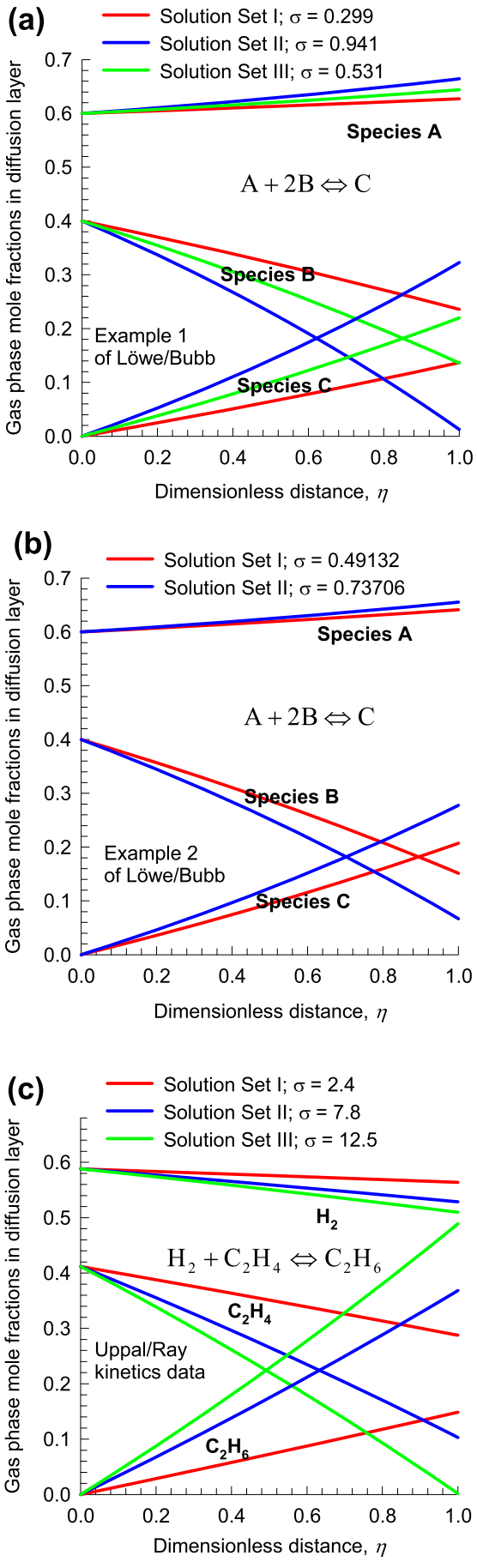

Experimental verification that the Gilliland solution set A is the physically realizable solution is provided by experimental data of Carty and Schrodt (1975) for diffusional evaporation of acetone/methanol into air. For the set of boundary conditions in their experiments, three solution sets are obtained. Of the three solution sets, only Gilliland set A yields composition profiles, and transfer fluxes, that are in agreement with the experimentally data; see Fig. S4. The use of the Prigogine principle of minimum entropy production, as suggested in this work, obviates the need for using experimental data to decide on the choice of the physically realizable solution.

For steady-state equimolar diffusion in ternary gas mixtures, $N_1 + N_2 + N_3 = 0$, Toor (1957) has presented analytic solutions in parameter form, analogous to Eqs. (3) and (4); the Toor solutions also result in multiplicity of solutions. The Prigogine principle of minimum entropy production allows the selection of the physically realizable solution; see Supplementary material for detailed discussions and calculations.

From the results in Fig. 1a we must conclude that for accurate calculation of the ethanol/water fluxes, we must use Eq. (12); somewhat lower accuracy is obtained using the linearized Eq. (5). For 2-propanol/water/inert system, the linearized solution is practically identical to the results from the exact Krishna-Standart model; see Fig. 1b. This is because the 2-propanol/water/inert system was investigated at a lower temperature of 313.15 K at which the compositions of both 2-propanol and water in the gas phase are low. The separation efficacy, quantified by N_2/N_1, appears to correlate with $\sqrt{M_3}$, broadly in agreement with the experimental results of Singh and Prasad (2011) for ethanol/water separations in a wetted-wall column using different inert gases. Simulations of transient diffusion between a liquid film and a stagnant vapor slab, more representative of wetted-wall columns, lead to the same conclusions regarding the influence of the choice of the inert gas; see Figs. S12–S16 of the Supplementary material.

5. Imposition of porous barriers between liquid and vapor phases

In view of scale-up limitations of wetted-wall columns, porous barriers are often interposed between the liquid and vapor phases (Breure et al., 2008) in experimental set-ups for diffusion distillation. Fig. 3 shows a schematic of vapor/liquid transfer across an inert porous barrier. From the conceptual point of view, the porous barrier is also to be considered as an "inert" fourth component in the quaternary system alcohol(1)/water(2)/inert gas (3)/inert barrier(component m). Extending Eq. (5), we may write for a barrier (membrane) with pore diameter, d_p (see (Krishna, 2016) for further background information)

$$\begin{pmatrix} N_1 \\ N_2 \end{pmatrix} = \frac{c_t}{\delta} \frac{\begin{bmatrix} \frac{y_1}{\mathcal{D}_{12}} + \frac{y_3}{\mathcal{D}_{23}} + \frac{1}{\mathcal{D}_{2,Kn}} & \frac{y_1}{\mathcal{D}_{12}} \\ \frac{y_2}{\mathcal{D}_{12}} & \frac{y_2}{\mathcal{D}_{12}} + \frac{y_3}{\mathcal{D}_{13}} + \frac{1}{\mathcal{D}_{1,Kn}} \end{bmatrix}}{\left(\frac{y_1}{\mathcal{D}_{12}}\left(\frac{y_3}{\mathcal{D}_{13}} + \frac{1}{\mathcal{D}_{1,Kn}}\right) + \frac{y_2}{\mathcal{D}_{12}}\left(\frac{y_3}{\mathcal{D}_{23}} + \frac{1}{\mathcal{D}_{2,Kn}}\right) + \left(\frac{y_3}{\mathcal{D}_{13}} + \frac{1}{\mathcal{D}_{1,Kn}}\right)\left(\frac{y_3}{\mathcal{D}_{23}} + \frac{1}{\mathcal{D}_{2,Kn}}\right)\right)} \begin{pmatrix} y_{10} - y_{1\delta} \\ y_{20} - y_{2\delta} \end{pmatrix} \tag{14}$$

where the Knudsen diffusivity values are used to quantify the friction with the pore walls of the barrier

$$D_{i,Kn} = \frac{d_p}{3}\sqrt{\frac{8RT}{\pi M_i}} \tag{15}$$

Fig. 5. Composition profiles in the gas film external to the catalyst surface with heterogeneous chemical reactions (a, b) A + 2B ⟺ C, and (c) $H_2 + C_2H_4 \Longleftrightarrow C_2H_6$. The calculations are all based on Eq. (9). Depending on the starting guess, different composition profiles are obtained, corresponding to one of the solution sets I, II, and III. The rates of entropy production, σ, for each solution set are also indicated. The input data and computational details are provided in the Supplementary material.

Fig. 4 presents calculations of the ratio of fluxes N_2/N_1 for 2-propanol (1)/water (2)/inert gas (3), plotted as a function of pore diameter, d_p, of the barrier interposed between the vapor and liquid phases. For each of the five inert gases investigated, increase in the pore diameter improves the separation performance; i.e. introduction of the porous barrier decreases the efficacy of separation. The results in Fig. 4 also lead to the conclusion that separations are most effective in the "bulk" diffusion regime, as compared to the "Knudsen" regime; the same conclusion has been drawn by Breure et al. (2008).

6. Applying the Prigogine principle for diffusion with heterogeneous catalytic reaction

For diffusion with heterogeneously catalyzed reversible reaction $A + 2B \Longleftrightarrow C$, following Langmuir-Hinshelwood kinetics, Löwe and Bub (1976) have demonstrated the possibility of multiple solutions with the aid of Example 1 and Example 2, each with different kinetic constants. We re-trace their analysis, using the Krishna-Standart analytic solution for calculation of the steady-state fluxes in the diffusion "film"; the reaction takes place at the position $\eta = z/\delta = 1$, corresponding to the catalytic surface. The analysis is also relevant in the context of reactive distillation for which multiple steady-states are often reported (Higler et al., 1999; Taylor and Krishna, 2000).

For Example 1, depending on the starting guess values, three different solutions sets I, II, and II are obtained. The composition profiles in the "film", calculated using Eq. (9), are shown in Fig. 5a. The obtained results are, precisely the same as those reported by Löwe and Bub (1976) as should be expected. The dimensionless rate of entropy production, $\sigma\delta^2/(c_t Đ R)$, for the three sets are 0.299, 0.941, and 0.531, respectively; calculation details are provided in the Supplementary material. Invoking the Prigogine principle, we conclude that the stable steady state is Solution Set I.

For Example 2, two different solutions are obtained; the composition profiles in the "film" are shown in Fig. 5b. The dimensionless rate of entropy production, $\sigma\delta^2/(c_t Đ R)$, for the two sets; the values are 0.49132, and 0.73706, respectively. Invoking the Prigogine principle, we conclude that the stable steady state is Solution Set I. Löwe and Bub (1976) present a detailed stability analysis to conclude that for both Examples 1, and 2, the Solution set I is the stable steady-state. The use of the Prigogine principle of minimum entropy production obviates the need for performing a detailed stability analysis.

Three different steady-state solutions are also realized in the analysis of diffusion and catalytic hydrogenation of ethene to produce ethane using platinum/alumina catalyst. For Langmuir-Hinshelwood kinetics and input data from Uppal and Ray (1977), the composition profiles calculated using Eq. (9), are shown in Fig. 5c. Application of the Prigogine principle leads us to conclude that the stable steady-state corresponds to solution set I, which is the low-conversion steady-state.

7. Conclusions

In this article, the Maxwell-Stefan diffusion equations have been used to investigate the strategy of introduction of an inert component for effecting the separation of azeotropic 2-propanol/water, and ethanol/water mixtures. The following major conclusions emerge from the analysis presented in this paper.

(1) The use of the Gilliland parametric solutions to the M-S diffusion equations results in three different set of transfer fluxes, depending on the starting guess values. Of these, only Gilliland set A solution is physically realizable, because it conforms with the Prigogine principle of minimum entropy production.
(2) The Krishna-Standart analytic solution yields results in precise agreement with the Gilliland A set. The method is computationally robust, and converges quickly.
(3) The linearized solution method employing Eq. (5) is of reasonable accuracy and may be used for preliminary design and screening purposes.
(4) The efficacy of separation of alcohol(1)/water(2) mixtures of azeotropic composition by introduction of an inert gaseous component (3) essentially relies on *differences* in 1–2 and 2–3 friction in the vapor phase. Such differences increase with increasing molar mass of the inert component 3. Inert gases such as CO_2 and Xe are more effective than lighter inerts such as air, nitrogen or helium.
(5) If porous barriers (membranes) are interposed between the vapor and liquid phases, the pore size of the barrier material must be chosen to be large enough to ensure that the diffusion regime within the pores corresponds to bulk diffusion. In other words, the operations should not be in the Knudsen regime.
(6) For diffusion with heterogeneous chemical reaction, the Prigogine principle can also be gainfully employed to determine the stable steady-state.

Appendix A. Supplementary material

Supplementary data associated with this article can be found, in the online version, at http://dx.doi.org/10.1016/j.ces.2017.01.060.

References

Banat, F.A., Al-Rub, F.A., Jumah, R., Shannag, M., 1999a. On the effect of inert gases in breaking the formic acid-water azeotrope by gas-gap membrane distillation. Chem. Eng. J. 99, 37–42.
Banat, F.A., Al-Rub, F.A., Shannag, M., 1999b. Modeling of dilute ethanol-water mixture separation by membrane distillation. Sep. Purif. Technol. 16, 119–131.
Breure, B., Peters, E.A.J.F., Kerkhof, P.J.A.M., 2008. Separation of azeotropic mixtures of alcohols and water with FricDiff. Sep. Purif. Technol. 62, 349–362.
Bröcker, S., Schulze, W., 1991. A new method of calculating ternary mass transfer with a non transferring species based on the Gilliland's parameter solution of the Maxwell-Stefan equations for the film model. Chem. Eng. Commun. 107, 163–172.
Carty, R., Schrodt, T., 1975. Concentration profiles in ternary gaseous diffusion. Ind. Eng. Chem. Fundam. 14, 276–278.
Cichelli, M.T., Weatherford, W.D., Bowman, J.R., 1951. Sweep diffusion gas separation process. Part I. Chem. Eng. Prog. 47 (2), 63–74.
Fullarton, D., Schlünder, E.U., 1986. Diffusion distillation – a new separation. process for azeotropic mixtures – Part I: selectivity and transfer efficiency. Chem. Eng. Process. 20, 255–263.
Fuller, E.N., Schettler, P.D., Giddings, J.C., 1966. A new method for prediction of binary gas-phase diffusion coefficients. Ind. Eng. Chem. 58, 19–27.
Higler, A.P., Taylor, R., Krishna, R., 1999. Nonequilibrium modelling of reactive distillation: multiple steady states in MTBE synthesis. Chem. Eng. Sci. 54, 1389–1395.
Keyes, J.J., Pigford, R.L., 1957. Diffusion in a ternary gas system with application to gas separation. Chem. Eng. Sci. 6, 215–226.
Krishna, R., 1977. A generalized film model for mass transfer in nonideal fluid mixtures. Chem. Eng. Sci. 32, 659–667.
Krishna, R., 1981. An alternative linearized theory of multicomponent mass transfer. Chem. Eng. Sci. 36, 219–222.
Krishna, R., 2016. Investigating the validity of the Knudsen diffusivity prescription for mesoporous and macroporous materials. Ind. Eng. Chem. Res. 55, 4749–4759.
Krishna, R., Standart, GL., 1976. A multicomponent film model incorporating a general matrix method of solution to the Maxwell-Stefan equations. AIChE J. 22, 383–389.
Löwe, A., Bub, G., 1976. Multiple steady states for isothermal catalytic gas-solid reactions with a positive reaction order. Chem. Eng. Sci. 31, 175–178.
Prigogine, I., 1961. Thermodynamics of Irreversible Processes. Interscience, New York U.S.A.
PTC, 2013. MathCad 15.0. PTC Corporate Headquarters, Needham. <http://www.ptc.com/> (3 November 2015). .
Sherwood, T.K., 1937. Absorption and Extraction. McGraw-Hill, New York.

Sherwood, T.K., Pigford, R.L., Wilke, C.R., 1975. Mass Transfer. Mc-Graw Hill, New York, U.S.A.
Singh, N., Prasad, R., 2011. Experimental studies on the effect of inert gases on diffusion distillation of ethanol–water mixtures. J. Chem. Technol. Biotechnol. 86, 1495–1500.
Singh, N., Prasad, R., 2015. Performance of diffusion distillation column for production of fuel grade ethanol. J. Chem. Technol. Biotechnol. 90, 1847–1854.
Standart, G.L., Taylor, R., Krishna, R., 1979. The Maxwell-Stefan formulation of irreversible thermodynamics for simultaneous heat and mass transfer. Chem. Eng. Commun. 3, 277–289.
Taylor, R., Krishna, R., 1993. Multicomponent Mass Transfer. John Wiley, New York.
Taylor, R., Krishna, R., 2000. Modelling reactive distillation. Chem. Eng. Sci. 55, 5183–5229.
Toor, HL., 1957. Diffusion in three-component gas mixtures. AIChE J. 3, 198–207.
Uppal, A., Ray, W.H., 1977. On the steady-state and dynamic behaviour of permeable, isothermal catalysts. Chem. Eng. Sci. 32, 649–657.
Ziobrowski, Z., Rotkegel, A., Krupiczka, R., 2009. Evaporation of a binary liquid film in the presence of stagnant inert gas. Chem. Process Eng. 30, 13–24.

Supplementary material to accompany:

Highlighting Multiplicity in the Gilliland Solution to the Maxwell-Stefan Equations Describing Diffusion Distillation

Rajamani Krishna

Van 't Hoff Institute for Molecular Sciences, University of Amsterdam, Science Park 904,

1098 XH Amsterdam, The Netherlands

email: r.krishna@contact.uva.nl

Table of Contents

1. Preamble 3
2. The Maxwell-Stefan formulation for *n*-component diffusion 3
3. The bootstrap relations in distillation separations 6
4. Second law, and the rate of entropy production 7
5. Non-equimolar effects for binary distillation 8
6. The Krishna-Standart solution to the M-S equations for non-equimolar distillation of ternary mixtures 14
7. The Krishna-Standart solution to the M-S equations for equimolar distillation of ternary mixtures 18
8. The Toor (1957) analytic solutions to the M-S equations for equimolar distillation 19
9. Non-equimolar distillation of acetic acid (1) – water (2) – methanol (3) mixtures 20
10. Non-equimolar distillation of 2-pentane (1) – ethanol (2) – water (3) mixtures 22
11. Multiplicity of solutions for equimolar diffusion in $H_2(1)/N_2(2)/CO_2(3)$ gas mixtures 23
12. The Maxwell-Stefan formulation for diffusion distillation 25
13. Krishna-Standart exact analytic solution for diffusion distillation 27
14. Gilliland exact analytic solution for diffusion distillation 30
15. The linearized solution for diffusion distillation 31
16. Carty-Schrodt experiments for diffusional evaporation of acetone/methanol into air 31
17. Diffusional evaporation of acetone/methanol into Xe 33
18. Absorption of $NH_3(1)$ and $H_2O(2)$ from Air(3) into water 35
19. Multiplicity of solutions for acetone/benzene diffusion in inert helium 37
20. Multiplicity of solutions for 2-propanol/water diffusion in inert CO_2 39
21. Multiplicity of solutions for ethanol/water diffusion in inert CO_2 43
22. Multiplicity of solutions for ethanol/water diffusion into Ar 46
23. Diffusion distillation with porous barrier: Exact analytic solutions for fluxes 50
24. Diffusion distillation with porous barrier: Linearized solutions for flux calculations 54
25. Diffusional evaporation of acetone/methanol into inert gas 56
26. Transient diffusional evaporation of 2-propanol/water/inert mixture 57
27. Transient diffusional evaporation of ethanol/water into inert gas 60
28. Diffusion with heterogeneous chemical reaction 62
29. Diffusional coupling effects in CVD reactor for W deposition 67
30. Multiplicity of solutions for hydrogenation of ethene 68
31. Multiplicity of solutions in the Löwe-Bubb reaction system 72
32. Notation 77

33. References 81
34. Caption for Figures 83

1. Preamble

The Supplementary material (*e*-content) accompanying the manuscript *Highlighting Multiplicity in the Gilliland Solution to the Maxwell-Stefan Equations Describing Diffusion Distillation* provides (a) Detailed derivation of the Maxwell-Stefan equations applicable to non-equimolar distillation, and diffusion distillation. (b) Calculation details of simulation model, and input data used to elucidate the principle of diffusion distillation for separation of azeotropic mixtures. (c) Analysis of multicomponent distillation with heterogeneous chemical reaction.

All the calculations and simulations presented in this article were performed using MathCad 15.[1]

For ease of reading, this Supplementary material has been written as a stand-alone document. Consequently, there is some degree of overlap with the main article.

2. The Maxwell-Stefan formulation for *n*-component diffusion

The approach we adopt to describe diffusion distillation stems from the pioneering works of James Clerk Maxwell [2] and Josef Stefan [3] who analyzed diffusion in ideal gas mixtures. The Maxwell-Stefan (M-S) formulation is best understood by considering *z*-directional diffusion in a binary gas mixture consisting of species 1 and 2, contained within the control volume shown schematically in Figure **1**. The cross-sectional area available for diffusion is 1 m^2 and the length of the diffusion path is dz. If the change in the partial pressure of component *i* across the diffusion distance dz is $-dp_i$, the force acting on species *i* per m^3 is $-\frac{dp_i}{dz}$. The number of moles of species *i* per m^3, $c_i = \frac{p_i}{RT}$, and therefore the force acting per mole of species *i* is $-\frac{RT}{p_i}\frac{dp_i}{dz}$ which for an ideal gas mixture at constant temperature also

equals the chemical potential gradient $-\frac{d\mu_i}{dz}$. This force is balanced by friction between the diffusing species 1 and 2, each diffusing with a velocity u_i (cf. Figure **2**). We may expect that the frictional drag to be proportional to the velocity difference $(u_1 - u_2)$, and we write $-\frac{d\mu_1}{dz} = \frac{RT}{Đ_{12}} y_2 (u_1 - u_2)$ where the term $\frac{RT}{Đ_{12}}$ is to be interpreted as the drag coefficient. The multiplier y_2 in the right member represents the mole fraction of component 2; this factor is introduced because we expect the friction to be dependent on the number of molecules of component 2 relative to that of component 1. The Maxwell-Stefan diffusivity $Đ_{12}$ has the units $m^2\ s^{-1}$ and the physical significance of an inverse drag coefficient. The extension to *n*-component mixtures is intuitively obvious [4, 5]:

$$-\frac{1}{RT}\frac{d\mu_i}{dz} = \sum_{\substack{j=1 \\ j\neq i}}^{n} \frac{y_j (u_i - u_j)}{Đ_{ij}}; \quad i = 1,2,\ldots n \tag{1}$$

The pair diffusivity $Đ_{ij}$ can be interpreted as an inverse "drag coefficient" between species *i* and species *j*. Equation (1) is consistent with the theory of irreversible thermodynamics. The Onsager reciprocal relations demand the symmetry constraint $Đ_{ij} = Đ_{ji}; \quad i, j = 1,2,\ldots n$. Multiplying both sides of Equation (1) by y_i we obtain

$$-\frac{y_i}{RT}\frac{d\mu_i}{dz} = \sum_{\substack{j=1 \\ j\neq i}}^{n} \frac{y_i y_j (u_i - u_j)}{Đ_{ij}}; \quad i = 1,2,\ldots n \tag{2}$$

The M-S pair diffusivities $Đ_{ij}$ for gaseous mixtures at low pressures, below about 10 bar, can be estimated to a good level of accuracy using the Fuller-Schettler-Giddings (FSG)[6] method

$$Đ_{ij} = \frac{1.43\times 10^{-7} T^{1.75}}{p\sqrt{M_{ij}}\left[\left(v_i^{1/3}\right) + \left(v_i^{1/3}\right)\right]^2} \quad m^2 s^{-1}$$ where *p* is the pressure (expressed in bars), $M_{ij} = \frac{2}{\frac{1}{M_i} + \frac{1}{M_j}}$ is the mean molecular weight of the mixture (expressed in g mol^{-1}), v_i, and v_j are the diffusion volumes (expressed in $cm^3\ mol^{-1}$) whose values are obtained by summing the contributions of the volumes of the

constituent atoms in the molecular species (the values are tabulated in Table 11.1 of Reid, Prausnitz, and Poling[7]). According to the FSG estimation procedure, the product of $Đ_{ij}$ and the total pressure, p, is a function only of temperature and is also independent of composition.

For mixtures of ideal gases, $\frac{y_i}{RT}\frac{d\mu_i}{dz} = \frac{dy_i}{dz}$; in this case, equation (2) simplifies to yield

$$-\frac{dy_i}{dz} = \sum_{\substack{j=1 \\ j\neq i}}^{n} \frac{y_i y_j \left(u_i - u_j\right)}{Đ_{ij}}; \quad i = 1,2,\ldots n \tag{3}$$

Equation (3) is entirely consistent with the kinetic theory of gases, and the pair diffusivities $Đ_{ij}$ can be identified with the diffusivity in the *binary* gas mixture of species *i* and species *j*.

All the calculations presented in this article are for ideal gas mixtures.

Only n-1 of the equations (2) are independent because the mole fractions sum to unity and the mole fraction gradients sum to zero $\sum_{i=1}^{n} y_i = 1; \quad \frac{dy_1}{dz} + \frac{dy_2}{dz} + \ldots \frac{dy_n}{dz} = 0$.

The molar fluxes N_i in the laboratory fixed reference frame are

$$N_i \equiv c_i u_i = c_t y_i u_i; \quad i = 1,2,\ldots n \tag{4}$$

The molar average mixture velocity u is $u = x_1 u_1 + x_2 u_2 + \cdots x_n u_n$. We may also define diffusion fluxes J_i with respect to the chosen molar average reference velocity frame u:

$$J_i \equiv c_i\left(u_i - u\right); \quad i = 1,2,..n \tag{5}$$

We have the inter-relation between the two fluxes

$$N_i \equiv c_i u_i = J_i + y_i N_t; \quad N_t = \sum_{i=1}^{n} N_i = c_t u \tag{6}$$

The diffusion fluxes J_i sum to zero

$$\sum_{i=1}^{n} J_i = \sum_{i=1}^{n} c_i u_i - \sum_{i=1}^{n} c_i u = \sum_{i=1}^{n} N_i - \sum_{i=1}^{n} c_i u = 0 \tag{7}$$

The n-1 independent diffusion fluxes J_i can be determined by solving the n-1 independent equations (3). The determination of the n independent molar fluxes N_i in the laboratory fixed reference frame requires an additional relationship, called the *bootstrap* relation by Krishna and Standart.[8]

A variety of bootstrap relations are applicable in a variety of situations; these are discussed in the following section.

3. The bootstrap relations in distillation separations

Consider first, vapor/liquid transfer in distillation, in the absence of an inert gas. Application of the proper energy balances to the vapor and liquid phases, it can be shown that the proper constraint on the interfacial molar fluxes is[9]

$$\sum_{i=1}^{n} N_i\left(\overline{H_i^V} - \overline{H_i^L}\right) = 0 \tag{8}$$

Let us denote the molar heats of vaporization as $\lambda_i \equiv \left(\overline{H_i^V} - \overline{H_i^L}\right)$. So, the additional bootstrap relation is

$$\sum_{i=1}^{n} N_i \lambda_i = 0 \tag{9}$$

Equations (3), in combination with the bootstrap relation (9) are sufficient to determine the n independent molar fluxes N_i.

Table 1 lists some typical values for the molar heats of vaporization of various molecules. For water/methanol, and water/ethanol mixtures, the molar heats of vaporization are close to one another and therefore, as an approximation, we get

$$\sum_{i=1}^{n} N_i \approx 0; \quad \text{equimolar counter-diffusion} \tag{10}$$

The assumption of equimolar counter-diffusion is commonly invoked in the analysis of mass transfer effects in distillation.

Consider the reactive distillation process for the manufacture of methyl tert-butyl ether (MTBE) by heterogeneously catalysed reaction of isobutene with methanol. The molar heats of vaporization of the species involved (at 40 ^{o}C) are: isobutene: 19.6 kJ/mol; methanol: 36.5 kJ/mol; MTBE: 29.5 kJ/mol. In the mass transfer modelling of this process a proper account is to be taken of these differences, as demonstrated in the detailed analysis of Sundmacher and Hoffmann.[10]

In diffusional distillation, the *n*th component is an inert gas that does not transfer across the vapor/liquid interface into or out of the liquid phase $u_n = 0; \quad N_n = 0$.

4. Second law, and the rate of entropy production

The second law of thermodynamics dictates that the rate of entropy production must be positive definite

$$\sigma = -\frac{1}{T}\sum_{i=1}^{n}\frac{d\mu_i}{dz}J_i \geq 0 \tag{11}$$

Equation (11) simplifies for ideal gas mixtures to

$$\sigma = -R\sum_{i=1}^{n} J_i \frac{1}{y_i}\frac{dy_i}{dz} \geq 0; \quad \text{(ideal gas mixtures)} \tag{12}$$

Equation (12) may also be re-written as

$$\sigma = -R\sum_{i=1}^{n} \frac{c_i}{y_i}\left(u_i - u\right)\frac{dy_i}{dz} \geq 0; \quad \text{(ideal gas mixtures)} \tag{13}$$

For equimolar counter-diffusion, the molar average reference velocity $u = 0$, and so equation (13) simplifies to $\sigma = -R\sum_{i=1}^{n}\frac{N_i}{y_i}\frac{dy_i}{dz}$. For equimolar counter-diffusion across a film thickness δ, the integral average rate of entropy production is

$$\sigma = \frac{R}{\delta}\left[N_1\frac{\Delta y_1}{y_{1,av}} + N_2\frac{\Delta y_2}{y_{2,av}} + N_3\frac{\Delta y_3}{y_{3,av}}\right]; \quad \text{equimolar counter - diffusion} \tag{14}$$

For a ternary gas mixture, the molar average reference velocity of the mixture $u = y_1u_1 + y_2u_2 + y_3u_3$, equation (13) yields

$$-\frac{\sigma}{c_tR} = (u_1 - y_1u_1 - y_2u_2 - y_3u_3)\frac{dy_1}{dz} + (u_2 - y_1u_1 - y_2u_2 - y_3u_3)\frac{dy_2}{dz} + (u_3 - y_1u_1 - y_2u_2 - y_3u_3)\frac{dy_3}{dz} \geq 0$$

For diffusion distillation, we have $u_3 = 0$. Therefore,

$$-\frac{\sigma}{c_tR} = (u_1 - y_1u_1 - y_2u_2)\frac{dy_1}{dz} + (u_2 - y_1u_1 - y_2u_2)\frac{dy_2}{dz} + (-y_1u_1 - y_2u_2)\left(-\frac{dy_1}{dz} - \frac{dy_2}{dz}\right) \geq 0; \quad (15)$$

In Equation (15)), we have introduced the constraint $-\frac{dy_1}{dz} - \frac{dy_2}{dz} = \frac{dy_3}{dz}$. Equation (15) simplifies to

$$\sigma = -c_tR(u_1)\frac{dy_1}{dz} - c_tR(u_2)\frac{dy_2}{dz} \geq 0; \quad (16)$$

In terms of the molar fluxes, equation (16) can be written

$$\sigma = -R\left[N_1\frac{1}{y_1}\frac{dy_1}{dz} + N_2\frac{1}{y_2}\frac{dy_2}{dz}\right] \geq 0 \quad (17)$$

For diffusion across a film thickness δ, with boundary conditions $\begin{matrix}\eta = 0; & z = 0; & (y) = (y_0)\\ \eta = 1; & z = \delta; & (y) = (y_\delta)\end{matrix}$, the integral average rate of entropy production can be approximated as follows

$$\sigma = -R\int_{z=0}^{z=\delta}\left[N_1\frac{1}{y_1}\frac{dy_1}{dz} + N_2\frac{1}{y_2}\frac{dy_2}{dz}\right]dz \approx \frac{R}{\delta}\left[N_1\frac{\Delta y_1}{y_{1,av}} + N_2\frac{\Delta y_2}{y_{2,av}}\right] \geq 0 \quad (18)$$

In equation (18), we use the arithmetic average vapor compositions $y_{i,av} = \frac{y_{i0} + y_{i\delta}}{2}$ and define the driving forces as $\Delta y_1 = y_{10} - y_{1\delta}$, and $\Delta y_2 = y_{20} - y_{2\delta}$.

5. Non-equimolar effects for binary distillation

Let us examine the influence of non-equimolar diffusion for binary distillation. There is only one independent diffusion flux

$$J_1 \equiv c_1(u_1 - u) = -c_t Đ_{12} \frac{dy_1}{dz} = -J_2 = c_t Đ_{12} \frac{dy_2}{dz} \tag{19}$$

The bootstrap relation is $\lambda_1 N_1 + \lambda_2 N_2 = 0; \quad N_2 = -\frac{\lambda_1 N_1}{\lambda_2}$. So,

$$N_1 = J_1 + y_1\left(N_1 - \frac{\lambda_1 N_1}{\lambda_2}\right) = J_1 - y_1 N_1\left(\frac{\lambda_1 - \lambda_2}{\lambda_2}\right) = \frac{\lambda_2}{\lambda_2 + y_1(\lambda_1 - \lambda_2)} J_1 \tag{20}$$

Combining equation (19) and (20) yields

$$N_1 = -c_t \frac{\lambda_2}{\lambda_2 + y_1(\lambda_1 - \lambda_2)} Đ_{12} \frac{dy_1}{dz} \tag{21}$$

The flux equation (21) can be integrated for the boundary conditions $\begin{matrix} z = 0; & y_1 = y_{10} \\ z = \delta; & y_1 = y_{1\delta} \end{matrix}$ to obtain

$$N_1 = \frac{c_t Đ_{12}}{\delta} \frac{\lambda_2}{(\lambda_1 - \lambda_2)} \ln\left(\frac{\lambda_2 + y_{10}(\lambda_1 - \lambda_2)}{\lambda_2 + y_{1\delta}(\lambda_1 - \lambda_2)}\right) \tag{22}$$

The corresponding expression for equimolar counter-diffusion is

$$N_1 = \frac{c_t Đ_{12}}{\delta}(y_{10} - y_{1\delta}); \quad \text{equimolar counter - diffusion} \tag{23}$$

The influence of non-equimolar transfer is given by the factor

$$F = \frac{\frac{\lambda_2}{(\lambda_1 - \lambda_2)} \ln\left(\frac{\lambda_2 + y_{10}(\lambda_1 - \lambda_2)}{\lambda_2 + y_{1\delta}(\lambda_1 - \lambda_2)}\right)}{(y_{10} - y_{1\delta})} \tag{24}$$

The total flux N_t is non-zero

$$N_t = N_1 + N_2 = N_1 - \frac{\lambda_1 N_1}{\lambda_2} = -N_1 \frac{\lambda_1 - \lambda_2}{\lambda_2} = \frac{c_t Đ_{12}}{\delta} \ln\left(\frac{\lambda_2 + y_{1\delta}(\lambda_1 - \lambda_2)}{\lambda_2 + y_{10}(\lambda_1 - \lambda_2)}\right) \tag{25}$$

Let us consider the narrow vertical slice of froth on a distillation tray in Figure 3. The liquid phase is the vertical slice will be assumed to be well mixed and have bulk phase composition liquid composition

x_i. The vapor phase is assumed to rise through the liquid in plug flow. The composition of the vapor phase depends on the distance above the tray.

Let v_i represents the molar flow rate of component *i* in the vapor phase, $V = \sum_{i=1}^{n} v_i$ the total vapor flow rate, *a* the interfacial area per unit volume of froth, h_f the froth height, and A_b the active bubbling area. The component material balance for the vapor phase may be written as (See Section 12.1.1 of Taylor and Krishna[4] for more detailed background and derivations)

$$\frac{dv_i}{dh} = -N_i a A_b; \quad i = 1,2,...n \tag{26}$$

Where N_i is the molar flux of species *i* across the vapor liquid interface, directed from the vapor to the liquid phase. For the *n*-component mixture, we may sum equation (26) to give

$$\frac{dV}{dh} = -N_t a A_b \tag{27}$$

The non-zero net-transfer flux N_t will cause an increase or decrease in the molar flow rate of the vapor phase during vapor/liquid contacting in a tray column or packed column. Depending on the direction of net transfer, the vapor flow rate will either increase or decrease. Increase in the vapor flow rate will result in a reduction in the contact time between vapor and liquid phases, causing perhaps a reduction in the Murphree efficiency. Conversely, a decrease in the vapor flow rate will result in an increase in the contact time between vapor and liquid phases, leading perhaps to an increase in the component Murphree efficiency, defined by $E_i = \frac{y_{iE} - y_{iL}}{y_{iE} - y_{i,eq}} = 1 - \frac{y_{iL} - y_{i,eq}}{y_{iE} - y_{i,eq}} = 1 - \frac{\Delta y_{iL}}{\Delta y_{iE}}; \quad i = 1,2,...n$ where y_{iE}, and y_{iL} are, respectively, the vapor phase mole fractions, entering and leaving a tray, and $y_{i,eq}$ is the vapor composition in thermodynamic equilibrium with the liquid leaving the tray; see schematic in Figure 3. For a tray in thermodynamic equilibrium, the component efficiencies are 100% for each component. Mass transfer resistances on either side of the vapor/liquid interface reduce the component efficiencies to values below 100%. For binary distillation, the Murphree component efficiencies are bounded, i.e.

$0 \le E_{1,} = E_2 \le 1$. For multicomponent distillation, with the number of species $n \ge 3$, coupled diffusion effects in either vapor or liquid phases cause the component efficiencies to be distinctly different from one another, $E_1 \ne E_2 \ne E_3$. Phenomena such as osmotic diffusion, diffusion barrier, and uphill diffusion lead to component efficiencies that are unbounded ($E_i \to \pm\infty$), zero ($E_i = 0$), or negative ($E_i < 0$); this has been demonstrated in several experimental studies.[11-19]

Substituting $N_i = J_i + y_i(N_t)$ in equation (26) and writing $v_i = y_i V$ we obtain

$$V\frac{dy_i}{dh} + y_i\frac{dV}{dh} = -J_i a A_b - y_i N_t a A_b; \quad i = 1,2,...n \tag{28}$$

In view of equation (27), the right members of both sides of equation (28) cancel each other and we get

$$V\frac{dy_i}{dh} = -J_i a A_b; \quad i = 1,2,...n \tag{29}$$

Due to non-equimolar transfers, the vapor flow rate V is not constant during the traverse upwards through the froth. Consequently, the set of equations (27) and (29) need to be solved simultaneously in order to determine the composition changes and Murphree point efficiencies.

To illustrate the influence of differences in the molar heats of vaporization on interfacial transfer fluxes we consider a set of three binary mixtures:

Acetic acid/water

2-pentane/ethanol

Water/tri-ethylene glycol

For all three binary mixtures, we assume that the interphase mass transfer process is governed by molecular diffusion in the vapor phase. A well-mixed binary liquid mixture of equimolar composition (x_1=0.5) is brought into contact with a bulk vapor phase of equimolar composition (y_{10}=0.5). The composition of the vapor mixture at the interface, $y_{1\delta}$, is determined from NRTL models describing vapor/liquid equilibrium.

Acetic acid (1)/water (2) mixture

Operating pressure, p = 101.3 kPa, Temperature, T = 374.74 K. Total molar concentration of the vapor mixture c_t = 32.5 mol m^{-3}.

The bulk vapor composition is y_{10}=0.5.

Acetic acid is less volatile, the interface composition, $y_{1\delta}$ = 0.328.

Molar heats of vaporization: λ_1 = 23.5 kJ mol^{-1}; λ_2 = 40.7 kJ mol^{-1}.

Estimated value of mass transfer coefficient in the vapor phase, $k = \frac{\mathcal{D}_{12}}{\delta}$ = 0.0158 m s^{-1}.

The acetic acid transfer flux N_1, calculated from equation (22) is $N_1 = 0.1071$ mol m^{-2} s^{-1}. The acetone flux is positive, i.e. directed from the bulk vapor to the liquid phase because it is the component with the lower volatility.

The total mixture transfer flux N_t, calculated from equation (25) is $N_t = 0.0454$ mol m^{-2} s^{-1}. The total flux is positive, i.e. directed from the bulk vapor to the liquid phase; this implies there will be a reduction in the molar flow rate of the vapor mixture as it traverses the distillation tray or packing. The contact time will be effectively increased due to decreased vapor flow causing an increase in the Murphree efficiency.

The influence of non-equimolar transfer, F, calculated from equation (24) is $F = 1.2137$. Non-equimolar effects cannot be ignored.

2-pentane (1)/ethanol(2) mixture

Operating pressure, p = 101.3 kPa, Temperature, T = 301.4 K. Total molar concentration of the vapor mixture c_t = 40.4 mol m^{-3}.

The bulk vapor composition is y_{10}=0.5.

2-pentane is more volatile, the interface composition, $y_{1\delta}$ = 0.9276.

Molar heats of vaporization: λ_1 = 24.7 kJ mol^{-1}; λ_2 = 38.8 kJ mol^{-1}.

Estimated value of mass transfer coefficient in the vapor phase, $k = \frac{\mathcal{D}_{12}}{\delta}$ = 0.00375 m s^{-1}.

The 2-pentane transfer flux N_1, calculated from equation (22) is $N_1 = -0.0879$ mol m^{-2} s^{-1}. The 2-pentane flux is negative i.e. directed from the interface to the bulk vapor because it is the component with the higher volatility.

The total mixture transfer flux N_t, calculated from equation (25) is $N_t = -0.032$ mol m^{-2} s^{-1}. The total flux is negative, i.e. directed from the interface to the bulk vapor phase; this implies there will be a increase in the molar flow rate of the vapor mixture as it traverses the distillation tray or packing. The contact time will be effectively reduced due to increased vapor flow causing a reduction in the Murphree efficiency.

The influence of non-equimolar transfer, F, calculated from equation (24) is $F = 1.35$. Non-equimolar effects cannot be ignored.

water (1)/tri-ethyleneglycol(2) mixture

Operating pressure, p = 101.3 kPa, Temperature, T = 401.2 K. Total molar concentration of the vapor mixture c_t = 30 mol m^{-3}.

The bulk vapor composition is y_{10}=0.5.

water is more volatile, the interface composition, $y_{1\delta}$ = 0.99907.

Molar heats of vaporization: λ_1 = 40.5 kJ mol^{-1}; λ_2 = 70 kJ mol^{-1}.

Estimated value of mass transfer coefficient in the vapor phase, $k = \frac{\mathcal{D}_{12}}{\delta} = 0.015$ m s^{-1}.

The water transfer flux N_1, calculated from equation (22) is $N_1 = -0.335$ mol m^{-2} s^{-1}. The water flux is negative i.e. directed from the interface to the bulk vapor because it is the component with the higher volatility.

The total mixture transfer flux N_t, calculated from equation (25) is $N_t = -0.141$ mol m^{-2} s^{-1}. The total flux is negative, i.e. directed from the interface to the bulk vapor phase; this implies there will be a increase in the molar flow rate of the vapor mixture as it traverses the distillation tray or packing. The contact time will be effectively reduced due to increased vapor flow causing a reduction in the Murphree efficiency.

The influence of non-equimolar transfer, F, calculated from equation (24) is $F = 1.473$. Non-equimolar effects cannot be ignored.

It is to be noted that for water/TEG mixtures, the liquid phase transfer resistance is significant and the Illustrative Example 12.1.2 of Taylor and Krishna[4] provides a good illustration of how both transfer resistances should be accounted for the calculations of non-equimolar distillation. It is however to be noted that the model calculations in Example 12.1.2 of Taylor and Krishna[4] do not consider the variation of the vapor flow rate V along the height of the distillation froth; in other words, equation (27) was not invoked. For a proper evaluation of non-equimolar effects, we need to account for the alteration in vapor flow as it traverses the distillation tray.

6. The Krishna-Standart solution to the M-S equations for non-equimolar distillation of ternary mixtures

We generalize the analysis in the foregoing section to non-equimolar distillation of n-component mixtures. The Maxwell-Stefan diffusion equations for n-component mixtures are

$$-\frac{dy_i}{dz} = \sum_{\substack{j=1 \\ j\neq i}}^{n} \frac{y_j N_i - y_i N_j}{c_t Đ_{ij}} = \sum_{\substack{j=1 \\ j\neq i}}^{n} \frac{y_j J_i - y_i J_j}{c_t Đ_{ij}}; \quad i = 1,2,\ldots n \tag{30}$$

Only n-1 of the fluxes J_i are independent. The Fick diffusivity matrix $[D]$ is commonly defined by the n-1 dimensional matrix equation

$$(J) = -c_t [D] \frac{d(y)}{dz} \tag{31}$$

For ternary mixtures, the Fick diffusivity matrix $[D]$ can be evaluated explicitly from equation (30)

$$[D] = \begin{bmatrix} \dfrac{x_1}{Đ_{13}} + \dfrac{x_2}{Đ_{12}} + \dfrac{x_3}{Đ_{13}} & -x_1\left(\dfrac{1}{Đ_{12}} - \dfrac{1}{Đ_{13}}\right) \\ -x_2\left(\dfrac{1}{Đ_{12}} - \dfrac{1}{Đ_{23}}\right) & \dfrac{x_2}{Đ_{23}} + \dfrac{x_1}{Đ_{12}} + \dfrac{x_3}{Đ_{23}} \end{bmatrix}^{-1} \tag{32}$$

$$= \frac{\begin{bmatrix} Đ_{13}\left(y_1 Đ_{23} + (1-y_1)Đ_{12}\right) & y_1 Đ_{23}\left(Đ_{13} - Đ_{12}\right) \\ y_2 Đ_{13}\left(Đ_{23} - Đ_{12}\right) & Đ_{23}\left(y_2 Đ_{13} + (1-y_2)Đ_{12}\right) \end{bmatrix}}{y_1 Đ_{23} + y_2 Đ_{13} + y_3 Đ_{12}}$$

For 3-component ideal gas mixtures, the M-S equations reduce to

$$-c_t \frac{dy_1}{dz} = \frac{y_2 N_1 - y_1 N_2}{Đ_{12}} + \frac{(1-y_1-y_2)N_1 - y_1 N_3}{Đ_{13}}$$
$$-c_t \frac{dy_2}{dz} = \frac{y_1 N_2 - y_2 N_1}{Đ_{12}} + \frac{(1-y_1-y_2)N_2 - y_2 N_3}{Đ_{23}} \qquad (33)$$

The bootstrap relation is

$$\lambda_1 N_1 + \lambda_2 N_2 + \lambda_3 N_3 = 0; \quad N_3 = -\frac{\lambda_1 N_1 + \lambda_2 N_2}{\lambda_3} \qquad (34)$$

Therefore, there are only two independent fluxes, and 2 independent driving forces. The molar fluxes N_i in the laboratory-fixed reference are linearly related to the diffusion fluxes J_i with respect to the molar average reference velocity $u = x_1 u_1 + x_2 u_2 + \cdots x_n u_n$ via the 2-dimensional bootstrap matrix $[\beta]$

$$\begin{pmatrix} N_1 \\ N_2 \end{pmatrix} = [\beta] \begin{pmatrix} J_1 \\ J_2 \end{pmatrix}; \quad [\beta] = \begin{bmatrix} 1 - y_1 \dfrac{\lambda_1 - \lambda_3}{\lambda_1 y_1 + \lambda_2 y_2 + \lambda_3 y_3} & y_1 \dfrac{\lambda_2 - \lambda_3}{\lambda_1 y_1 + \lambda_2 y_2 + \lambda_3 y_3} \\ -y_2 \dfrac{\lambda_1 - \lambda_3}{\lambda_1 y_1 + \lambda_2 y_2 + \lambda_3 y_3} & 1 - y_2 \dfrac{\lambda_2 - \lambda_3}{\lambda_1 y_1 + \lambda_2 y_2 + \lambda_3 y_3} \end{bmatrix}$$

Krishna and Standart[8] have developed exact solutions to equation (33) for explicit evaluation of the fluxes for steady-state transfer across a film of thickness δ. The Krishna-Standart method, as applied to non-equimolar distillation is described hereunder.

We define a dimensionless distance: $\eta = \dfrac{z}{\delta}$ and re-write equation (33) as follows

$$\frac{d(y)}{d\eta} = [\Phi](y) + (\phi) \qquad (35)$$

In equation (35) we define a two-dimensional square matrix of dimensionless fluxes

$[\Phi]=\dfrac{\delta}{c_t}\begin{bmatrix}\dfrac{N_2}{Đ_{12}}+\dfrac{N_1}{Đ_{13}}+\dfrac{N_3}{Đ_{13}} & -N_1\left(\dfrac{1}{Đ_{12}}-\dfrac{1}{Đ_{13}}\right)\\ -N_2\left(\dfrac{1}{Đ_{12}}-\dfrac{1}{Đ_{23}}\right) & \dfrac{N_1}{Đ_{12}}+\dfrac{N_2}{Đ_{23}}+\dfrac{N_3}{Đ_{23}}\end{bmatrix}$. We also define a column matrix of dimensionless fluxes $(\phi)=-\dfrac{\delta}{c_t}\begin{pmatrix}\dfrac{N_1}{Đ_{13}}\\ \dfrac{N_2}{Đ_{23}}\end{pmatrix}$. The boundary conditions are $\begin{matrix}\eta=0; & z=0; & (y)=(y_0)\\ \eta=1; & z=\delta; & (y)=(y_\delta)\end{matrix}$.

For steady-state transfer across a film, the matrices $[\Phi]$ and (ϕ) are both η-invariant. Therefore equation (35) represents a system of coupled *ordinary* differential equations with *constant coefficients* $[\Phi]$ and (ϕ).

The system of equations can be solved analytically to obtain the mole fraction profiles within the diffusion layer $(y_\eta - y_0)=-[\exp[\Phi]\eta-[I]][\exp[\Phi]-[I]]^{-1}(y_0-y_\delta)$ where $[I]$ is the identity matrix with Kronecker delta δ_{ik} as elements.

The Sylvester theorem, detailed in Equation (A.5.17) of Taylor and Krishna,[4] is required for explicit calculation of $[\exp[\Phi]\eta-[I]][\exp[\Phi]-[I]]^{-1}$. For the case of distinct eigenvalues, λ_1 and λ_2 of the 2-dimensional square matrix $[\Phi]$, the Sylvester theorem yields

$$[\exp[\Phi]\eta-[I]][\exp[\Phi]-[I]]^{-1}=\left(\frac{\exp(\lambda_1\eta)-1}{\exp(\lambda_1)-1}\right)\frac{[[\Phi]-\lambda_2[I]]}{(\lambda_1-\lambda_2)}+\left(\frac{\exp(\lambda_2\eta)-1}{\exp(\lambda_2)-1}\right)\frac{[[\Phi]-\lambda_1[I]]}{(\lambda_2-\lambda_1)} \qquad (36)$$

The composition gradient at the position $\eta=\dfrac{z}{\delta}$ can be obtained by differentiation of equation (36); we get $\dfrac{d(y_\eta)}{d\eta}=-[\Phi][\exp[\Phi]\eta][\exp[\Phi]-[I]]^{-1}(y_0-y_\delta)$. The steady-state transfer fluxes of components 1, and 2 can be determined from

$\begin{pmatrix} N_1 \\ N_2 \end{pmatrix} = -\frac{c_t}{\delta}[\beta_\eta][D_\eta]\frac{d(y_\eta)}{d\eta} = \frac{c_t}{\delta}[\beta_\eta][D_\eta][\Phi][\exp[\Phi]\eta][\exp[\Phi]-[I]]^{-1}(y_0 - y_\delta)$ where the Fick diffusivity matrix at position η is $[D_\eta] = \frac{\begin{bmatrix} Đ_{13}(y_{1\eta}Đ_{23}+(1-y_{1\eta})Đ_{12}) & y_{1\eta}Đ_{23}(Đ_{13}-Đ_{12}) \\ y_{2\eta}Đ_{13}(Đ_{23}-Đ_{12}) & Đ_{23}(y_{2\eta}Đ_{13}+(1-y_{2\eta})Đ_{12}) \end{bmatrix}}{y_{1\eta}Đ_{23}+y_{2\eta}Đ_{13}+y_{3\eta}Đ_{12}}$. Without loss of generality, we may evaluate $\left[\beta_\eta\right]$ and $\left[D_\eta\right]$ at position $\eta = \frac{z}{\delta} = 0$, and obtain

$$\begin{pmatrix} N_1 \\ N_2 \end{pmatrix} = -\frac{c_t}{\delta}[\beta_{\eta=0}][D_{\eta=0}]\left.\frac{d(y)}{d\eta}\right|_{\eta=0} = \frac{c_t}{\delta}[\beta_{\eta=0}][D_{\eta=0}][\Phi][\exp[\Phi]-[I]]^{-1}(y_0 - y_\delta) \tag{37}$$

The Sylvester theorem, detailed in Equation (A.5.17) of Taylor and Krishna,[4] is required for explicit calculation of $[\Phi][\exp[\Phi]-[I]]^{-1}$. For the case of distinct eigenvalues, λ_1 and λ_2 of the 2-dimensional square matrix $[\Phi]$, the Sylvester theorem yields

$$[\Phi][\exp[\Phi]-[I]]^{-1} = \left(\frac{\lambda_1}{\exp(\lambda_1)-1}\right)\frac{[[\Phi]-\lambda_2[I]]}{(\lambda_1-\lambda_2)} + \left(\frac{\lambda_2}{\exp(\lambda_2)-1}\right)\frac{[[\Phi]-\lambda_1[I]]}{(\lambda_2-\lambda_1)} \tag{38}$$

Though the expression (37) appears to be explicit in the fluxes, it is to be noted that the matrix $[\Phi][\exp[\Phi]-[I]]^{-1}$ is also a function of the fluxes. In the limit of vanishingly small transfer fluxes we have the limiting behavior $[\Phi][\exp[\Phi]-[I]]^{-1} \to [I]$. Equation (37) can be solved using the Given-Find solve block of MathCad 15 using $\begin{pmatrix} N_1 \\ N_2 \end{pmatrix} = \frac{c_t}{\delta}[\beta][D](y_0 - y_\delta)$ as starting guess values for the fluxes; in these guess values, we evaluate the matrices $[\beta]$ and $[D]$ at the arithmetic average vapor compositions $y_{i,av} = \frac{y_{i0}+y_{i\delta}}{2}$.

7. The Krishna-Standart solution to the M-S equations for equimolar distillation of ternary mixtures

When the molar latent heats of vaporization of the three components are close together, we may assume the equimolar distillation prevails, i.e. $N_1 + N_2 + N_3 = 0;\quad N_3 = -(N_1 + N_2)$. The bootstrap matrix $\left[\beta\right]$ degenerates to the identity matrix, and therefore $[\beta] = [I];\ \begin{pmatrix} N_1 \\ N_2 \end{pmatrix} = \begin{pmatrix} J_1 \\ J_2 \end{pmatrix}$. One of the eigenvalues of $[\Phi] = \dfrac{\delta}{c_t}\begin{bmatrix} \dfrac{N_2}{Đ_{12}} + \dfrac{N_1}{Đ_{13}} + \dfrac{N_3}{Đ_{12}} & -N_1\left(\dfrac{1}{Đ_{12}} - \dfrac{1}{Đ_{13}}\right) \\ -N_2\left(\dfrac{1}{Đ_{12}} - \dfrac{1}{Đ_{23}}\right) & \dfrac{N_1}{Đ_{12}} + \dfrac{N_2}{Đ_{23}} + \dfrac{N_3}{Đ_{23}} \end{bmatrix}$ vanishes; see Krishna and Standart[8] for details. Explicitly, the two eigenvalues are $\lambda_1 = \left[N_1\left(\dfrac{1}{Đ_{12}} - \dfrac{1}{Đ_{23}}\right) + N_2\left(\dfrac{1}{Đ_{12}} - \dfrac{1}{Đ_{13}}\right)\right]\dfrac{\delta}{c_t}$ and $\lambda_2 = 0$. The application of Sylvester's theorem for evaluation of $[\Phi][\exp[\Phi] - [I]]^{-1}$ has to be done with care, because $\dfrac{\lambda_2}{\exp(\lambda_2) - 1}$ needs to be evaluated by use of L'Hôpital's rule: $\dfrac{\lambda_2}{\exp(\lambda_2) - 1} \to 1$. So,

$$[\Phi][\exp[\Phi] - [I]]^{-1} = \left(\frac{\lambda_1}{\exp(\lambda_1) - 1}\right)\frac{[\Phi]}{(\lambda_1)} - \frac{[\Phi] - \lambda_1[I]}{(\lambda_1)}$$

The two independent fluxes can be evaluated explicitly

$$\begin{pmatrix} N_1 \\ N_2 \end{pmatrix} = -\frac{c_t}{\delta}[D_{\eta=0}]\frac{d(y)}{d\eta}\bigg|_{\eta=0} = \frac{c_t}{\delta}[D_{\eta=0}][\Phi][\exp[\Phi] - [I]]^{-1}(y_0 - y_\delta) \tag{39}$$

For the determination of the composition profiles, we need to evaluate $[\exp[\Phi]\eta - [I]][\exp[\Phi] - [I]]^{-1}$ by use of L'Hôpital's rule: $\left(\dfrac{\exp(\lambda_2\eta) - 1}{\exp(\lambda_2) - 1}\right) \to \eta$. So

$$[\exp[\Phi]\eta - [I]][\exp[\Phi] - [I]]^{-1} = \left(\frac{\exp(\lambda_1\eta) - 1}{\exp(\lambda_1) - 1}\right)\frac{[\Phi]}{(\lambda_1)} - \eta\frac{[\Phi] - \lambda_1[I]}{(\lambda_1)}$$

Equation (39) can be solved using the Given-Find solve block of MathCad 15 using $\begin{pmatrix} N_1 \\ N_2 \end{pmatrix} = \frac{c_t}{\delta}[D](y_0 - y_\delta)$ as starting guess values for the fluxes; in these guess values, we evaluate $[D]$ at the arithmetic average vapor compositions $y_{i,av} = \frac{y_{i0} + y_{i\delta}}{2}$.

8. The Toor (1957) analytic solutions to the M-S equations for equimolar distillation

Toor[20] has published analytic solutions to the M-S equations describing equimolar diffusion in parametric form:

$$\left[N_1\left(\frac{1}{Đ_{12}} - \frac{1}{Đ_{23}}\right) + N_2\left(\frac{1}{Đ_{12}} - \frac{1}{Đ_{13}}\right)\right]\frac{\delta}{c_t} = \ln\left(\frac{\dfrac{y_{1\delta}}{N_1} - \dfrac{y_{2\delta}}{N_2} - \dfrac{\left(\dfrac{1}{Đ_{13}} - \dfrac{1}{Đ_{23}}\right)}{N_1\left(\dfrac{1}{Đ_{12}} - \dfrac{1}{Đ_{23}}\right) + N_2\left(\dfrac{1}{Đ_{12}} - \dfrac{1}{Đ_{13}}\right)}}{\dfrac{y_{10}}{N_1} - \dfrac{y_{20}}{N_2} - \dfrac{\left(\dfrac{1}{Đ_{13}} - \dfrac{1}{Đ_{23}}\right)}{N_1\left(\dfrac{1}{Đ_{12}} - \dfrac{1}{Đ_{23}}\right) + N_2\left(\dfrac{1}{Đ_{12}} - \dfrac{1}{Đ_{13}}\right)}}\right) \tag{40}$$

$$\left[\frac{N_1}{Đ_{13}}\left(\frac{1}{Đ_{12}} - \frac{1}{Đ_{23}}\right) + \frac{N_2}{Đ_{23}}\left(\frac{1}{Đ_{12}} - \frac{1}{Đ_{13}}\right)\right]\frac{\delta}{c_t} = \left[\left(\frac{1}{Đ_{12}} - \frac{1}{Đ_{23}}\right)(y_{10} - y_{1\delta}) + \left(\frac{1}{Đ_{12}} - \frac{1}{Đ_{13}}\right)(y_{20} - y_{2\delta})\right]$$

The left member of the first of the two Equations (39), $\lambda_1 = \left[N_1\left(\frac{1}{Đ_{12}} - \frac{1}{Đ_{23}}\right) + N_2\left(\frac{1}{Đ_{12}} - \frac{1}{Đ_{13}}\right)\right]\frac{\delta}{c_t}$, is the first non-zero eigenvalue of $[\Phi] = \frac{\delta}{c_t}\begin{bmatrix} \frac{N_2}{Đ_{12}} + \frac{N_1}{Đ_{13}} + \frac{N_3}{Đ_{12}} & -N_1\left(\frac{1}{Đ_{12}} - \frac{1}{Đ_{13}}\right) \\ -N_2\left(\frac{1}{Đ_{12}} - \frac{1}{Đ_{23}}\right) & \frac{N_1}{Đ_{12}} + \frac{N_2}{Đ_{23}} + \frac{N_3}{Đ_{23}} \end{bmatrix}$. The set of two Equations (39) can be solved simultaneously using the Given-Find solve block of MathCad 15; using starting guess values for the two fluxes N_1 and N_2.

9. Non-equimolar distillation of acetic acid (1) – water (2) – methanol (3) mixtures

As illustration of flux calculations for non-equimolar distillation, we consider the ternary mixture acetic acid (1) – water (2) – methanol (3). We assume that the liquid mixture has the composition x_1 = 0.64, x_2 = 0.24, x_3 = 0.12. At a total pressure of 101.3 kPa, the composition of the vapor phase in equilibrium with the liquid mixture is $y_{1\delta}$ = 0.33869, $y_{2\delta}$ = 0.33078, $y_{3\delta}$ = 0.33053; the bubble temperature is 371.25 K. Let us consider vapor phase diffusion across a film of thickness δ = 1 mm. The compositions at the two edges of the film are taken to be $(y_0) = \begin{pmatrix} 0.64 \\ 0.2 \end{pmatrix}$; $(y_\delta) = \begin{pmatrix} 0.3386 \\ 0.33078 \end{pmatrix}$ where we use 2-dimensional column matrices to represent the two independent compositions. The molar heats of vaporization are: λ_1 = 23.5 kJ mol^{-1}; λ_2 = 40.7 kJ mol^{-1}; λ_3 = 35.43 kJ mol^{-1}. The heat of vaporization of acetic acid is significantly lower than that of water and methanol.

The bootstrap matrix evaluated at $(y_0) = \begin{pmatrix} 0.64 \\ 0.2 \end{pmatrix}$ is $[\beta_{\eta=0}] = \begin{bmatrix} 1.26351 & -0.11707 \\ 0.09882 & 0.9561 \end{bmatrix}$.

The values of the vapor phase M-S diffusivities of the three binary pairs are: $Đ_{12} = 2.45$; $Đ_{13} = 1.5$; $Đ_{23} = 3.04 \times 10^{-5}$ m^{2}s^{-1}; these diffusivities are independent of composition.

The Fick diffusivity matrix $[D_{\eta=0}] = \begin{bmatrix} 1.63091 & -0.71169 \\ 0.08216 & 2.59929 \end{bmatrix} \times 10^{-5}$ m^2 s^{-1}. Solving equations (37) yields $\begin{pmatrix} N_1 \\ N_2 \end{pmatrix} = \begin{pmatrix} 0.222 \\ -0.04648 \end{pmatrix}$; $N_3 = -0.09368$ mol m^{-2} s^{-1}.

We re-analyze distillation of the ternary mixture acetic acid (1) – water (2) – methanol (3) imposing the assumption of equimolar counter-diffusion. The bootstrap matrix for equimolar transfers is the identity matrix, $[\beta_{\eta=0}] = \begin{bmatrix} 1 & 0 \\ 0 & 1 \end{bmatrix}$. The Fick diffusivity matrix $[D_{\eta=0}] = \begin{bmatrix} 1.63091 & -0.71169 \\ 0.08216 & 2.59929 \end{bmatrix} \times 10^{-5}$ m^2 s^{-1} has the same values as in the set of calculations in the foregoing paragraph. Solving equations (39) yields $\begin{pmatrix} N_1 \\ N_2 \end{pmatrix} = \begin{pmatrix} 0.18166 \\ -0.06983 \end{pmatrix}$; $N_3 = -0.11184$ mol m^{-2} s^{-1}. Comparing with the corresponding values for

non-equmolar distillation $\begin{pmatrix} N_1 \\ N_2 \end{pmatrix} = \begin{pmatrix} 0.222 \\ -0.04648 \end{pmatrix}$; $N_3 = -0.09368$ mol m^{-2} s^{-1} shows that the proper accounting of differences in molar latent heats leads to a higher flux of the acetic acid (component 1) with the lowest molar heat of vaporization.

The observed influences of non-equimolar transfer are easily rationalized by comparing the constraints $\lambda_1 N_1 + \lambda_2 N_2 + \lambda_3 N_3 = 0$ with that for equimolar transfers $N_1 + N_2 + N_3 = 0$. Forcing the equimolar transfer constraint $N_1 + N_2 + N_3 = 0$ will have the effect of reducing the flux of the component with the lowest molar heat of vaporization; concomitantly the flux of component with the highest molar heat of vaporization will be increased.

Let us perform the flux calculations for equimolar distillation using the Toor analytic solution given by equations (40). Let us use the starting guess values $N_1 = 0.2$ $N_2 = -0.06$ mol m^{-2} s^{-1} that is close to the final solution determined using the Krishna-Standart method in the foregoing section. The solution to equations (40), using the Given-Find solve block of MathCad 15[1] yields $\begin{pmatrix} N_1 \\ N_2 \end{pmatrix} = \begin{pmatrix} 0.18166 \\ -0.06983 \end{pmatrix}$; $N_3 = -0.11184$ mol m^{-2} s^{-1}, that is identical to the Krishna-Standart model for equimolar distillation. The rate of entropy production can be calculated from Equation (13) that reduces to $\sigma = \frac{R}{\delta}\left[N_1 \frac{\Delta y_1}{y_{1,av}} + N_2 \frac{\Delta y_2}{y_{2,av}} + N_3 \frac{\Delta y_3}{y_{3,av}} \right]$ because the molar average mixture velocity $u = 0$; we obtain $\sigma = 1.98$ kJ m^{-3} K^{-1} s^{-1}.

Using a slightly poorer starting guess values $N_1 = 0.2$ $N_2 = -0.018$ mol m^{-2} s^{-1} yields $\begin{pmatrix} N_1 \\ N_2 \end{pmatrix} = \begin{pmatrix} 0.57187 \\ 0.178 \end{pmatrix}$; $N_3 = -0.75617$ mol m^{-2} s^{-1} using the Toor analytic solution given by equations (40). The rate of entropy production can be calculated from $\sigma = \frac{R}{\delta}\left[N_1 \frac{\Delta y_1}{y_{1,av}} + N_2 \frac{\Delta y_2}{y_{2,av}} + N_3 \frac{\Delta y_3}{y_{3,av}} \right]$; we obtain $\sigma = 8.36$ kJ m^{-3} K^{-1} s^{-1}. Invoking the Prigogine principle, we conclude that the physically

realizable solution is the one that produces entropy at the lower rate. Therefore the physically realizable fluxes are $\begin{pmatrix} N_1 \\ N_2 \end{pmatrix} = \begin{pmatrix} 0.18166 \\ -0.06983 \end{pmatrix}$; N_3 = -0.11184 mol m^{-2} s^{-1}.

The Krishna-Standart solution always converges to the solution that corresponds to the minimum rate of entropy production, *irrespective of the starting guess values.*

10. Non-equimolar distillation of 2-pentane (1) – ethanol (2) – water (3) mixtures

We now analyze the influence of non-equimolar transfers for distillation of pentane-2 (1) – ethanol (2) – water (3) mixtures; the analysis is essentially the same as that reported by Krishna.[9] The total pressure of 100 kPa, and the bubble temperature is 346 K. The composition of the vapor phase in equilibrium with the liquid mixture is $y_{1\delta}$ = 0.6, $y_{2\delta}$ = 0.1, $y_{3\delta}$ = 0.3. Let us consider vapor phase diffusion across a film of thickness δ = 0.01 mm. The compositions at the two edges of the film are taken to be $(y_0) = \begin{pmatrix} 0.62 \\ 0.16 \end{pmatrix}$; $(y_\delta) = \begin{pmatrix} 0.6 \\ 0.1 \end{pmatrix}$ where we use 2-dimensional column matrices to represent the two independent compositions. The molar heats of vaporization are: λ_1 = 22.5 kJ mol^{-1}; λ_2 = 40.5 kJ mol^{-1}; λ_3 = 42 kJ mol^{-1}. The heat of vaporization of 2-pentane is significantly lower than that of ethanol and water.

The bootstrap matrix evaluated at $(y_0) = \begin{pmatrix} 0.62 \\ 0.16 \end{pmatrix}$ is $[\beta_{\eta=0}] = \begin{bmatrix} 1.40741 & 0.03134 \\ 0.10516 & 1.00809 \end{bmatrix}$.

The values of the vapor phase M-S diffusivities of the three binary pairs are: $Đ_{12} = 0.727$; $Đ_{13} = 1.44$; $Đ_{23} = 2.09 \times 10^{-5}$ m^{2}s^{-1}; these diffusivities are independent of composition.

The Fick diffusivity matrix $[D_{\eta=0}] = \begin{bmatrix} 1.34257 & 0.54794 \\ 0.18625 & 1.042539 \end{bmatrix} \times 10^{-5}$ m^2 s^{-1}. Solving equations (39) yields $\begin{pmatrix} N_1 \\ N_2 \end{pmatrix} = \begin{pmatrix} 2.99 \\ 2.46 \end{pmatrix}$; N_3 = -3.98 mol m^{-2} s^{-1}.

We re-analyze distillation of the ternary mixture pentane-2 (1) – ethanol (2) – water (3) imposing the assumption of equimolar counter-diffusion. The bootstrap matrix for equimolar transfers is the identity matrix, $\left[\beta_{\eta=0}\right]=\begin{bmatrix}1 & 0\\ 0 & 1\end{bmatrix}$. The Fick diffusivity matrix $\left[D_{\eta=0}\right]=\begin{bmatrix}1.34257 & 0.54794\\ 0.18625 & 1.042539\end{bmatrix}\times 10^{-5}$ $\mathrm{m^2\ s^{-1}}$ has the same values as in the set of calculations in the foregoing paragraph. Solving equations (39) yields $\begin{pmatrix}N_1\\ N_2\end{pmatrix}=\begin{pmatrix}2.09\\ 2.27\end{pmatrix}$; $N_3 = -4.36$ mol $\mathrm{m^{-2}\ s^{-1}}$. Comparing with the corresponding values for non-equmolar distillation $\begin{pmatrix}N_1\\ N_2\end{pmatrix}=\begin{pmatrix}2.99\\ 2.46\end{pmatrix}$; $N_3 = -3.98$ mol $\mathrm{m^{-2}\ s^{-1}}$, shows that the proper accounting of differences in molar latent heats leads to a 30% higher flux of the 2-pentane (component 1) with the lowest molar heat of vaporization.

For azeotropic mixtures, differences in the molar heats of vaporization will have no influence on the transfer fluxes that will be zero because there is no driving force for transfer. To break azeotropes we allow diffusion through an inert gas, as explained below.

11. Multiplicity of solutions for equimolar diffusion in $H_2(1)/N_2(2)/CO_2(3)$ gas mixtures

Consider equimolar counter-diffusion in ternary $H_2(1)/N_2(2)/CO_2(3)$ gas mixtures at 101.3 kPa and 308.35 K. The length of the diffusion path, δ = 1 mm. The compositions at the two ends are

$y_{10} = 0.00000; y_{20} = 0.50086; y_{30} = 0.49914$
$y_{1\delta} = 0.25061; y_{2\delta} = 0.49982; y_{3\delta} = 0.24957$

The driving forces for $H_2(1)$, and $N_2(2)$ are: $\Delta y_1 = -0.25061$; $\Delta y_2 = 0.001035$. The M-S diffusivities for the three binary pairs at T = 308.3 K are $Đ_{12} = 8.33\times 10^{-5}$ $\mathrm{m^2\ s^{-1}}$, $Đ_{13} = 6.8\times 10^{-5}$ $\mathrm{m^2\ s^{-1}}$, $Đ_{23} = 1.68\times 10^{-5}$ $\mathrm{m^2\ s^{-1}}$. The Fick diffusivity matrix is

calculated: $\left[D_{\eta=0}\right]=\begin{bmatrix}7.48894 & 0\\ -2.99443 & 1.68\end{bmatrix}\times 10^{-5}$ m^2 s^{-1}. Solving equations (39) yields

$\begin{pmatrix}N_1\\ N_2\end{pmatrix}=\begin{pmatrix}-0.748\\ 0.328\end{pmatrix}$; $N_3=0.421$ mol m^{-2} s^{-1}.

Let us perform the flux calculations for equimolar counter-diffusion using the Toor analytic solution given by equations (40). Let us use the starting guess values $N_1=-0.7$ $N_2=0.3$ mol m^{-2} s^{-1} that is close to the final solution determined using the Krishna-Standart method in the foregoing section. The solution to equations (40), using the Given-Find solve block of MathCad 15[1] yields $\begin{pmatrix}N_1\\ N_2\end{pmatrix}=\begin{pmatrix}-0.748\\ 0.328\end{pmatrix}$; $N_3=0.421$ mol m^{-2} s^{-1}, that is identical to the Krishna-Standart model. The rate of entropy production can be calculated from Equation (13) that reduces to $\sigma=\frac{R}{\delta}\left[N_1\frac{\Delta y_1}{y_{1,av}}+N_2\frac{\Delta y_2}{y_{2,av}}+N_3\frac{\Delta y_3}{y_{3,av}}\right]$ because the molar average mixture velocity $u=0$; we obtain $\sigma=14.8$ kJ m^{-3} K^{-1} s^{-1}.

Using slightly poorer starting guess values $N_1=-0.7$ $N_2=0.01$ mol m^{-2} s^{-1} yields $\begin{pmatrix}N_1\\ N_2\end{pmatrix}=\begin{pmatrix}0.22\\ -3.89\end{pmatrix}$; $N_3=3.66$ mol m^{-2} s^{-1} using the Toor analytic solution given by equations (40). The rate of entropy production can be calculated from $\sigma=\frac{R}{\delta}\left[N_1\frac{\Delta y_1}{y_{1,av}}+N_2\frac{\Delta y_2}{y_{2,av}}+N_3\frac{\Delta y_3}{y_{3,av}}\right]$; we obtain $\sigma=16.6$ kJ m^{-3} K^{-1} s^{-1}. Invoking the Prigogine principle, we conclude that the physically realizable solution is the one that produces entropy at the lower rate. Therefore the physically realizable fluxes are $\begin{pmatrix}N_1\\ N_2\end{pmatrix}=\begin{pmatrix}-0.748\\ 0.328\end{pmatrix}$; $N_3=0.421$ mol m^{-2} s^{-1}.

The Krishna-Standart solution always converges to the solution that corresponds to the minimum rate of entropy production, *irrespective of the starting guess values.*

12. The Maxwell-Stefan formulation for diffusion distillation

In diffusional distillation, the *n*th component is an inert gas that does not transfer across the vapor/liquid interface into or out of the liquid phase, i.e. $u_n = 0; \quad N_n = 0$. The n-1 non-zero molar fluxes N_i are related to the n-1 independent diffusion fluxes J_i by the bootstrap relation (for further details see Section 7.2 of Taylor and Krishna[4]) $(N) = [\beta](J); \quad \beta_{ik} = \delta_{ik} + \frac{y_i}{y_n}; \quad i,k = 1,2,..n-1$. In view of $u_n = 0; \quad N_n = 0$, Equation (2) can be re-written in terms the n-1 non-vanishing fluxes N_i as

$$-\frac{dy_i}{dz} = \sum_{\substack{j=1 \\ j \neq i}}^{n} \frac{y_j N_i - y_i N_j}{c_t Đ_{ij}}; \quad i = 1,2,\ldots n-1 \tag{41}$$

Equations (41) are applicable also to situations in which there is a temperature gradient along the diffusion path; in this case the molar concentration of the mixture

$$c_t = \frac{p_t}{RT} \tag{42}$$

is to be evaluated at the average temperature in the diffusion layer.

For solving equations (41), it is convenient to re-cast these equations into (n-1) dimensional matrix notation

$$-c_t \frac{d(y)}{dz} = [B](N) \tag{43}$$

where we define a (n-1) × (n-1) dimensional matrix of *inverse* diffusivities $[B]$ whose elements are given by $B_{ii} = \sum_{\substack{k=1 \\ k \neq i}}^{n} \frac{y_k}{Đ_{ik}}; \quad B_{ij(i \neq j)} = -\frac{y_i}{Đ_{ij}}; \quad i,j = 1,2...n-1$. Equations (43) may be re-written in (n-1) dimensional matrix notation to yield an explicit expression for the n-1 non-vanishing fluxes N_i

$(N) = -c_t [D] \frac{d(y)}{dz}$. The ($n$-1) × ($n$-1) dimensional Fick diffusivity matrix [D] is

$$[D]=[B]^{-1};\quad [B]=\begin{bmatrix} \dfrac{y_2}{Đ_{12}}+\dfrac{y_3}{Đ_{13}} & -\dfrac{y_1}{Đ_{12}} \\ -\dfrac{y_2}{Đ_{12}} & \dfrac{y_1}{Đ_{12}}+\dfrac{y_3}{Đ_{23}} \end{bmatrix};\quad \begin{bmatrix} D_{11} & D_{12} \\ D_{21} & D_{22} \end{bmatrix}=\begin{bmatrix} \dfrac{y_2}{Đ_{12}}+\dfrac{y_3}{Đ_{13}} & -\dfrac{y_1}{Đ_{12}} \\ -\dfrac{y_2}{Đ_{12}} & \dfrac{y_1}{Đ_{12}}+\dfrac{y_3}{Đ_{23}} \end{bmatrix}^{-1} \tag{44}$$

The inversion of the matrix [B] can be performed explicitly and the 2 × 2 dimensional matrix [D] are explicitly related to the pair M-S diffusivities $Đ_{12}$, $Đ_{13}$, and $Đ_{23}$

$$[D]=\begin{bmatrix} D_{11} & D_{12} \\ D_{21} & D_{22} \end{bmatrix}=\frac{\begin{bmatrix} \dfrac{y_1}{Đ_{12}}+\dfrac{y_3}{Đ_{23}} & \dfrac{y_1}{Đ_{12}} \\ \dfrac{y_2}{Đ_{12}} & \dfrac{y_2}{Đ_{12}}+\dfrac{y_3}{Đ_{13}} \end{bmatrix}}{\left(\dfrac{y_1y_3}{Đ_{12}Đ_{13}}+\dfrac{y_2y_3}{Đ_{12}Đ_{23}}+\dfrac{y_3y_3}{Đ_{13}Đ_{23}}\right)} \tag{45}$$

Note that the Fick diffusivity matrix is defined in a distinctly different manner to that in equation (31). For diffusion distillation, the matrix [D] equals

$$[D]=\begin{bmatrix} 1+\dfrac{y_1}{y_3} & \dfrac{y_1}{y_3} \\ \dfrac{y_2}{y_3} & 1+\dfrac{y_2}{y_3} \end{bmatrix}\begin{bmatrix} \dfrac{x_1}{Đ_{13}}+\dfrac{x_2}{Đ_{12}}+\dfrac{x_3}{Đ_{13}} & -x_1\left(\dfrac{1}{Đ_{12}}-\dfrac{1}{Đ_{13}}\right) \\ -x_2\left(\dfrac{1}{Đ_{12}}-\dfrac{1}{Đ_{23}}\right) & \dfrac{x_2}{Đ_{23}}+\dfrac{x_1}{Đ_{12}}+\dfrac{x_3}{Đ_{23}} \end{bmatrix}^{-1}.$$

For 3-component ideal gas mixtures, equations (41) reduce to

$$\begin{aligned} -c_t\frac{dy_1}{dz}&=\frac{y_2N_1-y_1N_2}{Đ_{12}}+\frac{y_3N_1}{Đ_{13}};\\ -c_t\frac{dy_2}{dz}&=\frac{y_1N_2-y_2N_1}{Đ_{12}}+\frac{y_3N_2}{Đ_{23}} \end{aligned} \tag{46}$$

Combining equations (68), and (45), we obtain

$$\begin{pmatrix} N_1 \\ N_2 \end{pmatrix}=-c_t[D]\begin{pmatrix} \dfrac{dy_1}{dz} \\ \dfrac{dy_2}{dz} \end{pmatrix}=-c_t\frac{\begin{bmatrix} \dfrac{y_1}{Đ_{12}}+\dfrac{y_3}{Đ_{23}} & \dfrac{y_1}{Đ_{12}} \\ \dfrac{y_2}{Đ_{12}} & \dfrac{y_2}{Đ_{12}}+\dfrac{y_3}{Đ_{13}} \end{bmatrix}}{\left(\dfrac{y_1y_3}{Đ_{12}Đ_{13}}+\dfrac{y_2y_3}{Đ_{12}Đ_{23}}+\dfrac{y_3y_3}{Đ_{13}Đ_{23}}\right)}\begin{pmatrix} \dfrac{dy_1}{dz} \\ \dfrac{dy_2}{dz} \end{pmatrix} \tag{47}$$

13. Krishna-Standart exact analytic solution for diffusion distillation

Krishna and Standart[8] have developed exact solutions to equation (41) for explicit evaluation of the fluxes for steady-state transfer across a film of thickness δ. The Krishna-Standart method, as applied to diffusion distillation is described hereunder.

We define a dimensionless distance: $\eta = \frac{z}{\delta}$, introduce the equality $y_3 = 1 - y_1 - y_2$, and re-write equation (46) as follows

$$\begin{aligned} \frac{dy_1}{d\eta} &= \left(\frac{-y_2 N_1 + y_1 N_2}{Đ_{12}} + \frac{(y_1 + y_2) N_1}{Đ_{13}} - \frac{N_1}{Đ_{13}} \right) \frac{\delta}{c_t}; \\ \frac{dy_2}{d\eta} &= \left(\frac{-y_1 N_2 + y_2 N_1}{Đ_{12}} + \frac{(y_1 + y_2) N_2}{Đ_{23}} - \frac{N_2}{Đ_{23}} \right) \frac{\delta}{c_t} \end{aligned} \tag{48}$$

We define a two-dimensional square matrix of dimensionless fluxes

$$[\Phi] = \frac{\delta}{c_t} \begin{bmatrix} \frac{N_1}{Đ_{13}} + \frac{N_2}{Đ_{12}} & -N_1 \left(\frac{1}{Đ_{12}} - \frac{1}{Đ_{13}} \right) \\ -N_2 \left(\frac{1}{Đ_{12}} - \frac{1}{Đ_{23}} \right) & \frac{N_2}{Đ_{23}} + \frac{N_1}{Đ_{12}} \end{bmatrix} \tag{49}$$

We also define a column matrix of dimensionless fluxes

$$(\phi) = -\frac{\delta}{c_t} \begin{pmatrix} \frac{N_1}{Đ_{13}} \\ \frac{N_2}{Đ_{23}} \end{pmatrix} \tag{50}$$

With definitions (49), and (50), we can re-write equation (48) in 2-dimensional matrix form

$$\frac{d(y)}{d\eta} = [\Phi](y) + (\phi) \tag{51}$$

The boundary conditions are

$$\begin{aligned} &\eta = 0; \quad z = 0; \quad (y) = (y_0) \\ &\eta = 1; \quad z = \delta; \quad (y) = (y_\delta) \end{aligned} \tag{52}$$

For steady-state transfer across a film, the matrices $[\Phi]$ and (ϕ) are both η-invariant. Therefore equation (51) represents a system of coupled *ordinary* differential equations with *constant coefficients* $[\Phi]$ and (ϕ).

The system of equations can be solved analytically to obtain the mole fraction profiles within the diffusion layer $(y_\eta - y_0) = -[\exp[\Phi]\eta - [I]][\exp[\Phi] - [I]]^{-1}(y_0 - y_\delta)$ where $[I]$ is the identity matrix with Kronecker delta δ_{ik} as elements.

The Sylvester theorem, detailed in Equation (A.5.17) of Taylor and Krishna,[4] is required for explicit calculation of $[\exp[\Phi]\eta - [I]][\exp[\Phi] - [I]]^{-1}$. For the case of distinct eigenvalues, λ_1 and λ_2, of the 2-dimensional square matrix $[\Phi]$, the Sylvester theorem yields

$$[\exp[\Phi]\eta - [I]][\exp[\Phi] - [I]]^{-1} = \left(\frac{\exp(\lambda_1\eta)-1}{\exp(\lambda_1)-1}\right)\frac{[[\Phi]-\lambda_2[I]]}{(\lambda_1-\lambda_2)} + \left(\frac{\exp(\lambda_2\eta)-1}{\exp(\lambda_2)-1}\right)\frac{[[\Phi]-\lambda_1[I]]}{(\lambda_2-\lambda_1)}$$

For a ternary gas mixture, the two eigenvalues of $[\Phi]$ can be derived explicitly; these are

$$\lambda_1 = \left(\frac{N_1}{Đ_{13}} + \frac{N_2}{Đ_{23}}\right)\frac{\delta}{c_t};\ \lambda_2 = \left(\frac{N_1+N_2}{Đ_{12}}\right)\frac{\delta}{c_t}.$$

If the two eigenvalues are equal to each other, we need to use the confluent form of the Sylvester's theorem; see equation (29) of Toor.[21]

$$[\exp[\Phi]\eta - [I]][\exp[\Phi] - [I]]^{-1} =$$
$$\left(\frac{\exp(\lambda_1\eta)-1}{\exp(\lambda_1)-1}\right)[I] + \frac{(\exp(\lambda_1)-1)\eta\exp(\lambda_1\eta) - (\exp(\lambda_1\eta)-1)\exp(\lambda_1)}{(\exp(\lambda_1)-1)^2}[[\Phi]-\lambda_1[I]]$$

The composition gradient at the position $\eta = \frac{z}{\delta}$ can be obtained by differentiation; we get

$$\frac{d(y_\eta)}{d\eta} = -[\Phi][\exp[\Phi]\eta][\exp[\Phi] - [I]]^{-1}(y_0 - y_\delta) \tag{53}$$

The steady-state transfer fluxes of components 1, and 2 can be determined by combining equation (47) and (53)

$$\begin{pmatrix} N_1 \\ N_2 \end{pmatrix} = -\frac{c_t}{\delta}\left[D_\eta\right]\frac{d\left(y_\eta\right)}{d\eta} = \frac{c_t}{\delta}\left[D_\eta\right]\left[\Phi\right]\left[\exp\left[\Phi\right]\eta\right]\left[\exp\left[\Phi\right]-\left[I\right]\right]^{-1}\left(y_0 - y_\delta\right) \tag{54}$$

The Fick diffusivity matrix $\left[D_\eta\right]$ is to be evaluated using equation (45) using the compositions corresponding to position $\eta = \frac{z}{\delta}$. Without loss of generality, we may evaluate the Fick diffusivity at position $\eta = \frac{z}{\delta} = 0$, and obtain

$$\begin{pmatrix} N_1 \\ N_2 \end{pmatrix} = -\frac{c_t}{\delta}\left[D_{\eta=0}\right]\left.\frac{d\left(y\right)}{d\eta}\right|_{\eta=0} = \frac{c_t}{\delta}\left[D_{\eta=0}\right]\left[\Phi\right]\left[\exp\left[\Phi\right]-\left[I\right]\right]^{-1}\left(y_0 - y_\delta\right) \tag{55}$$

The Sylvester theorem, detailed in Equation (A.5.17) of Taylor and Krishna,[4] is required for explicit calculation of $\left[\Phi\right]\left[\exp\left[\Phi\right]-\left[I\right]\right]^{-1}$. For the case of distinct eigenvalues, λ_1 and λ_2 of the 2-dimensional square matrix $\left[D\right]$, the Sylvester theorem yields

$$\left[\Phi\right]\left[\exp\left[\Phi\right]-\left[I\right]\right]^{-1} = \left(\frac{\lambda_1}{\exp\left(\lambda_1\right)-1}\right)\frac{\left[\left[\Phi\right]-\lambda_2\left[I\right]\right]}{\left(\lambda_1-\lambda_2\right)} + \left(\frac{\lambda_2}{\exp\left(\lambda_2\right)-1}\right)\frac{\left[\left[\Phi\right]-\lambda_1\left[I\right]\right]}{\left(\lambda_2-\lambda_1\right)} \tag{56}$$

If the two eigenvalues are equal to each other, we need to use the confluent form of the Sylvester's theorem; see equation (29) of Toor.[21]

$$\left[\Phi\right]\left[\exp\left[\Phi\right]-\left[I\right]\right]^{-1} =$$
$$\left(\frac{\lambda_1}{\exp\left(\lambda_1\right)-1}\right)\left[I\right] + \frac{\left(\exp\left(\lambda_1\right)-1\right)-\lambda_1\exp\left(\lambda_1\right)}{\left(\exp\left(\lambda_1\right)-1\right)^2}\left[\left[\Phi\right]-\lambda_1\left[I\right]\right]$$

Though the expression (55) appears to be explicit in the fluxes, it is to be noted that the matrix $\left[\Phi\right]\left[\exp\left[\Phi\right]-\left[I\right]\right]^{-1}$ is also a function of the fluxes. $\left[\Phi\right]\left[\exp\left[\Phi\right]-\left[I\right]\right]^{-1} \to \left[I\right]$. Equation (37) can be solved using the Given-Find solve block of MathCad 15 using $\begin{pmatrix} N_1 \\ N_2 \end{pmatrix} = \frac{c_t}{\delta}\left[D\right]\left(y_0 - y_\delta\right)$ as starting guess values

for the fluxes; in these guess values, we evaluate $[D]$ at the arithmetic average vapor compositions $y_{i,av} = \frac{y_{i0} + y_{i\delta}}{2}$.

14. Gilliland exact analytic solution for diffusion distillation

The earliest example of the use of the Maxwell-Stefan equations to calculate steady-state transfer fluxes in ternary mixtures is provided by Edwin Richard Gilliland, one of the pioneering founding fathers of the chemical engineering profession. Gilliland developed an exact analytic solution to the Maxwell-Stefan equations (41) for the set of boundary conditions

$$\begin{aligned} &z = 0; \quad (y) = (y_0) \\ &z = \delta; \quad (y) = (y_\delta) \end{aligned} \tag{57}$$

The Gilliland solutions are in parametric form:

$$\lambda_1 = \left(\frac{N_1}{Đ_{13}} + \frac{N_2}{Đ_{23}}\right)\frac{\delta}{c_t} = \ln\left(\frac{y_{3\delta}}{y_{30}}\right)$$

$$\lambda_2 = \left(\frac{N_1 + N_2}{Đ_{12}}\right)\frac{\delta}{c_t} = \ln\left(\frac{y_{1\delta}\dfrac{N_1+N_2}{N_1} - \dfrac{\left(\dfrac{1}{Đ_{12}} - \dfrac{1}{Đ_{13}}\right)}{\left(\dfrac{1}{Đ_{12}} - \dfrac{1}{Đ_{23}}\right)}\dfrac{N_1+N_2}{N_2}y_{2\delta} - \dfrac{\left(\dfrac{1}{Đ_{13}} - \dfrac{1}{Đ_{23}}\right)}{\left(\dfrac{1}{Đ_{12}} - \dfrac{1}{Đ_{23}}\right)}}{y_{10}\dfrac{N_1+N_2}{N_1} - \dfrac{\left(\dfrac{1}{Đ_{12}} - \dfrac{1}{Đ_{13}}\right)}{\left(\dfrac{1}{Đ_{12}} - \dfrac{1}{Đ_{23}}\right)}\dfrac{N_1+N_2}{N_2}y_{20} - \dfrac{\left(\dfrac{1}{Đ_{13}} - \dfrac{1}{Đ_{23}}\right)}{\left(\dfrac{1}{Đ_{12}} - \dfrac{1}{Đ_{23}}\right)}}\right) \tag{58}$$

The left members of Equations (58) are the two eigenvalues, λ_1 and λ_2, of $[\Phi] = \frac{\delta}{c_t}\begin{bmatrix} \frac{N_1}{Đ_{13}} + \frac{N_2}{Đ_{12}} & -N_1\left(\frac{1}{Đ_{12}} - \frac{1}{Đ_{13}}\right) \\ -N_2\left(\frac{1}{Đ_{12}} - \frac{1}{Đ_{23}}\right) & \frac{N_2}{Đ_{23}} + \frac{N_1}{Đ_{12}} \end{bmatrix}$. Equations (58) were published in the 1st edition of *Absorption and Extraction*, authored by Thomas Kilgore Sherwood[22], another pioneer in mass transfer and separations. The fluxes N_1, and N_2 may be determined with say the Excel solver, using starting

guess values for N_1, and N_2. All the calculations in this article were performed using the Given-Find solve block of MathCad 15.[1]

Sherwood[22] illustrated the utility of equation (58) by means of an illustrative example for absorption of NH_3 (1) and water vapor (component 2) from a gas phase containing air as an inert gas (component 3) into water. For a chosen set of conditions, three distinct sets of solutions for the fluxes N_1 and N_2 were obtained, depending on the guess values for the fluxes. On the basis of physical arguments, only one of these sets was considered to be physically realizable in practice. Later editions of the classic 1937 book of Sherwood, do not contain the any discussions of Maxwell-Stefan equations, and the Gilliland solutions are omitted. Equations (58) are also available in the paper of Toor.[20]

The use of the Gilliland equations for flux calculations is illustrated by the work of Bröcker and Schulze.[23]

15. The linearized solution for diffusion distillation

For analysis of diffusional distillation we may also use the simplified procedure suggested in earlier work.[24] We evaluate the matrix $[D]$ at the arithmetic average vapor compositions $y_{i,av} = \frac{y_{i0} + y_{i\delta}}{2}$. With this simplification, the fluxes can be evaluated explicitly as follows

$$\begin{pmatrix} N_1 \\ N_2 \end{pmatrix} = \frac{c_t}{\delta}[D_{av}]\begin{pmatrix} y_{10} - y_{1\delta} \\ y_{20} - y_{2\delta} \end{pmatrix} = \frac{c_t}{\delta}\frac{\begin{bmatrix} \frac{y_{1,av}}{Đ_{12}} + \frac{y_{3,av}}{Đ_{23}} & \frac{y_{1,av}}{Đ_{12}} \\ \frac{y_{2,av}}{Đ_{12}} & \frac{y_{2,av}}{Đ_{12}} + \frac{y_{3,av}}{Đ_{13}} \end{bmatrix}}{\left(\frac{y_{1,av}y_{3,av}}{Đ_{12}Đ_{13}} + \frac{y_{2,av}y_{3,av}}{Đ_{12}Đ_{23}} + \frac{y_{3,av}y_{3,av}}{Đ_{13}Đ_{23}} \right)}\begin{pmatrix} y_{10} - y_{1\delta} \\ y_{20} - y_{2\delta} \end{pmatrix} \tag{59}$$

16. Carty-Schrodt experiments for diffusional evaporation of acetone/methanol into air

Before examining diffusional distillation as a separation technique, let us validate the Krishna-Standart model for calculation of composition profiles and fluxes. Towards this end, we simulate the experimental data of Carty and Schrodt[25] for diffusional evaporation of acetone/methanol into air. Their

experiments were carried out in a Stefan tube; see Figure 4. The temperature is 328.5 K, and the total pressure is 99.4 kPa. The length of the diffusion path, $\delta = 0.238$ m. The composition at the liquid/vapor interface is: $y_{10} = 0.319$, $y_{20} = 0.528$, $y_{30} = 0.153$. The bulk vapor compositions at position $z = \delta$ are $y_{1\delta} = 0.0$, $y_{2\delta} = 0.0$, $y_{3\delta} = 1$. The values of the vapor phase M-S diffusivities of the three binary pairs, are provided in Table I of Carty and Schrodt[25]: $Đ_{12} = 8.48$; $Đ_{13} = 13.72$; $Đ_{23} = 19.91 \times 10^{-6}$ $m^2 s^{-1}$; these diffusivities are independent of composition.

The Gilliland Equations (58) yields three different solution sets.

With the starting guesses using equation (59), $\begin{pmatrix} N_1 \\ N_2 \end{pmatrix} = \frac{c_t}{\delta}[D_{av}]\begin{pmatrix} y_{10} - y_{1\delta} \\ y_{20} - y_{2\delta} \end{pmatrix} = \frac{c_t}{\delta} \frac{\begin{bmatrix} \frac{y_{1,av}}{Đ_{12}} + \frac{y_{3,av}}{Đ_{23}} & \frac{y_{1,av}}{Đ_{12}} \\ \frac{y_{2,av}}{Đ_{12}} & \frac{y_{2,av}}{Đ_{12}} + \frac{y_{3,av}}{Đ_{13}} \end{bmatrix}}{\left(\frac{y_{1,av}y_{3,av}}{Đ_{12}Đ_{13}} + \frac{y_{2,av}y_{3,av}}{Đ_{12}Đ_{23}} + \frac{y_{3,av}y_{3,av}}{Đ_{13}Đ_{23}} \right)} \begin{pmatrix} y_{10} - y_{1\delta} \\ y_{20} - y_{2\delta} \end{pmatrix}$, the Gilliland solution set A is obtained $\begin{pmatrix} N_1 \\ N_2 \end{pmatrix} = \begin{pmatrix} 1.783 \\ 3.128 \end{pmatrix} \times 10^{-3}$ mol m^{-2} s^{-1}. This solution set is identical to that obtained using the Krishna-Standart equations (55), using a head-to-tail iteration procedure. The eigenvalues of $[\Phi] = \frac{\delta}{c_t} \begin{bmatrix} \frac{N_1}{Đ_{13}} + \frac{N_2}{Đ_{12}} & -N_1\left(\frac{1}{Đ_{12}} - \frac{1}{Đ_{13}}\right) \\ -N_2\left(\frac{1}{Đ_{12}} - \frac{1}{Đ_{23}}\right) & \frac{N_2}{Đ_{23}} + \frac{N_1}{Đ_{12}} \end{bmatrix}$ are both real and distinct; $\lambda_1 = 1.877$; $\lambda_2 = 3.787$.

Figure 4 presents the experimental data (indicated by symbols) of Carty and Schrodt[25] for the vapor phase composition profiles in Stefan tube for acetone(1)/methanol(2)/air(3). The continuous solid lines are the calculations of the composition profiles $(y_\eta - y_0) = -[\exp[\Phi]\eta - [I]][\exp[\Phi] - [I]]^{-1}(y_0 - y_\delta)$ where $[\Phi] = \frac{\delta}{c_t} \begin{bmatrix} \frac{N_1}{Đ_{13}} + \frac{N_2}{Đ_{12}} & -N_1\left(\frac{1}{Đ_{12}} - \frac{1}{Đ_{13}}\right) \\ -N_2\left(\frac{1}{Đ_{12}} - \frac{1}{Đ_{23}}\right) & \frac{N_2}{Đ_{23}} + \frac{N_1}{Đ_{12}} \end{bmatrix}$ is calculated using the set of fluxes from the Gilliland solution set A. There is good agreement of the calculated profiles with experimental data. It

is also to be noted that the composition profiles in the diffusion layer are not linear. The transfer fluxes calculated using equation (55) yield $\begin{pmatrix} N_1 \\ N_2 \end{pmatrix} = \begin{pmatrix} 1.783 \\ 3.128 \end{pmatrix} \times 10^{-3}$ mol m^{-2} s^{-1}. These values are in good agreement with the experimentally determined fluxes $\begin{pmatrix} N_1 \\ N_2 \end{pmatrix} = \begin{pmatrix} 1.779 \\ 3.121 \end{pmatrix} \times 10^{-3}$ mol m^{-2} s^{-1}, as reported in Table I of Carty and Schrodt.[25]

With the starting guesses $\begin{pmatrix} N_1 \\ N_2 \end{pmatrix} = \begin{pmatrix} 0.65 \\ 0.0001 \end{pmatrix}$ mol m^{-2} s^{-1}, the Gilliland solution set B is obtained: $\begin{pmatrix} N_1 \\ N_2 \end{pmatrix} = \begin{pmatrix} 7.273 \\ -4.838 \end{pmatrix} \times 10^{-3}$ mol m^{-2} s^{-1}; the eigenvalues of $[\Phi] = \frac{\delta}{c_t} \begin{bmatrix} \frac{N_1}{Đ_{13}} + \frac{N_2}{Đ_{12}} & -N_1\left(\frac{1}{Đ_{12}} - \frac{1}{Đ_{13}}\right) \\ -N_2\left(\frac{1}{Đ_{12}} - \frac{1}{Đ_{23}}\right) & \frac{N_2}{Đ_{23}} + \frac{N_1}{Đ_{12}} \end{bmatrix}$ are equal to each other: $\lambda_1 = \lambda_2 = 1.877$. These fluxes are not in agreement with the experimental data of Carty and Schrodt.[25]

With the starting guesses $\begin{pmatrix} N_1 \\ N_2 \end{pmatrix} = \begin{pmatrix} -0.065 \\ 0.07 \end{pmatrix}$ mol m^{-2} s^{-1}, the Gilliland solution set C is obtained: $\begin{pmatrix} N_1 \\ N_2 \end{pmatrix} = \begin{pmatrix} 12.67 \\ -12.67 \end{pmatrix} \times 10^{-3}$ mol m^{-2} s^{-1}; the determinant of $[\Phi] = \frac{\delta}{c_t} \begin{bmatrix} \frac{N_1}{Đ_{13}} + \frac{N_2}{Đ_{12}} & -N_1\left(\frac{1}{Đ_{12}} - \frac{1}{Đ_{13}}\right) \\ -N_2\left(\frac{1}{Đ_{12}} - \frac{1}{Đ_{23}}\right) & \frac{N_2}{Đ_{23}} + \frac{N_1}{Đ_{12}} \end{bmatrix}$ is zero and therefore one of the eigenvalues is zero: $\lambda_1 = 1.877; \quad \lambda_2 = 0$. These fluxes are not in agreement with the experimental data of Carty and Schrodt.[25]

17. Diffusional evaporation of acetone/methanol into Xe

Let us examine the diffusional evaporation of acetone/methanol mixture into inert Xe. The conditions are chosen to be the same as in the Carty and Schrodt[25] experiments.The temperature is 328.5 K, and the total pressure is 99.4 kPa. The length of the diffusion path, δ = 0.238 m. The composition at the

liquid/vapor interface is: $y_{10} = 0.319$, $y_{20} = 0.528$, $y_{30} = 0.153$. The bulk vapor compositions at position $z = \delta$ are $y_{1\delta} = 0.0$, $y_{2\delta} = 0.0$, $y_{3\delta} = 1$. The values of the vapor phase M-S diffusivities of the three binary pairs, estimated using the Fuller-Schettler-Giddings[6] method, are $Đ_{12} = 10.87$; $Đ_{13} = 7.68$; $Đ_{23} = 12.61 \times 10^{-6}$ $m^2 s^{-1}$; these diffusivities are independent of composition.

The Gilliland Equations (58) yields three different solution sets.

With the starting guesses using equation (59), $\begin{pmatrix} N_1 \\ N_2 \end{pmatrix} = \frac{c_t}{\delta}[D_{av}]\begin{pmatrix} y_{10} - y_{1\delta} \\ y_{20} - y_{2\delta} \end{pmatrix} = \frac{c_t}{\delta} \frac{\begin{bmatrix} \frac{y_{1,av}}{Đ_{12}} + \frac{y_{3,av}}{Đ_{23}} & \frac{y_{1,av}}{Đ_{12}} \\ \frac{y_{2,av}}{Đ_{12}} & \frac{y_{2,av}}{Đ_{12}} + \frac{y_{3,av}}{Đ_{13}} \end{bmatrix}}{\left(\frac{y_{1,av}y_{3,av}}{Đ_{12}Đ_{13}} + \frac{y_{2,av}y_{3,av}}{Đ_{12}Đ_{23}} + \frac{y_{3,av}y_{3,av}}{Đ_{13}Đ_{23}} \right)} \begin{pmatrix} y_{10} - y_{1\delta} \\ y_{20} - y_{2\delta} \end{pmatrix}$, the Gilliland solution set A is obtained $\begin{pmatrix} N_1 \\ N_2 \end{pmatrix} = \begin{pmatrix} 0.998 \\ 1.98 \end{pmatrix} \times 10^{-3}$ mol m^{-2} s^{-1}. This solution set is identical to that obtained using the Krishna-Standart equations (55), using a head-to-tail iteration procedure. The eigenvalues of $[\Phi] = \frac{\delta}{c_t}\begin{bmatrix} \frac{N_1}{Đ_{13}} + \frac{N_2}{Đ_{12}} & -N_1\left(\frac{1}{Đ_{12}} - \frac{1}{Đ_{13}}\right) \\ -N_2\left(\frac{1}{Đ_{12}} - \frac{1}{Đ_{23}}\right) & \frac{N_2}{Đ_{23}} + \frac{N_1}{Đ_{12}} \end{bmatrix}$ are both real and distinct; $\lambda_1 = 1.877$; $\lambda_2 = 1.7925$.

The rate of entropy production calculated using equation (18): $\sigma = \frac{R}{\delta}\left[N_1 \frac{\Delta y_1}{y_{1,av}} + N_2 \frac{\Delta y_2}{y_{2,av}} \right]$ yields $\sigma = 0.2082$ J m^{-3} s^{-1} K^{-1}.

With the starting guesses $\begin{pmatrix} N_1 \\ N_2 \end{pmatrix} = \begin{pmatrix} 0.1 \\ 2 \end{pmatrix} \times 10^{-3}$ mol m^{-2} s^{-1}, the Gilliland solution set B is obtained: $\begin{pmatrix} N_1 \\ N_2 \end{pmatrix} = \begin{pmatrix} 0.778 \\ 2.34 \end{pmatrix} \times 10^{-3}$ mol m^{-2} s^{-1}; the eigenvalues of $[\Phi] = \frac{\delta}{c_t}\begin{bmatrix} \frac{N_1}{Đ_{13}} + \frac{N_2}{Đ_{12}} & -N_1\left(\frac{1}{Đ_{12}} - \frac{1}{Đ_{13}}\right) \\ -N_2\left(\frac{1}{Đ_{12}} - \frac{1}{Đ_{23}}\right) & \frac{N_2}{Đ_{23}} + \frac{N_1}{Đ_{12}} \end{bmatrix}$ are equal to each other: $\lambda_1 = \lambda_2 = 1.877$. The rate of entropy production for Gilliland set B, calculated

using equation (18), yields $\sigma = 0.21804$ J m^{-3} K^{-1} s^{-1}. Since the rate of entropy production for Gilliland set A is lower, the Prigogine principle of minimum entropy production indicates that only Gilliland set A fluxes will be realized in practice.

With the starting guesses $\begin{pmatrix} N_1 \\ N_2 \end{pmatrix} = \begin{pmatrix} 1 \\ -2 \end{pmatrix} \times 10^{-3}$ mol m^{-2} s^{-1}, the Gilliland solution set C is obtained: $\begin{pmatrix} N_1 \\ N_2 \end{pmatrix} = \begin{pmatrix} 5.64 \\ -5.64 \end{pmatrix} \times 10^{-3}$ mol m^{-2} s^{-1}; the determinant of $[\Phi] = \frac{\delta}{c_t} \begin{bmatrix} \frac{N_1}{Đ_{13}} + \frac{N_2}{Đ_{12}} & -N_1\left(\frac{1}{Đ_{12}} - \frac{1}{Đ_{13}}\right) \\ -N_2\left(\frac{1}{Đ_{12}} - \frac{1}{Đ_{23}}\right) & \frac{N_2}{Đ_{23}} + \frac{N_1}{Đ_{12}} \end{bmatrix}$ is zero and therefore one of the eigenvalues is zero: $\lambda_1 = 1.877; \quad \lambda_2 = 0$. The rate of entropy production for Gilliland set C, calculated using equation (18), yields $\sigma = 0$. A zero entropy production at steady-state is not a physically acceptable situation, and we conclude that Gilliland set C is not realizable in practice.

18. Absorption of NH_3(1) and H_2O(2) from Air(3) into water

Before examining diffusional distillation as a separation technique, we re-examine the tutorial example included in Sherwood[22] for absorption of NH_3 (1) and water vapor (component 2) from a gas phase containing air as an inert gas (component 3) into water. The total system pressure is 20.265 kPa and temperature is 328.15 K. The effective film thickness for gas phase mass transfer, δ = 1 mm. The bulk vapor composition is: y_{10} = 0.03, y_{20} = 0.0, y_{30} = 0.97. The compositions at the liquid/vapor interface: $z = \delta$ are $y_{1\delta}$ = 0.0, $y_{2\delta}$ = 0.36315, $y_{3\delta}$ = 0.83685. The values of the vapor phase M-S diffusivities of the three binary pairs are: $Đ_{12} = 14.75; \quad Đ_{13} = 10.752; \quad Đ_{23} = 12.45 \times 10^{-5}$ m^{2}s^{-1}; these diffusivities are independent of composition.

The transfer fluxes calculated using equation (55) yield $\begin{pmatrix} N_1 \\ N_2 \end{pmatrix} = \begin{pmatrix} 0.02115 \\ -0.4136 \end{pmatrix}$ mol m^{-2} s^{-1}.

The Gilliland Equations (58) yields three different solution sets.

The Gilliland solution set A is $\begin{pmatrix} N_1 \\ N_2 \end{pmatrix} = \begin{pmatrix} 0.02115 \\ -0.4136 \end{pmatrix}$ mol m^{-2} s^{-1}, that is identical with the Krishna-Standart solution. The eigenvalues of $[\Phi] = \frac{\delta}{c_t} \begin{bmatrix} \frac{N_1}{Đ_{13}} + \frac{N_2}{Đ_{12}} & -N_1\left(\frac{1}{Đ_{12}} - \frac{1}{Đ_{13}}\right) \\ -N_2\left(\frac{1}{Đ_{12}} - \frac{1}{Đ_{23}}\right) & \frac{N_2}{Đ_{23}} + \frac{N_1}{Đ_{12}} \end{bmatrix}$ are both real and distinct; $\lambda_1 = -0.42076; \lambda_2 = -0.35942$.

The rate of entropy production calculated using equation (18): $\sigma = \frac{R}{\delta}\left[N_1 \frac{\Delta y_1}{y_{1,av}} + N_2 \frac{\Delta y_2}{y_{2,av}} \right]$ yields $\sigma = 7.23$ kJ m^{-3} s^{-1} K^{-1}.

With the starting guesses $\begin{pmatrix} N_1 \\ N_2 \end{pmatrix} = \begin{pmatrix} -0.065 \\ -0.07 \end{pmatrix}$, the Gilliland solution set B is obtained: $\begin{pmatrix} N_1 \\ N_2 \end{pmatrix} = \begin{pmatrix} 0.44467 \\ -0.9041 \end{pmatrix}$ mol m^{-2} s^{-1}. The eigenvalues of $[\Phi] = \frac{\delta}{c_t} \begin{bmatrix} \frac{N_1}{Đ_{13}} + \frac{N_2}{Đ_{12}} & -N_1\left(\frac{1}{Đ_{12}} - \frac{1}{Đ_{13}}\right) \\ -N_2\left(\frac{1}{Đ_{12}} - \frac{1}{Đ_{23}}\right) & \frac{N_2}{Đ_{23}} + \frac{N_1}{Đ_{12}} \end{bmatrix}$ are both identical: $\lambda_1 = \lambda_2 = -0.42076$.

The rate of entropy production for Gilliland set B, calculated using equation (18), yields $\sigma = 22.42$ kJ m^{-3} K^{-1} s^{-1}. Since the rate of entropy production for Gilliland set A is lower, the Prigogine principle of minimum entropy production indicates that only Gilliland set A fluxes will be realized in practice.

With the starting guesses $\begin{pmatrix} N_1 \\ N_2 \end{pmatrix} = \begin{pmatrix} -0.065 \\ 0.07 \end{pmatrix}$, the Gilliland solution set C is obtained: $\begin{pmatrix} N_1 \\ N_2 \end{pmatrix} = \begin{pmatrix} 2.46 \\ -2.46 \end{pmatrix}$ mol m^{-2} s^{-1}. The determinant of $[\Phi] = \frac{\delta}{c_t} \begin{bmatrix} \frac{N_1}{Đ_{13}} + \frac{N_2}{Đ_{12}} & -N_1\left(\frac{1}{Đ_{12}} - \frac{1}{Đ_{13}}\right) \\ -N_2\left(\frac{1}{Đ_{12}} - \frac{1}{Đ_{23}}\right) & \frac{N_2}{Đ_{23}} + \frac{N_1}{Đ_{12}} \end{bmatrix}$ is zero and therefore one of the eigenvalues is zero: $\lambda_1 = -0.42076; \quad \lambda_2 = 0$. The rate of entropy

production calculated using equation (18): $\sigma = \frac{R}{\delta}\left[N_1 \frac{\Delta y_1}{y_{1,av}} + N_2 \frac{\Delta y_2}{y_{2,av}} \right]$ yields $\sigma = 0$; a zero rate of entropy production is only possible at thermodynamic equilibrium. Counter-diffusion of cannot be a physically realistic solution and Gilliland set C has to be discounted.

The rate of entropy production for Gilliland set C, calculated using equation (18), yields $\sigma = 0$. A zero entropy production at steady-state is not a physically acceptable situation, and we conclude that Gilliland set C is not realizable in practice.

19. Multiplicity of solutions for acetone/benzene diffusion in inert helium

Modine[26] has reported experimental data that demonstrate strong coupling effects for diffusion of acetone/benzene through stagnant helium. The experiments were carried out in a wetted-wall column. Our objective here is to demonstrate multiplicity of solutions that are possible using the Gillliland analytic solution. For our calculation purposes, we use the data as presented in Example 11.5.3 of Taylor and Krishna.[4] For illustration purposes we use the film model for mass transfer and assume that the mass transfer resistance is restricted to the vapor phase, and the effective film thickness of the gas phase resistance is $\delta = 1$ mm. The temperature is 309.15 K, and the total pressure is 129.81 kPa.

The composition at the liquid/vapor interface is: y_{10} = 0.03603, y_{20} = 0.1248, y_{30} = 0.83917. The bulk vapor compositions at position $z = \delta$ are $y_{1\delta}$ = 0.052354, $y_{2\delta}$ = 0.0, $y_{3\delta}$ = 0.947646. The values of the vapor phase M-S diffusivities of the three binary pairs, are: $Đ_{12} = 2.93$; $Đ_{13} = 31.8$; $Đ_{23} = 29 \times 10^{-6}$ m^{2}s^{-1}; these diffusivities are independent of composition.

The Gilliland Equations (58) yields three different solution sets.

With the starting guesses $\begin{pmatrix} N_1 \\ N_2 \end{pmatrix} = \frac{c_t}{\delta}\begin{pmatrix} Đ_{13}(y_{10} - y_{1\delta}) \\ Đ_{23}(y_{10} - y_{1\delta}) \end{pmatrix} = \begin{pmatrix} -0.02622 \\ 0.18279 \end{pmatrix}$ mol m^{-2} s^{-1}, the Gilliland solution set A is obtained $\begin{pmatrix} N_1 \\ N_2 \end{pmatrix} = \begin{pmatrix} 0.02636 \\ 0.15401 \end{pmatrix}$ mol m^{-2} s^{-1}. It is vital to note that uphill diffusion of acetone is predicted by Gilliland set A. Uphill diffusion of acetone is confirmed in the Modine experiments; see

the analysis by Krishna.[27] This solution set is identical to that obtained using the Krishna-Standart equations (55), using a head-to-tail iteration procedure. The eigenvalues of $[\Phi]=\frac{\delta}{c_t}\begin{bmatrix} \frac{N_1}{Đ_{13}}+\frac{N_2}{Đ_{12}} & -N_1\left(\frac{1}{Đ_{12}}-\frac{1}{Đ_{13}}\right) \\ -N_2\left(\frac{1}{Đ_{12}}-\frac{1}{Đ_{23}}\right) & \frac{N_2}{Đ_{23}}+\frac{N_1}{Đ_{12}} \end{bmatrix}$ are both real and distinct; $\lambda_1 = 0.12157;\ \ \lambda_2 = 1.21892$. The rate of entropy production calculated using equation (18): $\sigma = \frac{R}{\delta}\left[N_1 \frac{\Delta y_1}{y_{1,av}} + N_2 \frac{\Delta y_2}{y_{2,av}} \right]$ yields $\sigma = 2.48$ kJ m^{-3} s^{-1} K^{-1}. The rate of entropy production due to acetone (1) is negative, $\sigma_1 = \frac{R}{\delta}\left[N_1 \frac{\Delta y_1}{y_{1,av}} \right] = -0.08$ kJ m^{-3} s^{-1} K^{-1}. However, there is no violation of the second law of thermodynamics, because the second component benzene (2) produces entropy at a rate $\sigma_3 = \frac{R}{\delta}\left[N_2 \frac{\Delta y_2}{y_{2,av}} \right] = 2.56$ kJ m^{-3} s^{-1} K^{-1} that is high enough to ensure that the total rate of entropy production is positive definite, $\sigma = \sigma_1 + \sigma_2 = 2.48 \geq 0$ kJ m^{-3} s^{-1} K^{-1}.

With the starting guesses $\begin{pmatrix} N_1 \\ N_2 \end{pmatrix} = \begin{pmatrix} -0.02 \\ 0.5 \end{pmatrix}$ mol m^{-2} s^{-1}, the Gilliland solution set B is obtained: $\begin{pmatrix} N_1 \\ N_2 \end{pmatrix} = \begin{pmatrix} -1.81785 \\ 1.83584 \end{pmatrix}$ mol m^{-2} s^{-1}. The eigenvalues of $[\Phi]=\frac{\delta}{c_t}\begin{bmatrix} \frac{N_1}{Đ_{13}}+\frac{N_2}{Đ_{12}} & -N_1\left(\frac{1}{Đ_{12}}-\frac{1}{Đ_{13}}\right) \\ -N_2\left(\frac{1}{Đ_{12}}-\frac{1}{Đ_{23}}\right) & \frac{N_2}{Đ_{23}}+\frac{N_1}{Đ_{12}} \end{bmatrix}$ are equal to each other: $\lambda_1 = \lambda_2 = 0.12157$. The rate of entropy production calculated using equation (18): $\sigma = \frac{R}{\delta}\left[N_1 \frac{\Delta y_1}{y_{1,av}} + N_2 \frac{\Delta y_2}{y_{2,av}} \right]$ yields $\sigma = 36.1$ kJ m^{-3} s^{-1} K^{-1}; this value is significantly higher than that for the Gilliland set A. Consequently, Gilliland set A will be realized in practice, and not the Gilliland set B.

With the starting guesses $\begin{pmatrix} N_1 \\ N_2 \end{pmatrix} = \begin{pmatrix} 0.02 \\ 0.9 \end{pmatrix}$ mol m^{-2} s^{-1}, the Gilliland solution set C is obtained: $\begin{pmatrix} N_1 \\ N_2 \end{pmatrix} = \begin{pmatrix} -2.022 \\ 2.022 \end{pmatrix}$ mol m^{-2} s^{-1}. The determinant of $[\Phi] = \frac{\delta}{c_t}\begin{bmatrix} \frac{N_1}{Đ_{13}} + \frac{N_2}{Đ_{12}} & -N_1\left(\frac{1}{Đ_{12}} - \frac{1}{Đ_{13}}\right) \\ -N_2\left(\frac{1}{Đ_{12}} - \frac{1}{Đ_{23}}\right) & \frac{N_2}{Đ_{23}} + \frac{N_1}{Đ_{12}} \end{bmatrix}$ is zero and therefore one of the eigenvalues is zero: $\lambda_1 = 0.12157; \quad \lambda_2 = 0$. The rate of entropy production for Gilliland set C, calculated using equation (18), yields $\sigma = 0$. A zero entropy production at steady-state is not a physically acceptable situation, and we conclude that Gilliland set C is not realizable in practice.

20. Multiplicity of solutions for 2-propanol/water diffusion in inert CO_2

Consider mass transfer between the liquid and vapor phase for 2-propanol(1)/water(2)/CO_2(3). The mass transfer resistance is assumed to be restricted to the vapor phase, and the effective film thickness of the gas phase resistance is $\delta = 1$ mm.

Assume that the liquid phase is the binary mixture 2-propanol(1)/water(2) at T = 313.15 K. The azeotropic composition at this temperature can be calculated as x_1 = 0.62258, x_2 = 0.37742; the calculations are based on the NRTL parameters provided in Table 2. The ratio of the mole fraction of water to that of propanol in the liquid phase is $\frac{x_2}{x_1} = 0.60624$. Let us bring this liquid phase in contact with an inert gas phase consisting of the CO_2 (= species 3). The vapor pressure of 2-propanol at 313.15 K is 13.6 kPa, and the vapor pressure of water at 313.15 K is 7.36 kPa. The total gas phase pressure p_t =101.3 kPa. The composition of the vapor phase at the gas/liquid interface in equilibrium with the liquid mixture can be calculated from $y_i = \frac{\gamma_i x_i P_i^0}{p_t}$. This yields $y_{1\delta}$ = 0.09836, $y_{2\delta}$ = 0.05963, $y_{3\delta}$ = 0.84201; see Figure 5. The bulk vapor composition is taken to be: y_{10} = 0.0, y_{20} = 0.0, y_{30} = 1.0.

The driving forces are $\Delta y_1 = y_{10} - y_{1\delta} = -0.09836$, and $\Delta y_2 = y_{20} - y_{2\delta} = -0.05963$. Both driving forces are directed from liquid to the vapor phase. The ratio of driving forces $\frac{\Delta y_1}{\Delta y_2} = 1.65$.

The values of the vapor phase M-S diffusivities of the three binary pairs at 313.15 K, calculated using the Fuller-Schettler-Giddings[6] method, are $Đ_{12} = 1.47$; $Đ_{13} = 0.9$; $Đ_{23} = 2.27 \times 10^{-5}$ $m^2 s^{-1}$; these diffusivities are independent of composition.

Firstly, we consider the linearized method for estimation of the transfer fluxes and use equation (59). At the average composition $y_{i,av} = \frac{y_{i0} + y_{i\delta}}{2}$, the Fick matrix of diffusivities calculated using equation (45), yields $[D] = \begin{bmatrix} 0.959668 & 0.073178 \\ 0.044363 & 2.281643 \end{bmatrix} \times 10^{-5}$ m^2 s^{-1}. At steady-state, the transfer fluxes can be estimated as

$$\begin{pmatrix} N_1 \\ N_2 \end{pmatrix} = \frac{101300/(8.314 \times 313.15)}{10^{-3}} \begin{bmatrix} 0.959668 & 0.073178 \\ 0.044363 & 2.281643 \end{bmatrix} \times 10^{-5} \begin{pmatrix} 0 - 0.09836 \\ 0 - 0.005963 \end{pmatrix};$$

this yields $\begin{pmatrix} N_1 \\ N_2 \end{pmatrix} = \begin{pmatrix} -0.0384 \\ -0.0546 \end{pmatrix}$ mol m^{-2} s^{-1}. Both fluxes are directed from liquid to the vapor phase. The ratio of the flux of water to that of 2-propanol is $\frac{N_2}{N_1} = 1.42$. This ratio is significantly higher than the ratio of the compositions in the liquid phase $\frac{x_2}{x_1} = 0.60624$. This implies that the vapor phase gets relatively enriched with water vapor.

The Krishna-Standart exact analytic solution, using equation (55) and (56), following an head-to-tail iterative procedure (this procedure is explained in Example 8.3.1 of Taylor and Krishna[4]) yields $\begin{pmatrix} N_1 \\ N_2 \end{pmatrix} = \begin{pmatrix} -0.0385 \\ -0.0546 \end{pmatrix}$, i.e. $\frac{N_2}{N_1} = 1.416$. The exact solution is very close to the linearized solution. The

eigenvalues of $[\Phi]=\frac{\delta}{c_t}\begin{bmatrix} \frac{N_1}{Đ_{13}}+\frac{N_2}{Đ_{12}} & -N_1\left(\frac{1}{Đ_{12}}-\frac{1}{Đ_{13}}\right) \\ -N_2\left(\frac{1}{Đ_{12}}-\frac{1}{Đ_{23}}\right) & \frac{N_2}{Đ_{23}}+\frac{N_1}{Đ_{12}} \end{bmatrix}$ are both real and distinct; $\lambda_1 = -0.17196; \quad \lambda_2 = -0.16302$.

Depending on the starting guess used in an equation solver, there are three distinct sets of solutions to the Gilliland equations, called Gilliland A, Gilliland B, and Gilliland C. Our solutions are based on the Given-Find solve block of MathCad 15.[1]

The Gilliland A solution set is identical to that obtained using the Krishna-Standart matrix formulation. For the starting guess values, we use the values using the linearized solution: $\begin{pmatrix} N_1 \\ N_2 \end{pmatrix}=\begin{pmatrix} -0.0384 \\ -0.0546 \end{pmatrix}$. With this starting guess values, the equation yields the set of values that correspond precisely with the Krishna-Standart exact analytic solution: $\begin{pmatrix} N_1 \\ N_2 \end{pmatrix}=\begin{pmatrix} -0.0386 \\ -0.0546 \end{pmatrix}$, with $\frac{N_2}{N_1}=1.416$. The eigenvalues of $[\Phi]=\frac{\delta}{c_t}\begin{bmatrix} \frac{N_1}{Đ_{13}}+\frac{N_2}{Đ_{12}} & -N_1\left(\frac{1}{Đ_{12}}-\frac{1}{Đ_{13}}\right) \\ -N_2\left(\frac{1}{Đ_{12}}-\frac{1}{Đ_{23}}\right) & \frac{N_2}{Đ_{23}}+\frac{N_1}{Đ_{12}} \end{bmatrix}$ are both real and distinct; $\lambda_1 = -0.17196; \quad \lambda_2 = -0.16302$. The rate of entropy production calculated using equation (18): $\sigma=\frac{R}{\delta}\left[N_1\frac{\Delta y_1}{y_{1,av}}+N_2\frac{\Delta y_2}{y_{2,av}}\right]$ yields $\sigma = 1.55$ kJ m^{-3} s^{-1} K^{-1}.

If the starting guess values are chosen to be $\begin{pmatrix} N_1 \\ N_2 \end{pmatrix}=\begin{pmatrix} -0.03 \\ -0.05 \end{pmatrix}$, deviating slightly from the Gilliland A solution values, we obtain the Gilliland B solution set: $\begin{pmatrix} N_1 \\ N_2 \end{pmatrix}=\begin{pmatrix} -0.0352 \\ -0.0631 \end{pmatrix}$, yielding a flux ratio $\frac{N_2}{N_1}=1.79$. The eigenvalues of $[\Phi]=\frac{\delta}{c_t}\begin{bmatrix} \frac{N_1}{Đ_{13}}+\frac{N_2}{Đ_{12}} & -N_1\left(\frac{1}{Đ_{12}}-\frac{1}{Đ_{13}}\right) \\ -N_2\left(\frac{1}{Đ_{12}}-\frac{1}{Đ_{23}}\right) & \frac{N_2}{Đ_{23}}+\frac{N_1}{Đ_{12}} \end{bmatrix}$ are:

$\lambda_1 = \lambda_2 = -0.17196$. The rate of entropy production calculated using equation (18): $\sigma = \frac{R}{\delta}\left[N_1 \frac{\Delta y_1}{y_{1,av}} + N_2 \frac{\Delta y_2}{y_{2,av}} \right]$ yields $\sigma = 1.63$ kJ m^{-3} s^{-1} K^{-1}; this value is higher than that for the Gilliland set A. Consequently, Gilliland set A will be realized in practice, and not the Gilliland set B.

If the starting guess values are chosen to be $\begin{pmatrix} N_1 \\ N_2 \end{pmatrix} = \begin{pmatrix} -0.04 \\ 0.05 \end{pmatrix}$, we obtain the Gilliland C solution set: $\begin{pmatrix} N_1 \\ N_2 \end{pmatrix} = \begin{pmatrix} -0.0997 \\ 0.0997 \end{pmatrix}$, yielding a flux ratio $\frac{N_2}{N_1} = -1$. Indeed it is easy to check that $N_1 + N_2 = 0$ is always a solution to the equations (58). For this scenario, the determinant $|\Phi| = 0$ and consequently one of the eigenvalues is zero: $\lambda_1 = -0.17196$; $\lambda_2 = 0$. The rate of entropy production for Gilliland set C, calculated using equation (18), yields $\sigma = 0$. A zero entropy production at steady-state is not a physically acceptable situation, and we conclude that Gilliland set C is not realizable in practice. Counter-diffusion of alcohol and water cannot be a physically realistic solution and Gilliland set C should be discounted as unrealistic.

The existence of multiple Gilliland solutions is not restricted to the choice of CO_2 as inert. To demonstrate this, we performed analogous sets of calculations for helium, nitrogen, air, argon, and xenon. The calculated fluxes with different inert gases are compared in Figure 6. The *x*-axis is the square root of the molecular weight of the inert gas $\sqrt{M_3}$ .The linearized theory is in excellent agreement with the exact Krishna-Standart solution for all of the chosen inert gases. The Gilliland B set of solutions leads to serious error in all cases. With Xe as inert gas the predicted flux ratio for Gilliland B set is $\frac{N_2}{N_1} = 5.33$, compared to the physically correct ratio $\frac{N_2}{N_1} = 1.603$.

The simplest explanation of influence of the choice of the inert gas is as follows. From equation (59), the ratio of the flux of water (2) to that of 2-propanol (component 1) is

$$\frac{N_2}{N_1}=\frac{\frac{y_2}{Đ_{12}}(y_{10}-y_{1\delta})+\left(\frac{y_2}{Đ_{12}}+\frac{y_3}{Đ_{13}}\right)(y_{20}-y_{2\delta})}{\left(\frac{y_1}{Đ_{12}}+\frac{y_3}{Đ_{23}}\right)(y_{10}-y_{1\delta})+\left(\frac{y_1}{Đ_{12}}\right)(y_{20}-y_{2\delta})}$$

The choice of the inert gas influences the relative values of 1-3 friction and 1-2 friction. The friction is inversely proportion to the corresponding M-S diffusivity pairs $Đ_{ij}$. From the FSG equation $Đ_{ij}=\frac{1.43\times10^{-7}T^{1.75}}{p\sqrt{M_{ij}}\left[\left(v_i^{1/3}\right)+\left(v_i^{1/3}\right)\right]^2}$ $\mathrm{m^2s^{-1}}$, the M-S diffusivity $Đ_{ij}$ is inversely proportional to the square root of the mean molar mass of the pairs $\sqrt{M_{ij}}$. We should therefore expect the ratio of fluxes to depend on the square root of the molar mass of the inert gas, $\sqrt{M_3}$.

21. Multiplicity of solutions for ethanol/water diffusion in inert CO_2

Consider mass transfer between the liquid and vapor phase for ethanol(1)/water(2)/CO_2(3). The mass transfer resistance is assumed to be restricted to the vapor phase, and the effective film thickness of the gas phase resistance is $\delta = 1$ mm.

Assume that the liquid phase is the binary mixture ethanol(1)/water(2) at T = 343.15 K. The azeotropic composition at this temperature can be calculated as x_1 = 0.87, x_2 = 0.13; the calculations are based on the NRTL parameters provided in Table 2. Let us bring this liquid phase in contact with an inert gas phase consisting of the CO_2 (= species 3). The vapor pressure of ethanol at 343.15 K is 71.2 kPa, and the vapor pressure of water at 343.15 K is 31.2 kPa. The total gas phase pressure p_t =101.3 kPa. The composition of the vapor phase at the gas/liquid interface in equilibrium with the liquid mixture can be calculated from $y_i=\frac{\gamma_i x_i P_i^0}{p_t}$. This yields $y_{1\delta}$ = 0.6177, $y_{2\delta}$ = 0.09264, $y_{3\delta}$ = 0.2897; see Figure 5. The bulk vapor composition is taken to be: y_{10} = 0.0, y_{20} = 0.0, y_{30} = 1.0.

The driving forces are $\Delta y_1 = y_{10} - y_{1\delta} = -0.6177$, and $\Delta y_2 = y_{20} - y_{2\delta} = -0.09264$. Both driving forces are directed from liquid to the vapor phase. The ratio of driving forces $\frac{\Delta y_1}{\Delta y_2} = 6.67$.

The values of the vapor phase M-S diffusivities of the three binary pairs at 343.15 K, calculated using the Fuller-Schettler-Giddings[6] method, are $Đ_{12} = 2.05$; $Đ_{13} = 1.27$; $Đ_{23} = 2.67 \times 10^{-5}$ $m^2 s^{-1}$; these diffusivities are independent of composition.

Firstly, we consider the linearized method for estimation of the transfer fluxes and use equation (59). At the average composition $y_{i,av} = \frac{y_{i0} + y_{i\delta}}{2}$, the Fick matrix of diffusivities calculated using equation (45), yields $[D] = \begin{bmatrix} 1.922 & 0.7377 \\ 0.1106 & 2.590 \end{bmatrix} \times 10^{-5}$ m^2 s^{-1}. At steady-state, the transfer fluxes can be estimated as

$$\begin{pmatrix} N_1 \\ N_2 \end{pmatrix} = \frac{101300/(8.314 \times 343.15)}{10^{-3}} \begin{bmatrix} 1.922 & 0.7377 \\ 0.1106 & 2.590 \end{bmatrix} \times 10^{-5} \begin{pmatrix} 0 - 0.6177 \\ 0 - 0.09264 \end{pmatrix};$$ this yields

$\begin{pmatrix} N_1 \\ N_2 \end{pmatrix} = \begin{pmatrix} -0.44594 \\ -0.10947 \end{pmatrix}$ mol m^{-2} s^{-1}. Both fluxes are directed from liquid to the vapor phase. The ratio of the flux of water to ethanol is $\frac{N_2}{N_1} = 0.2455$. This ratio is significantly higher than the ratio of the compositions in the liquid phase $\frac{x_2}{x_1} = 0.15$. Diffusional evaporation leads to a relatively higher proportion of water in the vapor phase.

The Krishna-Standart analytic solution, using equation (55) and (56), following an head-to-tail iterative procedure (this procedure is explained in Example 8.3.1 of Taylor and Krishna[4]) yields $\begin{pmatrix} N_1 \\ N_2 \end{pmatrix} = \begin{pmatrix} -0.506 \\ -0.14 \end{pmatrix}$, i.e. $\frac{N_2}{N_1} = 0.225$. The eigenvalues of $[\Phi] = \frac{\delta}{c_t} \begin{bmatrix} \frac{N_1}{Đ_{13}} + \frac{N_2}{Đ_{12}} & -N_1\left(\frac{1}{Đ_{12}} - \frac{1}{Đ_{13}}\right) \\ -N_2\left(\frac{1}{Đ_{12}} - \frac{1}{Đ_{23}}\right) & \frac{N_2}{Đ_{23}} + \frac{N_1}{Đ_{12}} \end{bmatrix}$ are both real and distinct; $\lambda_1 = -1.239$; $\lambda_2 = -0.8514$. The exact solution leads to a flux ratio that is about 10% lower than the value determined from the linearized theory. For accurate modelling of diffusion distillation, it is necessary to employ the exact analytic solution of Krishna and Standart.[8]

Depending on the starting guess used in any equation solver, there are three distinct sets of solutions to the Gilliland equations, called Gilliland A, Gilliland B, and Gilliland C, are obtained. Our solutions are based on the Given-Find solve block of MathCad 15.[1]

The Gilliland A solution set is identical to that obtained using the Krishna-Standart matrix solution. For the starting guess values, we use the values using the linearized solution: $\begin{pmatrix} N_1 \\ N_2 \end{pmatrix} = \begin{pmatrix} -0.44594 \\ -0.10947 \end{pmatrix}$. With this starting guest, the equation yields the set of values that correspond exactly with the Krishna-Standart exact analytic solution: $\begin{pmatrix} N_1 \\ N_2 \end{pmatrix} = \begin{pmatrix} -0.506 \\ -0.114 \end{pmatrix}$, with $\frac{N_2}{N_1} = 0.225$. The eigenvalues of $[\Phi] = \frac{\delta}{c_t} \begin{bmatrix} \frac{N_1}{Đ_{13}} + \frac{N_2}{Đ_{12}} & -N_1\left(\frac{1}{Đ_{12}} - \frac{1}{Đ_{13}}\right) \\ -N_2\left(\frac{1}{Đ_{12}} - \frac{1}{Đ_{23}}\right) & \frac{N_2}{Đ_{23}} + \frac{N_1}{Đ_{12}} \end{bmatrix}$ are both real and distinct; $\lambda_1 = -1.239$; $\lambda_2 = -0.8514$.

The rate of entropy production calculated using equation (18): $\sigma = \frac{R}{\delta}\left[N_1 \frac{\Delta y_1}{y_{1,av}} + N_2 \frac{\Delta y_2}{y_{2,av}} \right]$ yields $\sigma = 10.31$ kJ m^{-3} s^{-1} K^{-1}.

If the starting guess values are chosen to be $\begin{pmatrix} N_1 \\ N_2 \end{pmatrix} = \begin{pmatrix} -0.3 \\ -0.27 \end{pmatrix}$, deviating somewhat from the Gilliland A solution values, we obtain the Gilliland B solution set: $\begin{pmatrix} N_1 \\ N_2 \end{pmatrix} = \begin{pmatrix} -0.2476 \\ -0.6546 \end{pmatrix}$, yielding a flux ratio $\frac{N_2}{N_1} = 2.64$. Remarkably, in this case the flux of water is significantly higher than the flux of ethanol. The eigenvalues of $[\Phi] = \frac{\delta}{c_t} \begin{bmatrix} \frac{N_1}{Đ_{13}} + \frac{N_2}{Đ_{12}} & -N_1\left(\frac{1}{Đ_{12}} - \frac{1}{Đ_{13}}\right) \\ -N_2\left(\frac{1}{Đ_{12}} - \frac{1}{Đ_{23}}\right) & \frac{N_2}{Đ_{23}} + \frac{N_1}{Đ_{12}} \end{bmatrix}$ are equal to each other; $\lambda_1 = \lambda_2 = -1.239$. The rate of entropy production calculated using equation (18):

$\sigma = \frac{R}{\delta}\left[N_1 \frac{\Delta y_1}{y_{1,av}} + N_2 \frac{\Delta y_2}{y_{2,av}} \right]$ yields $\sigma = 15$ kJ m^{-3} s^{-1} K^{-1}; this value is significantly higher than that for the Gilliland set A. Consequently, Gilliland set A will be realized in practice, and not the Gilliland set B.

If the starting guess values are chosen to be $\begin{pmatrix} N_1 \\ N_2 \end{pmatrix} = \begin{pmatrix} -0.3 \\ 0.1 \end{pmatrix}$, we obtain the Gilliland C solution set: $\begin{pmatrix} N_1 \\ N_2 \end{pmatrix} = \begin{pmatrix} -1.073 \\ 1.073 \end{pmatrix}$, yielding a flux ratio $\frac{N_2}{N_1} = -1$. Indeed it is easy to check that $N_1 + N_2 = 0$ is always a solution to the equations (58). The determinant $|\Phi| = 0$ and consequently one of the eigenvalues is zero: $\lambda_1 = -1.239$; $\lambda_2 = 0$. The rate of entropy production for Gilliland set C, calculated using equation (18), yields $\sigma = 0$. A zero entropy production at steady-state is not a physically acceptable situation, and we conclude that Gilliland set C is not realizable in practice. Counter-diffusion of alcohol and water cannot be a physically realistic solution and Gilliland set C should be discounted as unrealistic.

The existence of multiple Gilliland solutions is not restricted to the choice of CO_2 as inert gas. To demonstrate this we performed analogous sets of calculations for helium, nitrogen, air, argon, and xenon. The calculation details for Ar are provided below.

22. Multiplicity of solutions for ethanol/water diffusion into Ar

Consider mass transfer between the liquid and vapor phase for ethanol(1)/water(2)/Ar(3). The mass transfer resistance is assumed to be restricted to the vapor phase, and the effective film thickness of the gas phase resistance is $\delta = 1$ mm.

Assume that the liquid phase is the binary mixture ethanol(1)/water(2) at T = 343.15 K. The azeotropic composition at this temperature can be calculated as $x_1 = 0.87$, $x_2 = 0.13$; the calculations are based on the NRTL parameters provided in Table 2. Let us bring this liquid phase in contact with an inert gas phase consisting of the nitrogen (= species 3). The vapor pressure of ethanol at 343.15 K is

71.2 kPa, and the vapor pressure of water at 343.15 K is 31.2 kPa. The total gas phase pressure p_t =101.3 kPa. The composition of the vapor phase at the gas/liquid interface in equilibrium with the liquid mixture can be calculated from $y_i = \frac{\gamma_i x_i P_i^0}{p_t}$. This yields $y_{1\delta} = 0.6177$, $y_{2\delta} = 0.09264$, $y_{3\delta} = 0.2897$; see Figure 5. The bulk vapor composition is taken to be: $y_{10} = 0.0$, $y_{20} = 0.0$, $y_{30} = 1.0$.

The driving forces are $\Delta y_1 = y_{10} - y_{1\delta} = -0.6177$, and $\Delta y_2 = y_{20} - y_{2\delta} = -0.09264$. Both driving forces are directed from liquid to the vapor phase. The ratio of driving forces $\frac{\Delta y_1}{\Delta y_2} = 6.67$.

The values of the vapor phase M-S diffusivities of the three binary pairs at 343.15 K, calculated using the Fuller-Schettler-Giddings[6] method, are $Đ_{12} = 2.05$; $Đ_{13} = 1.51$; $Đ_{23} = 3.24 \times 10^{-5}$ $m^2 s^{-1}$; these diffusivities are independent of composition.

Firstly, we consider the linearized method for estimation of the transfer fluxes and use equation (59). At the average composition $y_{i,av} = \frac{y_{i0} + y_{i\delta}}{2}$, the Fick matrix of diffusivities calculated using equation (45), yields $[D] = \begin{bmatrix} 2.27 & 0.978 \\ 0.147 & 2.92 \end{bmatrix} \times 10^{-5}$ m^2 s^{-1}. At steady-state, the transfer fluxes can be estimated as $\begin{pmatrix} N_1 \\ N_2 \end{pmatrix} = \frac{101300/(8.314 \times 343.15)}{10^{-3}} \begin{bmatrix} 2.27 & 0.978 \\ 0.147 & 2.92 \end{bmatrix} \times 10^{-5} \begin{pmatrix} 0 - 0.6177 \\ 0 - 0.09264 \end{pmatrix}$; this yields $\begin{pmatrix} N_1 \\ N_2 \end{pmatrix} = \begin{pmatrix} -0.53 \\ -0.128 \end{pmatrix}$ mol m^{-2} s^{-1}. Both fluxes are directed from liquid to the vapor phase. The ratio of the flux of water to ethanol is $\frac{N_2}{N_1} = 0.2423$. This ratio is significantly higher than the ratio of the compositions in the liquid phase $\frac{x_2}{x_1} = 0.15$. Diffusional evaporation leads to a relatively higher proportion of water in the vapor phase.

The Krishna-Standart analytic solution, using equation (55) and (56), following an head-to-tail iterative procedure (this procedure is explained in Example 8.3.1 of Taylor and Krishna[4]) yields

$\begin{pmatrix} N_1 \\ N_2 \end{pmatrix} = \begin{pmatrix} -0.602 \\ -0.132 \end{pmatrix}$, i.e. $\frac{N_2}{N_1} = 0.22$. The eigenvalues of $[\Phi] = \frac{\delta}{c_t}\begin{bmatrix} \frac{N_1}{Đ_{13}} + \frac{N_2}{Đ_{12}} & -N_1\left(\frac{1}{Đ_{12}} - \frac{1}{Đ_{13}}\right) \\ -N_2\left(\frac{1}{Đ_{12}} - \frac{1}{Đ_{23}}\right) & \frac{N_2}{Đ_{23}} + \frac{N_1}{Đ_{12}} \end{bmatrix}$

are both real and distinct; $\lambda_1 = -1.239$; $\lambda_2 = -1.01$. Consequently, this solution is physically realizable. The exact solution leads to a flux ratio that is about 10% lower than the value determined from the linearized theory. For accurate modelling of diffusion distillation, it is necessary to employ the exact analytic solution of Krishna and Standart[8]

Depending on the starting guess used in any equation solver, there are three distinct sets of solutions to the Gilliland equations, called Gilliland A, Gilliland B, and Gilliland C, are obtained. Our solutions are based on the Given-Find solve block of MathCad 15.[1]

The Gilliland A solution set is identical to that obtained using the Krishna-Standart solution. For the starting guess values, we use the values using the linearized solution: $\begin{pmatrix} N_1 \\ N_2 \end{pmatrix} = \begin{pmatrix} -0.53 \\ -0.128 \end{pmatrix}$. With this starting guest, the equation yields the set of values that correspond exactly with the Krishna-Standart exact analytic solution: $\begin{pmatrix} N_1 \\ N_2 \end{pmatrix} = \begin{pmatrix} -0.602 \\ -0.132 \end{pmatrix}$ with $\frac{N_2}{N_1} = 0.22$. The eigenvalues of $[\Phi] = \frac{\delta}{c_t}\begin{bmatrix} \frac{N_1}{Đ_{13}} + \frac{N_2}{Đ_{12}} & -N_1\left(\frac{1}{Đ_{12}} - \frac{1}{Đ_{13}}\right) \\ -N_2\left(\frac{1}{Đ_{12}} - \frac{1}{Đ_{23}}\right) & \frac{N_2}{Đ_{23}} + \frac{N_1}{Đ_{12}} \end{bmatrix}$ are both real and distinct; $\lambda_1 = -1.239$; $\lambda_2 = -1.01$.

The rate of entropy production calculated using equation (18): $\sigma = \frac{R}{\delta}\left[N_1 \frac{\Delta y_1}{y_{1,av}} + N_2 \frac{\Delta y_2}{y_{2,av}} \right]$ yields $\sigma = 12.2$ kJ m^{-3} s^{-1} K^{-1}.

If the starting guess values are chosen to be $\begin{pmatrix} N_1 \\ N_2 \end{pmatrix} = \begin{pmatrix} -0.3 \\ -0.3 \end{pmatrix}$, deviating somewhat from the Gilliland A solution values, we obtain the Gilliland B solution set: $\begin{pmatrix} N_1 \\ N_2 \end{pmatrix} = \begin{pmatrix} -0.4559 \\ -0.4463 \end{pmatrix}$, yielding a flux ratio

$\frac{N_2}{N_1} = 0.979$. The eigenvalues of $[\Phi] = \frac{\delta}{c_t}\begin{bmatrix} \frac{N_1}{Đ_{13}} + \frac{N_2}{Đ_{12}} & -N_1\left(\frac{1}{Đ_{12}} - \frac{1}{Đ_{13}}\right) \\ -N_2\left(\frac{1}{Đ_{12}} - \frac{1}{Đ_{23}}\right) & \frac{N_2}{Đ_{23}} + \frac{N_1}{Đ_{12}} \end{bmatrix}$ are equal to each other; $\lambda_1 = \lambda_2 = -1.239$. The rate of entropy production calculated using equation (18): $\sigma = \frac{R}{\delta}\left[N_1 \frac{\Delta y_1}{y_{1,av}} + N_2 \frac{\Delta y_2}{y_{2,av}}\right]$ yields $\sigma = 15.0$ kJ m^{-3} s^{-1} K^{-1}. This rate of entropy production is higher than for the Gilliland set A; therefore the physically realizable solution corresponds to Gilliland set A.

If the starting guess values are chosen to be $\begin{pmatrix} N_1 \\ N_2 \end{pmatrix} = \begin{pmatrix} -0.3 \\ 0.1 \end{pmatrix}$, we obtain the Gilliland C solution set: $\begin{pmatrix} N_1 \\ N_2 \end{pmatrix} = \begin{pmatrix} -1.24 \\ 1.24 \end{pmatrix}$, yielding a flux ratio $\frac{N_2}{N_1} = -1$. Indeed it is easy to check that $N_1 + N_2 = 0$ is always a solution to the equations (58). The determinant $|\Phi| = 0$ and consequently one of the eigenvalues is zero: $\lambda_1 = -1.239; \quad \lambda_2 = 0$. The rate of entropy production calculated using equation (18): $\sigma = \frac{R}{\delta}\left[N_1 \frac{\Delta y_1}{y_{1,av}} + N_2 \frac{\Delta y_2}{y_{2,av}}\right]$ yields $\sigma = 0$ kJ m^{-3} s^{-1} K^{-1}; a zero rate of entropy production is only possible at thermodynamic equilibrium. Counter-diffusion of alcohol and water cannot be a physically realistic solution and Gilliland set C has to be discounted.

The calculated flux ratios using different inert gases are compared in Figure 7. The *x*-axis is the square root of the molecular weight of the inert gas $\sqrt{M_3}$ .The linearized theory is in reasonable agreement with the exact Krishna-Standart solution for all of the chosen inert gases. The Gilliland B set of solutions leads to serious error in all cases. With Xe as inert gas the predicted flux ratio for Gilliland B set is $\frac{N_2}{N_1} = 14.3$, compared to the physically correct ratio $\frac{N_2}{N_1} = 0.249$.

The simplest explanation of influence of the choice of the inert gas is as follows. From equation (59), the ratio of the flux of water (2) to that of ethanol (component 1) is

$$\frac{N_2}{N_1}=\frac{\frac{y_2}{Đ_{12}}(y_{10}-y_{1\delta})+\left(\frac{y_2}{Đ_{12}}+\frac{y_3}{Đ_{13}}\right)(y_{20}-y_{2\delta})}{\left(\frac{y_1}{Đ_{12}}+\frac{y_3}{Đ_{23}}\right)(y_{10}-y_{1\delta})+\left(\frac{y_1}{Đ_{12}}\right)(y_{20}-y_{2\delta})}$$

The choice of the inert gas influences the relative values of 1-3 friction and 1-2 friction. The friction is inversely proportion to the corresponding M-S diffusivity pairs $Đ_{ij}$. From the FSG equation $Đ_{ij}=\frac{1.43\times10^{-7}T^{1.75}}{p\sqrt{M_{ij}}\left[\left(v_i^{1/3}\right)+\left(v_i^{1/3}\right)\right]^2}$ $\mathrm{m^2s^{-1}}$, the M-S diffusivity $Đ_{ij}$ is inversely proportional to the square root of the mean molar mass of the pairs $\sqrt{M_{ij}}$. We should therefore expect the ratio of fluxes to depend on the square root of the molar mass of the inert gas, $\sqrt{M_3}$.

23. Diffusion distillation with porous barrier: Exact analytic solutions for fluxes

In view of scale-up limitations of using wetted-wall columns, porous barriers are often interposed between the liquid and vapor phases.[28] Figure 8 shows a schematic of vapor/liquid transfer across an inert porous barrier. From the conceptual point of view, the porous barrier is also to be considered as an "inert" fourth component in the quaternary system alcohol(1)/water(2)/inert gas (3)/inert barrier(component m). The quasi-stationary transfer fluxes are obtained by extending the linearized equation (80), to include the friction between the transferring components 1, and 2 and the barrier (m). The porous barriers used are, generally speaking, either meso-porous or macro-porous.

In recent works, a different approach to the description of diffusion in porous materials has been developed, using the Maxwell-Stefan approach,[29-34] employing chemical potential gradients as driving forces:

$$-\rho V_p\frac{c_i}{RT}\frac{d\mu_i}{dz}=\sum_{\substack{j=1\\ j\neq i}}^{n}\left(\frac{y_jN_i-y_iN_j}{Đ_{ij}}\right)+\frac{N_i}{Đ_i};\quad i=1,2...n \tag{60}$$

The fluxes N_i are defined as the moles transported per m^2 of total external surface area of the porous material

$$N_i \equiv \varepsilon \frac{p_i}{RT} u_i; \quad i = 1,2...n \tag{61}$$

The species velocities u_i are defined in a reference framework with respect to the pore walls. The porosity ε appears on the left member of equation (61) because only a fraction ε of the external surface is available for influx of guest molecules.

In equation (60), c_i is the molar concentration of species *i* based on the accessible pore volume, V_p (= m^3 pore volume per kg framework), and ρ is the material framework density. The quantity ρV_p is the fractional pore volume

$$\rho V_p = \left(\frac{\text{kg framework}}{\text{m}^3 \text{ framework}}\right)\left(\frac{\text{m}^3 \text{ pore volume}}{\text{kg framework}}\right) = \left(\frac{\text{m}^3 \text{ pore volume}}{\text{m}^3 \text{ framework}}\right) = \varepsilon \tag{62}$$

Equation (60) applies to microporous, mesoporous, and macroporous materials. For mesoporous, and macroporous materials with the fluid phase in the gaseous state, $c_i = \frac{p_i}{RT}; \quad \frac{d\mu_i}{dz} = \frac{RT}{p_i}\frac{dp_i}{dz}$, the left hand side of equation (60) simplifies to yield

$$-\varepsilon \frac{1}{RT}\frac{dp_i}{dz} = \sum_{\substack{j=1 \\ j\neq i}}^{n}\left(\frac{y_j N_i - y_i N_j}{Đ_{ij}}\right) + \frac{N_i}{Đ_i}; \quad i = 1,2...n \tag{63}$$

For pores with tortuosity τ, equation (63) may be modified as follows

$$-\frac{1}{RT}\frac{dp_i}{dz} = \sum_{\substack{j=1 \\ j\neq i}}^{n}\left(\frac{y_j N_i - y_i N_j}{(\varepsilon/\tau)Đ_{ij}}\right) + \frac{N_i}{(\varepsilon/\tau)Đ_i}; \quad i = 1,2...n \tag{64}$$

Equation (64) is comparable, but not equivalent with the corresponding Dusty-Gas Model (DGM)[35]

$$-\frac{p_t}{RT}\frac{dx_i}{dz} - \left(\frac{y_i}{RT}\right)\left(\frac{B_0 p_t}{\eta D_{i,Kn}} + 1\right)\frac{dp_t}{dz} = \sum_{\substack{j=1 \\ j\neq i}}^{n}\left(\frac{y_j N_i - y_i N_j}{(\varepsilon/\tau)Đ_{ij}}\right) + \frac{N_i}{(\varepsilon/\tau)D_{i,Kn}}; \quad i = 1,2...n \tag{65}$$

where the Knudsen diffusivity values are used to quantify the friction with the pore walls, with pore diameter, d_p, of the barrier

$$D_{i,Kn} = \frac{d_p}{3}\sqrt{\frac{8RT}{\pi M_i}} \tag{66}$$

In the M-S formulation (64), the M-S diffusivity $Đ_i$ describes the interaction between species *i* and the pore wall. The Maxwell-Stefan diffusion formulation is essentially a "friction formulation"; the M-S diffusivity $Đ_i$, is to be interpreted as an inverse drag coefficient between the guest molecule and the surface of the framework material; this diffusivity reflects both the Knudsen and surface diffusion characteristics. In other words, the surface diffusion is not separately accounted for. Furthermore, any viscous flow contribution is also subsumed into the M-S diffusivities $Đ_i$, and $Đ_{ij}$. Comparing equation (64) with the DGM equation (65) we may derive; see Krishna and Wesselingh[36]

$$Đ_i = D_{i,Kn}\left(1 + \frac{B_0 p_t}{\eta}\sum_{j=1}^{n}\frac{y_j}{D_{j,Kn}}\right); \quad i = 1,2...n \tag{67}$$

In all the flux calculations for diffusion distillation, we calculate the fluxes based on the surface area of the pores, and consequently we take $\varepsilon = 1$. For the purposes of our analysis of diffusion distillation with porous barriers, we also ignore the viscous flow contributions, and take the tortuosity $\tau = 1$. Consequently our analysis is based on the assumption that $(\varepsilon/\tau) = 1$.

For diffusion at constant total pressure, Equations (65) may be re-written in (*n*-1) dimensional matrix notation to yield an explicit expression for the *n*-1 non-vanishing fluxes N_i

$$(N) = -c_t[D]\frac{d(y)}{dz} \tag{68}$$

The Fick diffusivity matrix [*D*] can be evaluated explicitly from

$$[D]=[B]^{-1};\quad [B]=\begin{bmatrix} \dfrac{y_2}{Đ_{12}}+\dfrac{y_3}{Đ_{13}}+\dfrac{1}{D_{1,Kn}} & -\dfrac{y_1}{Đ_{12}} \\ -\dfrac{y_2}{Đ_{12}} & \dfrac{y_1}{Đ_{12}}+\dfrac{y_3}{Đ_{23}}+\dfrac{1}{D_{2,Kn}} \end{bmatrix} \tag{69}$$

For steady-state diffusion across a porous barrier of thickness δ, equations (65) can be solved analytically for the set of boundary conditions are $\begin{matrix}\eta=0;\quad z=0;\quad (y)=(y_0)\\ \eta=1;\quad z=\delta;\quad (y)=(y_\delta)\end{matrix}$ following the procedure described by Krishna.[37]

We re-write equations (65) in n-1 dimensional matrix notation

$$\frac{d(y)}{d\eta}=[\Phi](y)+(\phi) \tag{70}$$

with $[\Phi]=\dfrac{\delta}{c_t}\begin{bmatrix} \dfrac{N_1}{D_{1,Kn}}+\dfrac{N_1}{Đ_{13}}+\dfrac{N_2}{Đ_{12}} & -N_1\left(\dfrac{1}{Đ_{12}}-\dfrac{1}{Đ_{13}}\right) \\ -N_2\left(\dfrac{1}{Đ_{12}}-\dfrac{1}{Đ_{23}}\right) & \dfrac{N_2}{D_{2,Kn}}+\dfrac{N_2}{Đ_{23}}+\dfrac{N_1}{Đ_{12}} \end{bmatrix}$ and $(\phi)=-\dfrac{\delta}{c_t}\begin{pmatrix} \dfrac{N_1}{Đ_{13}}+\dfrac{N_1}{D_{1,kn}} \\ \dfrac{N_2}{Đ_{23}}+\dfrac{N_2}{D_{2,kn}} \end{pmatrix}$

The system of equations (70) can be solved analytically to obtain the mole fraction profiles within the diffusion layer $(y_\eta-y_0)=-[\exp[\Phi]\eta-[I]][\exp[\Phi]-[I]]^{-1}(y_0-y_\delta)$ where $[I]$ is the identity matrix with Kronecker delta δ_{ik} as elements. The Sylvester theorem, detailed in Equation (A.5.17) of Taylor and Krishna,[4] is required for explicit calculation of $[\exp[\Phi]\eta-[I]][\exp[\Phi]-[I]]^{-1}$. For the case of distinct eigenvalues, λ_1 and λ_2 of the 2-dimensional square matrix $[\Phi]$, the Sylvester theorem yields

$$[\exp[\Phi]\eta-[I]][\exp[\Phi]-[I]]^{-1}=\left(\frac{\exp(\lambda_1\eta)-1}{\exp(\lambda_1)-1}\right)\frac{[[\Phi]-\lambda_2[I]]}{(\lambda_1-\lambda_2)}+\left(\frac{\exp(\lambda_2\eta)-1}{\exp(\lambda_2)-1}\right)\frac{[[\Phi]-\lambda_1[I]]}{(\lambda_2-\lambda_1)}$$

The fluxes can be calculated from

$$\begin{pmatrix} N_1 \\ N_2 \end{pmatrix}=-\frac{c_t}{\delta}[D_{\eta=0}]\left.\frac{d(y)}{d\eta}\right|_{\eta=0}=\frac{c_t}{\delta}[D_{\eta=0}][\Phi][\exp[\Phi]-[I]]^{-1}(y_0-y_\delta) \tag{71}$$

Equation (71) can be solved using the Given-Find solve block of MathCad 15 with starting guess values for the fluxes $\begin{pmatrix} N_1 \\ N_2 \end{pmatrix} = \frac{c_t}{\delta}[D](y_0 - y_\delta)$ where $[D]$ is evaluated at the arithmetic average vapor compositions $y_{i,av} = \frac{y_{i0} + y_{i\delta}}{2}$.

We consider the separation of liquid phase binary mixture 2-propanol(1)/water(2) at T = 313.15 K. The azeotropic composition at this temperature can be calculated as x_1 = 0.62258, x_2 = 0.37742; the calculations are based on the NRTL parameters provided in Table 2. Let us bring this liquid phase in contact with an inert gas phase consisting of the CO_2 (= species 3) inside a pore of diameter d_p = 1 μm. The vapor pressure of 2-propanol at 313.15 K is 13.6 kPa, and the vapor pressure of water at 313.15 K is 7.36 kPa. The total gas phase pressure p_t =101.3 kPa. The composition of the vapor phase at the gas/liquid interface in equilibrium with the liquid mixture can be calculated from $y_i = \frac{\gamma_i x_i P_i^0}{p_t}$. This yields $y_{1\delta}$ = 0.09836, $y_{2\delta}$ = 0.05963, $y_{3\delta}$ = 0.84201; see Figure 5. The bulk vapor composition is taken to be: y_{10} = 0.0, y_{20} = 0.0, y_{30} = 1.0. The solution to Equation (71) yields $\begin{pmatrix} N_1 \\ N_2 \end{pmatrix} = \begin{pmatrix} -0.03547 \\ -0.04912 \end{pmatrix}$ mol m^{-2} s^{-1}, with $\frac{N_2}{N_1}$ = 1.385.

24. Diffusion distillation with porous barrier: Linearized solutions for flux calculations

Following the linearized model described in earlier works,[29, 38] we write for a barrier (membrane) with pore diameter, d_p, in which we evaluate the matrix $[D]$ at the arithmetic average vapor compositions $y_i = \frac{y_{i0} + y_{i\delta}}{2}$.

$$\begin{pmatrix} N_1 \\ N_2 \end{pmatrix} = \frac{c_t}{\delta} \begin{bmatrix} \frac{y_2}{Đ_{12}} + \frac{y_3}{Đ_{13}} + \frac{1}{D_{1,Kn}} & -\frac{y_1}{Đ_{12}} \\ -\frac{y_2}{Đ_{12}} & \frac{y_1}{Đ_{12}} + \frac{y_3}{Đ_{23}} + \frac{1}{D_{2,Kn}} \end{bmatrix}^{-1} \begin{pmatrix} y_{10} - y_{1\delta} \\ y_{20} - y_{2\delta} \end{pmatrix} \quad (72)$$

The matrix inversion in equation (72) can be performed explicitly to yield

$$\begin{pmatrix} N_1 \\ N_2 \end{pmatrix} = \frac{c_t}{\delta} \frac{\begin{bmatrix} \frac{y_1}{Đ_{12}} + \frac{y_3}{Đ_{23}} + \frac{1}{D_{2,Kn}} & \frac{y_1}{Đ_{12}} \\ \frac{y_2}{Đ_{12}} & \frac{y_2}{Đ_{12}} + \frac{y_3}{Đ_{13}} + \frac{1}{D_{1,Kn}} \end{bmatrix}}{\left(\frac{y_1}{Đ_{12}} \left(\frac{y_3}{Đ_{13}} + \frac{1}{D_{1,Kn}} \right) + \frac{y_2}{Đ_{12}} \left(\frac{y_3}{Đ_{23}} + \frac{1}{D_{2,Kn}} \right) + \left(\frac{y_3}{Đ_{13}} + \frac{1}{D_{1,Kn}} \right) \left(\frac{y_3}{Đ_{23}} + \frac{1}{D_{2,Kn}} \right) \right)} \begin{pmatrix} y_{10} - y_{1\delta} \\ y_{20} - y_{2\delta} \end{pmatrix} \quad (73)$$

The ratio of the flux of water to that of alcohol is

$$\frac{N_2}{N_1} = \frac{\frac{y_2}{Đ_{12}} (y_{10} - y_{1\delta}) + \left(\frac{y_2}{Đ_{12}} + \frac{y_3}{Đ_{13}} + \frac{1}{D_{1,Kn}} \right) (y_{20} - y_{2\delta})}{\left(\frac{y_1}{Đ_{12}} + \frac{y_3}{Đ_{23}} + \frac{1}{D_{2,Kn}} \right) (y_{10} - y_{1\delta}) + \left(\frac{y_1}{Đ_{12}} \right) (y_{20} - y_{2\delta})} \quad (74)$$

For the separation of liquid phase binary mixture 2-propanol(1)/water(2) at T = 313.15 K, under the same set of conditions as in the foregoing section, the fluxes are calculated to be yields $\begin{pmatrix} N_1 \\ N_2 \end{pmatrix} = \begin{pmatrix} -0.0352 \\ -0.04897 \end{pmatrix}$ mol m^{-2} s^{-1}, with $\frac{N_2}{N_1}$ = 1.39. The ratio of fluxes is within 1% of the value calculated using the exact analytic solution. Therefore, all porous barrier calculations reported below are obtained using the linearized solution.

Figure 9a presents calculations of the ratio of quasi-stationary fluxes $\frac{N_2}{N_1}$ for 2-propanol (1)/water (2)/inert gas (3), plotted as a function of pore diameter, d_p, of the barrier interposed between the vapor and liquid phases. For each of the five inert gases investigated, increase in the pore diameter improves the separation performance. Introduction of the porous barrier decreases the efficacy of separation. The results in Figure 9a also lead to the conclusion that separations are most effective in the "bulk" diffusion regime, as compared to the "Knudsen" regime.

In order to emphasize this point further, Figure 9b compares the ratio of quasi-stationary fluxes $\frac{N_2}{N_1}$ for 2-propanol (1)/water (2)/CO_2 (3) for the two scenarios, with and without inclusion of the porous

barrier. The separations without a porous barrier provides the upper limit for the separation. Precisely analogous conclusion can be drawn for ethanol (1)/water (2)/CO_2 (3) system; see the results in Figure 10.

25. Diffusional evaporation of acetone/methanol into inert gas

Diffusion distillation also applies to non-aqueous mixtures such as acetone/methanol. For quantitative demonstration of this separation, let us consider operation at a total pressure of 101.3 kPa and temperature of 323.15 K. The liquid composition is x_1 = 0.8025, x_2 = 0.19744; this composition corresponds to that of the azeotrope at 323.15 K, calculated using the NRTL parameters provided in Table 4.

We bring this liquid mixture into contact with gas phase containing pure CO_2 (component 3), interposing a porous barrier between the vapor and liquid phases.

The composition of the vapour phase in equilibrium with the binary liquid mixture is $y_{1\delta}$ = 0.66112, $y_{2\delta}$ = 0.16265, $y_{3\delta}$ = 0.17623. The ratio of the compositions of methanol (2) to that of acetone (1) at equilibrium, $\frac{y_{2\delta}}{y_{1\delta}}$ is that same as that of the ratio of water to ethanol in the liquid phase, $\frac{y_{2\delta}}{y_{1\delta}} = \frac{x_2}{x_1} = 0.246$.

Figure 11 presents calculations of the quasi-stationary fluxes $\frac{N_2}{N_1}$ for acetone (1)/methanol (2)/CO_2 (3) for two scenarios: with and without inclusion of the porous barrier. We note that the best separations are achieved by choosing smaller pore sizes and operating in the Knudsen regime. However, it is noteworthy that the maximum ratio of $\frac{N_2}{N_1} \approx 0.33$ achieved in diffusion distillation is only slightly higher than the ratio of azeotropic compositions, $\frac{y_{2\delta}}{y_{1\delta}} = \frac{x_2}{x_1} = 0.246$. In other words, diffusion distillation is unlikely to be a useful strategy that can be exploited in practice.

26. Transient diffusional evaporation of 2-propanol/water/inert mixture

A different method of illustrating the principle of diffusion distillation is to consider transient diffusion into a vapor "slab" of half-thickness δ (= 1 mm); see schematic in Figure **12**. The vapor slab is considered to be of "infinite" length in the vertical direction and the diffusion is limited to the transverse (z) direction.

At time t = 0, the bulk vapor phase consists of pure nitrogen: y_{10} = 0.0, y_{20} = 0.0, y_{30} = 1.0. At time t = 0, either side of the vapor slab is in contact with a binary liquid mixture of constant composition and maintained at 313.15 K. The liquid composition corresponds to the azeotrope: x_1 = 0.62258, x_2 = 0.37742. The vapor pressure of 2-propanol at 313.15 K is 13.6 kPa, and the vapor pressure of water at 341.15 K is 7.36 kPa. The total gas phase pressure p_t =101.3 kPa. The composition of the vapor phase at the gas/liquid interface in equilibrium with the liquid mixture can be calculated from $y_i = \dfrac{\gamma_i x_i P_i^0}{p_t}$. This yields $y_{1\delta}$ = 0.09836, $y_{2\delta}$ = 0.05963, $y_{3\delta}$ = 0.84201.

For a binary vapor mixture, the fractional *departure* from equilibrium is given by the matrix equation

$$\bar{y}(t) - y_{z=\delta} = Q\left(y_0 - y_{z=\delta}\right); \quad Q \equiv \sum_{m=0}^{\infty} \frac{8}{(2m+1)^2 \pi^2} \exp\left[-(2m+1)^2 \pi^2 \frac{Dt}{4\delta^2}\right] \tag{75}$$

This expression can be generalized for ternary vapor mixtures by using two-dimensional matrix notation by replacing the binary mixture diffusivity D by the Fick diffusivity matrix $[D]$; the justification for this procedure is provided in earlier works. [4, 24]

The expression for fractional *departure* from equilibrium for ternary vapor mixtures (inert species 3) is

$$\left(\bar{y}(t) - y_{z=\delta}\right) = [Q]\left(y_0 - y_{z=\delta}\right); \quad [Q] \equiv \sum_{m=0}^{\infty} \frac{8}{(2m+1)^2 \pi^2} \exp\left[-(2m+1)^2 \pi^2 \frac{[D]t}{4\delta^2}\right] \tag{76}$$

The Sylvester theorem, detailed in Appendix A of Taylor and Krishna,[4] is required for explicit calculation of $[Q]$. For the case of distinct eigenvalues, λ_1 and λ_2 of the 2-dimensional square matrix $[D]$, the Sylvester theorem yields

$$[Q] = \frac{f(\lambda_1)[[D]-\lambda_2[I]]}{(\lambda_1-\lambda_2)} + \frac{f(\lambda_2)[[D]-\lambda_1[I]]}{(\lambda_2-\lambda_1)} \tag{77}$$

In equation (77), $[I]$ is the identity matrix with elements δ_{ik}. The functions $f(\lambda_i)$ are obtained by substituting the eigenvalues λ_1 and λ_2 in place of the binary diffusivity in equation (75):

$$f(\lambda_i) = \sum_{m=0}^{\infty} \frac{8}{(2m+1)^2\pi^2} \exp\left[-(2m+1)^2\pi^2 \frac{\lambda_i t}{4\delta^2}\right] \tag{78}$$

The calculations can be easily implemented in MathCad 15.[1]

In Figure 13a, the spatial-averaged mole fractions $\left(\overline{y}(t)\right)$ of 2-propanol (1) and water (2) are plotted as a function of time, *t*. The ratio of the mole fraction of water (2) to that of 2-propanol (1) in the vapor phase as a function of time, *t* is plotted in Figure 13b; this ratio equilibrates to the value of $\frac{y_2}{y_1} = \frac{x_2}{x_1} = 0.60624$, as is expected. During the initial transience, $t < 0.01$ s, $\frac{y_2}{y_1} = 0.917$, i.e. the vapor phase is richer in water than the azeotropic composition. For effective separations, the contact time should be less than about 0.02 s. Also shown in Figure 13b are the calculations for δ= 5 mm. In this case, for $t < 0.02$ s, $\frac{y_2}{y_1} = 0.917$ and longer contact times are allowed before the system equilibrates to the azeotropic composition.

The choice of the inert gas is also important. Figure 13c compares the transient values of $\frac{y_2}{y_1}$ for helium, nitrogen, air (21% oxygen, 79% nitrogen), argon, CO_2, and xenon. The results obtained with air are indistinguishable from those with nitrogen. The separation performance increases with increasing molar mass of the inert gas. We note that best separations are obtained by choosing xenon as the inert gas.

Figure 13d presents a plot of the value of $\frac{y_2}{y_1}$ during the initial transience as a function of $\sqrt{M_3}$. The separation efficacy appears to correlate with $\sqrt{M_3}$, broadly in agreement with the experimental results of Singh and Prasad[39] for ethanol/water separations using different inert gases.

The simplest explanation of influence of the choice of the inert gas is as follows. From equation (59), at time *t*, that is close to the initial condition ($y_{1\delta} = 0; y_{2\delta} = 0$), the ratio of the flux of water (2) to that of 2-propanol (component 1) is

$$\frac{N_2}{N_1} = \frac{\frac{y_2}{Đ_{12}}(y_{10} - y_{1\delta}) + \left(\frac{y_2}{Đ_{12}} + \frac{y_3}{Đ_{13}}\right)(y_{20} - y_{2\delta})}{\left(\frac{y_1}{Đ_{12}} + \frac{y_3}{Đ_{23}}\right)(y_{10} - y_{1\delta}) + \left(\frac{y_1}{Đ_{12}}\right)(y_{20} - y_{2\delta})} \tag{79}$$

Since the vapor phase is dilute in both of the transferring components, the flux ratio is dictated predominantly by the relative values of 1-3 friction and 1-2 friction. The friction is inversely proportion to the corresponding M-S diffusivity pairs $Đ_{ij}$. From the FSG equation $Đ_{ij} = \frac{1.43\times10^{-7}T^{1.75}}{p\sqrt{M_{ij}}\left[\left(v_i^{1/3}\right)+\left(v_i^{1/3}\right)\right]^2}$ $\mathrm{m^2 s^{-1}}$, the M-S diffusivity $Đ_{ij}$ is inversely proportional to the square root of the mean molar mass of the pairs $\sqrt{M_{ij}}$. We should therefore expect the ratio of fluxes to depend on the square root of the molar mass of the inert gas, $\sqrt{M_3}$.

Figure 14 presents a plot of the ratio of quasi-stationary fluxes $\frac{N_2}{N_1}$, calculated using equation (59), as a function of $\sqrt{M_3}$. The trends are the same as for the ratio $\frac{y_2}{y_1}$. However, we note that $\frac{N_2}{N_1}$ is consistently higher than $\frac{y_2}{y_1}$ because the compositions are time averaged over the volume of the vapor slab.

The important conclusion that can be drawn from Figure 14 is that the ratio of quasi-stationary fluxes $\frac{N_2}{N_1}$ provides a reasonably good qualitative indication of the influence of inerts on the separation.

27. Transient diffusional evaporation of ethanol/water into inert gas

We illustrate the principle of diffusion distillation to separation ethanol(1)/water(2) azeotrope mixtures by considerng transient diffusion into a vapor "slab" of half-thickness δ (= 1mm); see schematic in Figure **12**. The vapor slab is considered to be of "infinite" length in the vertical direction and the diffusion is limited to the transverse (z) direction.

At time t = 0, the bulk vapor phase consists of pure CO_2: y_{10} = 0.0, y_{20} = 0.0, y_{30} = 1.0.

At time t = 0, either side of the vapor slab is in contact with a binary liquid mixture of constant composition and maintained at 343.15 K. The liquid composition corresponds to the azeotrope: x_1 = 0.869, x_2 = 0.131. The vapor pressure of ethanol at 343.15 K is 71.2 kPa, and the vapor pressure of water at 343.15 K is 31.2 kPa. The total gas phase pressure p_t =101.3 kPa. The composition of the vapor phase at the gas/liquid interface in equilibrium with the liquid mixture can be calculated from $y_{i0} = \frac{\gamma_i x_i P_i^0}{p_t}$. This yields $y_{1\delta}$ = 0.6177, $y_{2\delta}$ = 0.09264, $y_{3\delta}$ = 0.28971.

In Figure 15a, the spatial-averaged mole fractions $\left(\bar{y}(t)\right)$of ethanol (1) and water (2) are plotted as a function of time, t. The ratio of the mole fraction of water (2) to that of ethanol (1) in the vapor phase as a function of time, t is plotted in Figure 15b; this ratio equilibrates to the value of $\frac{y_2}{y_1} = \frac{x_2}{x_1} = 0.15$, as is expected. During the initial transience, however, $\frac{y_2}{y_1} > \frac{x_2}{x_1} = 0.15$, i.e. the vapor phase is richer in water than the azeotropic composition. Short contact times result in more effective separations.

The choice of the inert gas is also important. Figure 15c compares the transient values of $\frac{y_2}{y_1}$ for helium, nitrogen, air (21% oxygen, 79% nitrogen), argon, CO_2, and xenon. The results obtained with air

are indistinguishable from those with nitrogen. The separation performance increases with increasing molar mass of the inert gas. We note that best separations are obtained by choosing xenon as the inert gas.

Figure 15d presents a plot of the value of $\frac{y_2}{y_1}$ during the initial transience as a function of $\sqrt{M_3}$. The separation efficacy appears to correlate with $\sqrt{M_3}$, broadly in agreement with the experimental results of Singh and Prasad for ethanol/water separations using different inert gases.[39] The data in Figure 15d also includes the separation efficacies at temperatures T = 333.15 K, 323.15 K, and 318.15 K. We note that the separations are more effective at lower temperatures; these results also agree with the experimental findings of Singh and Prasad at different temperatures.[39]

The simplest explanation of influence of the choice of the inert gas is as follows. From equation (59), at time *t*, that is close to the initial condition ($y_{1\delta} = 0; y_{2\delta} = 0$), the ratio of the flux of water (2) to that of ethanol (component 1) is

$$\frac{N_2}{N_1} = \frac{\frac{y_2}{Đ_{12}}(y_{10} - y_{1\delta}) + \left(\frac{y_2}{Đ_{12}} + \frac{y_3}{Đ_{13}}\right)(y_{20} - y_{2\delta})}{\left(\frac{y_1}{Đ_{12}} + \frac{y_3}{Đ_{23}}\right)(y_{10} - y_{1\delta}) + \left(\frac{y_1}{Đ_{12}}\right)(y_{20} - y_{2\delta})} \tag{80}$$

The choice of the inert gas influences the relative values of 1-3 friction and 1-2 friction. The friction is inversely proportion to the corresponding M-S diffusivity pairs $Đ_{ij}$. From the FSG equation $Đ_{ij} = \frac{1.43\times10^{-7}T^{1.75}}{p\sqrt{M_{ij}}\left[\left(v_i^{1/3}\right)+\left(v_i^{1/3}\right)\right]^2}$ $\mathrm{m^2 s^{-1}}$, the M-S diffusivity $Đ_{ij}$ is inversely proportional to the square root of the mean molar mass of the pairs $\sqrt{M_{ij}}$. We should therefore expect the ratio of fluxes to depend on the square root of the molar mass of the inert gas, $\sqrt{M_3}$.

Figure 16 presents a plot of the ratio of quasi-stationary fluxes $\frac{N_2}{N_1}$, calculated using equation (59), as a function of $\sqrt{M_3}$. The trends are the same as for the ratio $\frac{y_2}{y_1}$. However, we note that $\frac{N_2}{N_1}$ is consistently higher than $\frac{y_2}{y_1}$ because the compositions are time averaged over the volume of the vapor slab.

The important conclusion that can be drawn from Figure 16 is that the ratio of quasi-stationary fluxes $\frac{N_2}{N_1}$ provides a reasonably good qualitative indication of the influence of inerts on the separation.

28. Diffusion with heterogeneous chemical reaction

Löwe and Bubb[40] have presented an analysis of the diffusion with heterogeneous chemical reaction $\mathrm{A} + 2\mathrm{B} \rightleftarrows \mathrm{C}$ to demonstrate the possibility of multiplicity of solutions. For that reason, we present a general analysis of diffusion with heterogeneous chemical reaction in this Section.

For steady-state diffusion across a film of thickness δ, the Maxwell-Stefan diffusion equations for n-component mixtures are written as

$$-\frac{dy_i}{dz} = \sum_{\substack{j=1 \\ j\neq i}}^{n} \frac{y_j N_i - y_i N_j}{c_t Đ_{ij}} = \sum_{\substack{j=1 \\ j\neq i}}^{n} \frac{y_j J_i - y_i J_j}{c_t Đ_{ij}}; \quad i = 1,2,\ldots n \tag{81}$$

Only n-1 of the fluxes J_i are independent.

The Fick diffusivity matrix $[D] = [B]^{-1}$ is commonly defined by the n-1 dimensional matrix equation

$$(J) = -c_t [D] \frac{d(y)}{dz}; \quad [D] = [B]^{-1} \tag{82}$$

In equation (82) we define a (n-1) × (n-1) matrix of inverse diffusivities $[B]$ whose elements are given by

$$B_{ii} = \frac{x_i}{Đ_{in}} + \sum_{\substack{k=1 \\ k\neq i}}^{n} \frac{x_k}{Đ_{ik}}; \quad B_{ij(i\neq j)} = -x_i\left(\frac{1}{Đ_{ij}} - \frac{1}{Đ_{in}}\right); \quad i, j = 1,2...n-1 \tag{83}$$

We define a dimensionless distance: $\eta = \frac{z}{\delta}$. The bulk vapor compositions are specified as follows $\eta = 0; \quad z = 0; \quad (y) = (y_0)$. At the other end of the film, the boundary conditions are $\eta = 1; \quad z = \delta; \quad (y) = (y_\delta)$; at this position we have a catalytic surface with the heterogeneous reaction $\nu_1 A_1 + \nu_2 A_2 + \nu_3 A_3 + ...\nu_n A_n = 0$. In contrast to the model calculations heretofore for equimolar diffusion, non-equimolar diffusion, and Stefan diffusion, the mole fractions at the surface of the catalyst are *not* known.

In typical practical examples, the bulk vapor compositions $\eta = 0; \quad z = 0; \quad (y) = (y_0)$ are specified or known. The *n*-1 independent compositions at the catalytic surface $\eta = 1; \quad z = \delta; \quad (y) = (y_\delta)$ are all unknown. Since the flux ratios are fixed, there is only one unknown flux, say N_1. For the determination of total of *n* unknowns (N_1, and *n*-1 independent compositions $y_{i\delta}$), requires the specification of the chemical reaction rate at the surface, say expressed in terms of moles of component 1 converted per m^2 of surface per second.

The ratios of the fluxes N_i, in the laboratory fixed reference velocity frame, are determined by the reaction stoichiometry and so $\frac{N_1}{\nu_1} = \frac{N_2}{\nu_2} = \frac{N_3}{\nu_3} = ... = \frac{N_n}{\nu_n}$.

For ammonia synthesis reaction $N_2 + 3H_2 \rightleftarrows 2NH_3$, for example, we have the constraint $\frac{N_1}{1} = \frac{N_2}{3} = \frac{N_3}{-2}$.

In the chemical vapor deposition (CVD) process for production of tungsten by surface reaction on a wafer $WF_6 + 3H_2 \rightarrow W_{(s)} + 6HF$, the gas phase mixture consists of four species WF_6 (1), H_2 (2), HF (3), along with inert gas Ar (4). The molar masses of the four species are, respectively: 297.83, 2, 20, and 40 kg mol^{-1}. The flux ratios are $\nu_2/\nu_1 = 3$; $\nu_3/\nu_1 = -6$; $\nu_4/\nu_1 = 0$.

For the catalytic dehydrogenation of ethanol to acetaldehyde $C_2H_5OH \rightleftarrows CH_3CHO + H_2$, the flux ratios are are $\nu_2/\nu_1 = -1$; $\nu_3/\nu_1 = -1$.

The total mixture flux can be expressed in terms of the flux of component 1: $N_t = N_1\left(1+\frac{\nu_2}{\nu_1}+\frac{\nu_3}{\nu_1}+....+\frac{\nu_n}{\nu_1}\right)$.

The ratio of the total flux to the flux of component i is $\frac{N_t}{N_i} = \left(1+\frac{\nu_2}{\nu_1}+\frac{\nu_3}{\nu_1}+....+\frac{\nu_n}{\nu_1}\right)\frac{\nu_1}{\nu_i}$. Each of the molar fluxes N_i are related to the corresponding diffusion fluxes J_i by $N_i = \frac{J_i}{\left(1-y_i\frac{N_t}{N_i}\right)} = \frac{J_i}{\left(1-y_i\left(1+\frac{\nu_2}{\nu_1}+\frac{\nu_3}{\nu_1}+....+\frac{\nu_n}{\nu_1}\right)\frac{\nu_1}{\nu_i}\right)}$. Only n-1 of the fluxes J_i are independent. The n-1 × n-1 dimensional bootstrap matrix, defined by $(N) = [\beta](J)$, has the elements $\beta_{ik} = \frac{\delta_{ik}}{\left(1-y_i\left(1+\frac{\nu_2}{\nu_1}+\frac{\nu_3}{\nu_1}+....+\frac{\nu_n}{\nu_1}\right)\frac{\nu_1}{\nu_i}\right)}$.

A different approach for the calculation of the fluxes N_i is to define effective diffusivities, $D_{i,eff}$ for each component i as follows

$$N_i = -c_t D_{i,eff}\frac{dy_i}{dz}; \quad i = 1,2,\ldots n \tag{84}$$

Equation (81) allows us to obtain an explicit expression for the effective diffusivity

$$\frac{1}{D_{i,eff}} = \sum_{\substack{j=1\\ j\neq i}}^{n}\frac{x_j}{Đ_{ij}}\left(1-\frac{x_i N_j}{x_j N_i}\right) = \sum_{\substack{j=1\\ j\neq i}}^{n}\frac{x_j}{Đ_{ij}}\left(1-\frac{x_i \nu_j}{x_j \nu_i}\right); \quad i = 1,2,\ldots n \tag{85}$$

We illustrate the effective diffusivity approach using Equation (85) by considering: chemical vapor deposition (CVD). Consider the specific example of the CVD process for deposition of tungsten, by surface reaction on a wafer

$$WF_6 + 3H_2 \rightarrow W_{(s)} + 6HF \tag{86}$$

The gas phase mixture consists of four species WF_6, H_2, HF, along with inert gas Ar. The molar masses of the four species are, respectively: 297.83, 2, 20, and 40 kg mol^{-1}. For example, in a tungsten CVD reactor with the species WF_6 (1), H_2 (2), HF (3) and inert Ar (4), the flux ratios are $\nu_2/\nu_1 = 3$; $\nu_3/\nu_1 = -6$; $\nu_4/\nu_1 = 0$. Calculations of the effective diffusivities according to eq. (84) are illustrated in Figure **17** for conditions in which the ratio of the compositions $x_2/x_1 = 2$, and the composition of Ar is held constant at $x_4 = 0.3$. At the chosen temperature (673 K) and pressure conditions (100 Pa), use of the Peng-Robinson equation of state reveals that ideal gas behavior prevails despite the presence of the "heavy" WF_6. The effective diffusivity of H_2 is about an order of magnitude higher than that of WF_6. Also noteworthy is that the effective diffusivities are practically composition independent. The large differences in the effective diffusivities of WF_6 (1), H_2 (2), HF (3) have a significant influence on the composition profiles in the effective diffusion layer between the bulk gas phase and the surface of the wafer. We take the opportunity to note that the effective diffusivity calculations presented in earlier work [36] are erroneous.

The exact analytic solution of Krishna and Standart[8] is now applied for the calculation of the fluxes. In terms of the n-1 independent mole fraction gradients, equation (33) can be cast into n-1 dimensional matrix notation

$$\frac{d(y)}{d\eta} = [\Phi](y) + (\phi)$$
$$\Phi_{ii} = \left(\frac{\nu_i}{\nu_1 Đ_{in}} + \sum_{k=1;k\approx i}^{k=n} \frac{\nu_k}{\nu_1 Đ_{ik}} \right) \frac{\delta}{c_t} N_1; \quad \Phi_{ik;k\neq i} = -\left(\frac{\nu_i}{\nu_1 Đ_{ik}} - \frac{\nu_i}{\nu_1 Đ_{in}} \right) \frac{\delta}{c_t} N_1 \tag{87}$$
$$\phi_i = -\left(\frac{\nu_i}{\nu_1 Đ_{in}} \right) \frac{\delta}{c_t} N_1$$

For steady-state transfer across a film, the matrices $[\Phi]$ and (ϕ) are both η-invariant. Therefore equation (87) represents a system of coupled *ordinary* differential equations with *constant coefficients* $[\Phi]$ and (ϕ).

The system of equations can be solved analytically to obtain the mole fraction profiles within the diffusion layer

$$\left(y_\eta - y_0\right) = -\left[\exp[\Phi]\eta - [I]\right]\left[\exp[\Phi] - [I]\right]^{-1}\left(y_0 - y_\delta\right) \tag{88}$$

In equation (88), $[I]$ is the identity matrix with Kronecker delta δ_{ik} as elements.

The Sylvester theorem, detailed in Equation (A.5.17) of Taylor and Krishna,[4] is required for explicit calculation of $\left[\exp[\Phi]\eta - [I]\right]\left[\exp[\Phi] - [I]\right]^{-1}$. The composition gradient at the position $\eta = \frac{z}{\delta}$ can be obtained by differentiation of equation (88); we get

$$\frac{d\left(y_\eta\right)}{d\eta} = -\left[\Phi\right]\left[\exp[\Phi]\eta\right]\left[\exp[\Phi] - [I]\right]^{-1}\left(y_0 - y_\delta\right) \tag{89}$$

The steady-state transfer fluxes of components 1,2,..n-1 can be determined from

$$\left(N\right) = -\frac{c_t}{\delta}\left[\beta_\eta\right]\left[D_\eta\right]\frac{d\left(y_\eta\right)}{d\eta} = \frac{c_t}{\delta}\left[\beta_\eta\right]\left[D_\eta\right]\left[\Phi\right]\left[\exp[\Phi]\eta\right]\left[\exp[\Phi] - [I]\right]^{-1}\left(y_0 - y_\delta\right)$$ where the Fick diffusivity matrix at position η is $\left[D_\eta\right]$ is calculated from equations (82) and (83). Without loss of generality, we may evaluate $\left[\beta_\eta\right]$ and $\left[D_\eta\right]$ at position $\eta = \frac{z}{\delta} = 0$, and obtain

$$\left(N\right) = -\frac{c_t}{\delta}\left[\beta_{\eta=0}\right]\left[D_{\eta=0}\right]\left.\frac{d\left(y\right)}{d\eta}\right|_{\eta=0} = \frac{c_t}{\delta}\left[\beta_{\eta=0}\right]\left[D_{\eta=0}\right]\left[\Phi\right]\left[\exp[\Phi] - [I]\right]^{-1}\left(y_0 - y_\delta\right) \tag{90}$$

The Sylvester theorem, detailed in Equation (A.5.17) of Taylor and Krishna,[4] is required for explicit calculation of $\left[\Phi\right]\left[\exp[\Phi] - [I]\right]^{-1}$.

Using effective diffusivities, as defined in equation (85), the fluxes are calculated from

$$\left(N\right) = - = \frac{c_t}{\delta}\begin{bmatrix} D_{1,eff} & 0 & 0 & 0 & 0 \\ 0 & D_{3,eff} & 0 & 0 & 0 \\ 0 & 0 & D_{3,eff} & 0 & 0 \\ 0 & 0 & 0 & \ddots & 0 \\ 0 & 0 & 0 & 0 & D_{n-1,eff} \end{bmatrix}\left[\Phi\right]\left[\exp[\Phi] - [I]\right]^{-1}\left(y_0 - y_\delta\right) \tag{91}$$

In Equation (91), the diagonal matrix of effective diffusivites is calculated using the compositions y_{i0} at position $\eta = \frac{z}{\delta} = 0$. Both equations (90) and (91) yield identical values for the fluxes, as they should.

29. Diffusional coupling effects in CVD reactor for W deposition

We shall now demonstrate the importance of proper modelling of diffusion processes in the chemical vapor deposition (CVD) process for production of tungsten by surface reaction on a wafer $WF_6 + 3H_2 \rightarrow W_{(s)} + 6HF$. The gas phase mixture consists of four species WF_6 (1), H_2 (2), HF (3), along with inert gas Ar (4). The flux ratios are $\nu_2/\nu_1 = 3$; $\nu_3/\nu_1 = -6$; $\nu_4/\nu_1 = 0$. The data inputs for the process are largely based on the paper by Kuijlaars et al.[41] The temperature in the CVD reactor is 673 K and the total pressure p_t = 100 Pa. The effective film thickness δ = 1 mm. Using the Fuller-Schettler-Giddings (FSG)[6], the M-S diffusivities of the constituent binary pairs are

$\mathcal{D}_{12} = 0.152 \quad \mathcal{D}_{13} = 0.04; \quad \mathcal{D}_{14} = 0.0295;$
$\mathcal{D}_{21} = 0.344 \quad \mathcal{D}_{24} = 0.343; \quad \mathcal{D}_{34} = 0.0946;$ $m^2\ s^{-1}$. Note that the diffusivities are about three orders of magnitude higher than the usual values at ambient pressure and temperature conditions. The reaction rate, *r*, expressed as moles of W deposited per m^2 of surface per second is calculated by the kinetic expression $r = 0.015\sqrt{p_{1\delta}}\ \sqrt{p_{2\delta}}$ where $p_{1\delta} = y_{1\delta} p_t$ and $p_{2\delta} = y_{2\delta} p_t$ are the partial pressures of WF_6 and H_2 at the surface of the wafer (position $\eta = 1; \quad z = \delta$. At steady-state, the flux of WF_6 equals the reaction rate, i.e.

$$N_1 = 0.015\sqrt{p_{1\delta}}\ \sqrt{p_{2\delta}} \tag{92}$$

For a chosen bulk gas mixture composition, $y_{10} = 0.15, y_{20} = 0.3, y_{30} = 0.3, y_{40} = 0.25$, Equations (90) and (92), four in total, need to be solved simultaneously to determine the four "unknowns" $N_1, y_{1\delta}, y_{2\delta}, y_{3\delta}$. The Given-Find solve block of MathCad 15 was used for solving the four set of

equations. The obtained results are: $\begin{matrix} N_1 = 0.08215 & \text{mol m}^{-2}\text{ s}^{-1} \\ y_{1\delta} = 0.01184 & \\ y_{2\delta} = 0.25336 & \\ y_{3\delta} = 0.50751 & \end{matrix}$. The composition profiles in the "film", calculated using equation (88) are shown as the continuous solid lines in Figure 18. If difference in the pair diffusivities are ignored and we assume that six pair diffusivities are equal to the diffusivity of WF_6 in Ar, i.e. 0.03 m^2 s^{-1}, the obtained results are $\begin{matrix} N_1 = 0.04579 & \text{mol m}^{-2}\text{ s}^{-1} \\ y_{1\delta} = 0.04907 & \\ y_{2\delta} = 0.01899 & \\ y_{3\delta} = 0.72155 & \end{matrix}$. In this case, the flux of WF_6 is about half of the value calculated above using the rigorous M-S equations with differing pair diffusivities. The corresponding composition profiles are shown as dashed lines in Figure 18. The calculations underscore the need for taking proper account of differences in pair diffusivities in the modelling of CVD reactors; this conclusion is also reached by Kuijlaars et al.[41]

30. Multiplicity of solutions for hydrogenation of ethene

We now analyze the influence of diffusion on the heterogeneously catalyzed hydrogenation of ethene to produce ethane, $H_2 + C_2H_4 \rightleftarrows C_2H_6$, using platinum/alumina catalyst at 293.15 K. We number the species as follows $H_2 = 1; C_2H_4 = 2; C_2H_6 = 3$. The stoichiometric coefficients are $\nu_1 = 1;\ \nu_2 = 1;\ \nu_3 = -1$. The flux ratios are $\nu_2/\nu_1 = 1;\ \nu_3/\nu_1 = -1$. According to the work of Uppal and Ray,[42] the system follows Langmuir-Hinshelwood kinetics. In the calculations presented below, the rate of reaction, expressed as mole H_2 (species 1) reacted per m^2 of external surface are per second is described by the Langmuir-Hinshelwood kinetic expression $r = \dfrac{k_1 K_A K_B p_{1\delta} p_{2\delta}}{1 + K_A p_{1\delta} + K_B p_{2\delta}}$ where $p_{1\delta} = y_{1\delta} p_t$ and $p_{2\delta} = y_{2\delta} p_t$ are the partial pressures of H_2 (species 1) and C_2H_4 (species 2) at the surface of the catalyst (position $\eta = 1;\quad z = \delta$). The total pressure of the gas mixture, $p_t = 20.4\times10^5$ Pa. The partial pressures of H_2 (species 1) and C_2H_4 (species 2) in the bulk gas phase at position $\eta = 0;\quad z = 0$ are $p_{10} = 12\times10^5$ Pa

and $p_{20} = 8.4\times10^{5}$ Pa. The total molar concentration of the gas mixture, $c_t = \dfrac{p_t}{RT}$ = 837 mol m^{-3}, is constant across the diffusion "film", whose thickness is taken to be, δ = 1 mm. The adsorption constants are $K_A = 0.5\times10^{-5}$ Pa^{-1}, and $K_B = 30\times10^{-5}$ Pa^{-1}. The reaction rate constant $k_1 = 4$ mol m^{-2} s^{-1}.

At the operating pressure and temperature conditions, the Maxwell-Stefan diffusivities of the binary pairs, calculated using the Fuller-Schettler-Giddings[6] method, are $Đ_{12} = 2.7;\quad Đ_{13} = 2.57;\quad Đ_{23} = 0.548\times10^{-6}$ m^{2}s^{-1}; these diffusivities are independent of composition.

The elements of the diagonal bootstrap matrix, $\left[\beta_{\eta=0}\right]$, evaluated at $\eta = \dfrac{z}{\delta} = 0$ are $\beta_{11} = \dfrac{1}{(1-y_{10})}$; $\beta_{22} = \dfrac{1}{(1-y_{20})}$.

At steady-state, the fluxes of H_2 (component 1) and C_2H_4 (Component 2) are given by the two-dimensional matrix equation

$\begin{pmatrix} N_1 \\ N_2 \end{pmatrix} = \dfrac{c_t}{\delta}\left[\beta_{\eta=0}\right]\left[D_{\eta=0}\right]\left[\Phi\right]\left[\exp[\Phi]-[I]\right]^{-1}(y_0 - y_\delta)$, where $[\Phi]$ is defined as in equation (87).

At steady-state, the flux of H_2 equals the reaction rate at $\eta = 1;\ z = \delta$, i.e. $N_1 = r = \dfrac{k_1 K_A K_B p_{1\delta} p_{2\delta}}{1 + K_A p_{1\delta} + K_B p_{2\delta}}$. In view of the reaction stoichiometry, the steady-state flux of C_2H_4 is $N_2 = N_1$. The steady-state flux of C_2H_6 is $N_3 = -N_1 = -N_2$. The total mixture flux $N_t = (1 + \nu_2 + \nu_3)N_1 = N_1$

The diffusion fluxes are calculated from Equation (93), that simplifies to

$J_1 = N_1 - y_1 N_t;\quad J_2 = N_2 - y_2 N_t;\quad J_3 = N_3 - y_3 N_t$

The calculations below are for $y_{10} = 0.58824;\ y_{20} = 0.41176$; these values are based on the partial pressures in the bulk gas mixture as in the work of Uppal and Ray.[42] For these mixture compositions, y_{10} and y_{20}, there are two independent flux relations that determine the compositions, and concentrations, at

the position $\eta = 1$; $z = \delta$: $c_{1\delta} = y_{1\delta} c_t$ and $c_{2\delta} = y_{2\delta} c_t$. We use the Given-Find solve block of MathCad 15 to determine the unknowns $y_{1\delta}$ and $y_{2\delta}$.

Depending on the starting guess values for N_1, $y_{1\delta}$ and $y_{2\delta}$, three different solution sets are obtained; these are called Solution set I, Solution set II, and Solution set III.

With the starting guesses: $N_1 = 0.1$ mol m^{-2} s^{-1}, $y_{1\delta}$ = 0.6 and $y_{2\delta}$ = 0.2, we obtain Solution set I: $N_1 = 0.1211$ mol m^{-2} s^{-1}, $y_{1\delta}$ = 0.56381, and $y_{2\delta}$ = 0.28786. The composition profiles, calculated using equation (88), are shown in Figure 19a. For this solution set I, the rate of entropy production is

$$\sigma = \frac{R}{\delta}\left[J_1 \frac{(y_{10} - y_{1\delta})}{(y_{10} + y_{1\delta})/2} + J_2 \frac{(y_{20} - y_{2\delta})}{(y_{20} + y_{2\delta})/2} + J_3 \frac{(y_{30} - y_{3\delta})}{(y_{30} + y_{3\delta})/2} \right] = 2.4 \text{ kJ m}^{-3} \text{ K}^{-1} \text{ s}^{-1}.$$

With the starting guesses: $N_1 = 0.1$ mol m^{-2} s^{-1}, $y_{1\delta}$ = 0.06 and $y_{2\delta}$ = 0.02, we obtain Solution set II: $N_1 = 0.2835$ mol m^{-2} s^{-1}, $y_{1\delta}$ = 0.52838, and $y_{2\delta}$ = 0.1023. The composition profiles, calculated using equation (88), are shown in Figure 19b. For this solution set II, the rate of entropy production is

$$\sigma = \frac{R}{\delta}\left[J_1 \frac{(y_{10} - y_{1\delta})}{(y_{10} + y_{1\delta})/2} + J_2 \frac{(y_{20} - y_{2\delta})}{(y_{20} + y_{2\delta})/2} + J_3 \frac{(y_{30} - y_{3\delta})}{(y_{30} + y_{3\delta})/2} \right] = 7.8 \text{ kJ m}^{-3} \text{ K}^{-1} \text{ s}^{-1}.$$

With the starting guesses: $N_1 = 0.1$ mol m^{-2} s^{-1}, $y_{1\delta}$ = 0.5 and $y_{2\delta}$ = 0.01, we obtain Solution set III: $N_1 = 0.36394$ mol m^{-2} s^{-1}, $y_{1\delta}$ = 0.50959, and $y_{2\delta}$ = 0.0014312. The composition profiles, calculated using equation (88), are shown in Figure 19c. For this solution set III, the rate of entropy production is

$$\sigma = \frac{R}{\delta}\left[J_1 \frac{(y_{10} - y_{1\delta})}{(y_{10} + y_{1\delta})/2} + J_2 \frac{(y_{20} - y_{2\delta})}{(y_{20} + y_{2\delta})/2} + J_3 \frac{(y_{30} - y_{3\delta})}{(y_{30} + y_{3\delta})/2} \right] = 12.5 \text{ kJ m}^{-3} \text{ K}^{-1} \text{ s}^{-1}.$$

Invoking the Prigogine principle, the stable, physically realizable, steady-state corresponds to the one that produces entropy at the minimum rate; this implies the realizable solution is Solution set I: $N_1 = 0.1211$ mol m^{-2} s^{-1}, $y_{1\delta}$ = 0.56381, and $y_{2\delta}$ = 0.28786 ; this is the "low conversion" steady-state as discussed by Uppal and Ray.[42]

What is the cause of multiplicity of steady-states? There are two possible reasons: (1) differences in the diffusivities of the pair M-S diffusivities, $Đ_{12}$; $Đ_{13}$; $Đ_{23}$, and (2) the "feedback" mechanism

implicit in the Langmuir-Hinshelwood kinetic expression $r = \frac{k_1 K_A K_B p_{1\delta} p_{2\delta}}{1 + K_A p_{1\delta} + K_B p_{2\delta}}$. To answer this question, we repeated the same set of calculations and taking $Đ_{12} = Đ_{13} = Đ_{23} = 0.6 \times 10^{-6}$ m^{2}s^{-1}. With this assumption, the Krishna and Standart[8] analytic solution, equation (37), simplifies to

$$\begin{pmatrix} N_1 \\ N_2 \end{pmatrix} = \frac{c_t}{\delta} \begin{bmatrix} \beta_{11} & 0 \\ 0 & \beta_{22} \end{bmatrix} \begin{bmatrix} Đ & 0 \\ 0 & Đ \end{bmatrix} \begin{bmatrix} \frac{\Phi}{\exp(\Phi)-1} & 0 \\ 0 & \frac{\Phi}{\exp(\Phi)-1} \end{bmatrix} \begin{pmatrix} y_{10} - y_{1\delta} \\ y_{20} - y_{2\delta} \end{pmatrix}$$ where the dimensionless flux is

$\Phi \equiv (1 + \nu_2 + \nu_3) \frac{N_1 \delta}{c_t Đ}$.

At steady-state, the flux of H_2 equals the reaction rate at $\eta = 1; \; z = \delta$, i.e. $N_1 = = \frac{c_t}{\delta} \beta_{11} Đ \frac{\Phi}{\exp(\Phi)-1} (y_{10} - y_{1\delta}) = \frac{k_1 K_A K_B p_{1\delta} p_{2\delta}}{1 + K_A p_{1\delta} + K_B p_{2\delta}}$. In view of the reaction stoichiometry, the steady-state flux of C_2H_4 is $N_2 = N_1 \frac{c_t}{\delta} \beta_{22} Đ \frac{\Phi}{\exp(\Phi)-1} (y_{20} - y_{2\delta})$. The steady-state flux of C_2H_6 is $N_3 = -N_1 = -N_2$. The total mixture flux $N_t = (1 + \nu_2 + \nu_3) N_1 = N_1$

Depending on the starting guess values for N_1, $y_{1\delta}$ and $y_{2\delta}$, three different solution sets are also obtained in this scenario with equal M-S pair diffusivities.

With the starting guesses: $N_1 = 0.1$ mol m^{-2} s^{-1}, $y_{1\delta}$ = 0.5 and $y_{2\delta}$ = 0.01, we obtain Solution set I: $N_1 = 0.11466$ mol m^{-2} s^{-1}, $y_{1\delta}$ = 0.48262, and $y_{2\delta}$ = 0.26089. The composition profiles, calculated using equation (88), are shown in Figure 20a. For this solution set I, the rate of entropy production is

$$\sigma = \frac{R}{\delta} \left[J_1 \frac{(y_{10} - y_{1\delta})}{(y_{10} + y_{1\delta})/2} + J_2 \frac{(y_{20} - y_{2\delta})}{(y_{20} + y_{2\delta})/2} + J_3 \frac{(y_{30} - y_{3\delta})}{(y_{30} + y_{3\delta})/2} \right] = 0.30338 \text{ J m}^{-3} \text{ K}^{-1} \text{ s}^{-1}.$$

With the starting guesses: $N_1 = 0.1$ mol m^{-2} s^{-1}, $y_{1\delta}$ = 0.1 and $y_{2\delta}$ = 0.1, we obtain Solution set II: $N_1 = 0.21437$ mol m^{-2} s^{-1}, $y_{1\delta}$ = 0.369, and $y_{2\delta}$ = 0.09857. The composition profiles, calculated using equation (88), are shown in Figure 20b. For this solution set II, the rate of entropy production is

$$\sigma = \frac{R}{\delta}\left[J_1 \frac{(y_{10} - y_{1\delta})}{(y_{10} + y_{1\delta})/2} + J_2 \frac{(y_{20} - y_{2\delta})}{(y_{20} + y_{2\delta})/2} + J_3 \frac{(y_{30} - y_{3\delta})}{(y_{30} + y_{3\delta})/2} \right] = 0.79003 \text{ J m}^{-3} \text{ K}^{-1} \text{ s}^{-1}.$$

With the starting guesses: $N_1 = 0.2$ mol m^{-2} s^{-1}, $y_{1\delta} = 0.01$ and $y_{2\delta} = 0.01$, we obtain Solution set III: $N_1 = 0.26612$ mol m^{-2} s^{-1}, $y_{1\delta} = 0.3005$, and $y_{2\delta} = 0.00072$. The composition profiles, calculated using equation (88), are shown in Figure 20c. For this solution set III, the rate of entropy production is

$$\sigma = \frac{R}{\delta}\left[J_1 \frac{(y_{10} - y_{1\delta})}{(y_{10} + y_{1\delta})/2} + J_2 \frac{(y_{20} - y_{2\delta})}{(y_{20} + y_{2\delta})/2} + J_3 \frac{(y_{30} - y_{3\delta})}{(y_{30} + y_{3\delta})/2} \right] = 1.23495 \text{ J m}^{-3} \text{ K}^{-1} \text{ s}^{-1}.$$

Invoking the Prigogine principle, the stable, physically realizable, steady-state corresponds to the one that produces entropy at the minimum rate; this implies the realizable solution is Solution set I: $N_1 = 0.11466$ mol m^{-2} s^{-1}, $y_{1\delta} = 0.48262$, and $y_{2\delta} = 0.26089$; this is also the "low conversion" steady-state as discussed by Uppal and Ray.[42]

The important conclusion we wish to draw is that the steady-state multiplicity is not caused by differences in the M-S pair diffusivities, but due to the "feedback" mechanism implicit in the Langmuir-Hinshelwood kinetics.

Having established this, we proceed to analyze the reaction system $A + 2B \rightleftarrows C$, with equal M-S pair diffusivities and Langmuir-Hinshelwood kinetics.

31. Multiplicity of solutions in the Löwe-Bubb reaction system

We now present a re-analysis of the multiplicity in the diffusion-reaction system considered by Löwe and Bubb.[40] Our objective is to demonstrate that the Prigogine principle of minimum entropy production can be gainfully employed in selecting the physically realizable, stable, solution.

The reaction scheme considered by Löwe and Bubb[40] is the heterogeneous catalyzed reversible reaction $A + 2B \rightleftarrows C$. We number the species 1 = A, 2 = B, 3 = C. The stoichiometric coefficients are $\nu_1 = 1$; $\nu_2 = 2$; $\nu_3 = -1$. The flux ratios are $\nu_2/\nu_1 = 2$; $\nu_3/\nu_1 = -1$. The M-S diffusivities of all species is

taken to be identical to one another, and equal to $Đ$. The elements of the diagonal bootstrap matrix $\left[\beta_{\eta=0}\right]$, evaluated at $\eta=\frac{z}{\delta}=0$ are $\beta_{11}=\frac{1}{(1-2y_{10})}$; $\beta_{22}=\frac{1}{(1-y_{20})}$.

The Krishna and Standart[8] analytic solution, equation (37), simplifies to

$$\begin{pmatrix}N_1\\N_2\end{pmatrix}=\frac{c_t}{\delta}\begin{bmatrix}\beta_{11}&0\\0&\beta_{22}\end{bmatrix}\begin{bmatrix}Đ&0\\0&Đ\end{bmatrix}\begin{bmatrix}\frac{\Phi}{\exp(\Phi)-1}&0\\0&\frac{\Phi}{\exp(\Phi)-1}\end{bmatrix}\begin{pmatrix}y_{10}-y_{1\delta}\\y_{20}-y_{2\delta}\end{pmatrix}$$ where the dimensionless flux is

$\Phi\equiv(1+\nu_2+\nu_3)\frac{N_1\delta}{c_tĐ}$.

The rate of reaction, expressed as mole A (species 1) reacted per m^2 of external surface are per second is described by the Langmuir-Hinshelwood kinetic expression $r=\frac{k_1c_{1\delta}c_{2\delta}}{1+k_2c_{1\delta}+k_3c_{2\delta}}$ where $c_{1\delta}=y_{1\delta}c_t$ and $c_{2\delta}=y_{2\delta}c_t$ are the molar concentrations of A (species 1) and B (species 2) at the surface of the catalyst (position $\eta=1;\quad z=\delta$). The total molar concentration of the gas mixture, $c_t=\frac{p_t}{RT}$.

At steady-state, the flux of A (component 1) is $N_1=\frac{c_t}{\delta}\beta_{11}Đ\frac{\Phi}{\exp(\Phi)-1}(y_{10}-y_{1\delta})=\frac{k_1c_{1\delta}c_{2\delta}}{1+k_2c_{1\delta}+k_3c_{2\delta}}$.

The flux of B (component 2) is $N_2=\nu_2N_1=\frac{c_t}{\delta}\beta_{22}Đ\frac{\Phi}{\exp(\Phi)-1}(y_{20}-y_{2\delta})$.

The flux of C (component 3) is $N_3=\nu_3N_1$. The total mixture flux $N_t=(1+\nu_2+\nu_3)N_1$

The diffusion fluxes are calculated from Equation (94), that simplifies to

$J_1=N_1-y_1N_t;\quad J_2=N_2-y_2N_t;\quad J_3=N_3-y_3N_t$

For a specified set of bulk gas mixture compositions, y_{10} and y_{20}, there are two independent flux relations that determine the compositions, and concentrations, at the position $\eta=1;\quad z=\delta$: $c_{1\delta}=y_{1\delta}c_t$ and $c_{2\delta}=y_{2\delta}c_t$. We use the Given-Find solve block of MathCad 15 to determine the unknowns $y_{1\delta}$ and $y_{2\delta}$.

Löwe and Bubb[40] have demonstrated the existence of multiple steady-states by considering two different examples, Example 1, and Example 2. The diffusivity and kinetic data used Löwe and Bubb[40] is presented in terms of dimensionless variables.

We shall first reproduce their published results for Example 1, for which the parameter values are

y_{10} =0.6, y_{20} = 0.4, y_{30} = 0; $\dfrac{k_1 c_t \delta}{Đ(1+k_3 c_t)^2} = 5.5\times 10^{-2}$; $\dfrac{k_3}{k_2} = 10^{-3}$, $\dfrac{k_3 c_t}{1+k_3 c_t} = 0.97$.

Depending on the starting guess values for $\dfrac{N_1\delta}{c_t D}$, $y_{1\delta}$ and $y_{2\delta}$, three different solutions are obtained in agreement with the findings of Löwe and Bubb.[40]

With the starting guesses: $\dfrac{N_1\delta}{c_t D} = 0.1$, $y_{1\delta}$ = 0.6 and $y_{2\delta}$ = 0.3, we obtain Solution set I: $\dfrac{N_1\delta}{c_t D} = 0.12103$, $y_{1\delta}$ = 0.62739, and $y_{2\delta}$ = 0.23568. The composition profiles, calculated using equation (88), are shown in Figure 21a. Since the composition profiles are practically linear, the rate of entropy production, Equation (12) simplifies to

$$\sigma = \frac{R}{\delta}\left[J_1 \frac{(y_{10}-y_{1\delta})}{(y_{10}+y_{1\delta})/2} + J_2 \frac{(y_{20}-y_{2\delta})}{(y_{20}+y_{2\delta})/2} + J_3 \frac{(y_{30}-y_{3\delta})}{(y_{30}+y_{3\delta})/2}\right] \tag{95}$$

In equation (95) we estimate the diffusion fluxes

$$J_1 = N_1 - \frac{(y_{10}+y_{1\delta})}{2}N_t; \quad J_2 = N_2 - \frac{(y_{20}+y_{2\delta})}{2}N_t; \quad J_3 = N_3 - \frac{(y_{30}+y_{3\delta})}{2}N_t$$

For this solution set I, the dimensionless rate of entropy production is

$$\frac{\sigma\delta^2}{c_t Đ R} = \left[J_1 \frac{(y_{10}-y_{1\delta})}{(y_{10}+y_{1\delta})/2} + J_2 \frac{(y_{20}-y_{2\delta})}{(y_{20}+y_{2\delta})/2} + J_3 \frac{(y_{30}-y_{3\delta})}{(y_{30}+y_{3\delta})/2}\right]\left(\frac{\delta}{c_t Đ}\right) = 0.36181.$$

With the starting guesses: $\dfrac{N_1\delta}{c_t D} = 0.1$, $y_{1\delta}$ = 0.6 and $y_{2\delta}$ = 0.01, we obtain Solution set II: $\dfrac{N_1\delta}{c_t D} = 0.24916$, $y_{1\delta}$ = 0.6646, and $y_{2\delta}$ = 0.01243. The composition profiles, calculated using equation (88), are shown in Figure 21b. For this solution set II, the dimensionless rate of entropy production is

$$\frac{\sigma\delta^2}{c_t \text{Đ} R} = \left[J_1 \frac{(y_{10} - y_{1\delta})}{(y_{10} + y_{1\delta})/2} + J_2 \frac{(y_{20} - y_{2\delta})}{(y_{20} + y_{2\delta})/2} + J_3 \frac{(y_{30} - y_{3\delta})}{(y_{30} + y_{3\delta})/2} \right] \left(\frac{\delta}{c_t \text{Đ}} \right) = 1.409 .$$

With the starting guesses: $\frac{N_1\delta}{c_t D} = 0.1$, $y_{1\delta}$ = 0.6 and $y_{2\delta}$ = 0.15, we obtain Solution set III: $\frac{N_1\delta}{c_t D} = 0.18232$, $y_{1\delta}$ = 0.644, and $y_{2\delta}$ = 0.13601. The composition profiles, calculated using equation (88), are shown in Figure 21c. For this solution set III, the dimensionless rate of entropy production is

$$\frac{\sigma\delta^2}{c_t \text{Đ} R} = \left[J_1 \frac{(y_{10} - y_{1\delta})}{(y_{10} + y_{1\delta})/2} + J_2 \frac{(y_{20} - y_{2\delta})}{(y_{20} + y_{2\delta})/2} + J_3 \frac{(y_{30} - y_{3\delta})}{(y_{30} + y_{3\delta})/2} \right] \left(\frac{\delta}{c_t \text{Đ}} \right) = 0.711 .$$

Invoking the Prigogine principle, the stable, physically realizable, steady-state corresponds to the one that produces entropy at the minimum rate; this implies the stable steady state solution is Solution set I: $\frac{N_1\delta}{c_t D} = 0.12103$, $y_{1\delta}$ = 0.62739 and $y_{2\delta}$ = 0.23568. It is noteworthy, that Löwe and Bubb[40] have reported identical results for Solution sets I, II, and III, as should be expected. Löwe and Bubb[40] present a detailed stability analysis to reach the same conclusion that Solution set I is the stable steady-state; see Figure 5 of their paper.

The multiple solutions obtained in Example 1 is a phenomenon that is distinctly different from diffusion distillation, because the multiplicity is also exhibited by the exact analytic solution of Krishna and Standart.[8]

We now reproduce the results for multiplicity for Example 2 of Löwe and Bubb.[40] In this case the reaction kinetics and diffusivity data are chosen by Löwe and Bubb[40] to correspond with the Eley-Rideal reaction mechanism as described by equation (9) in the paper by Löwe and Bubb.[40] The bulk phase compositions are the same as in Example 1, i.e.

y_{10} =0.6, y_{20} = 0.4, y_{30} = 0.0

Two different solutions are reported by Löwe and Bubb;[40] referred to here as Solution set I and Solution set II.

For Solution set I: $y_{1\delta}$ = 0.6414 and $y_{2\delta}$ = 0.1514, $\frac{N_1\delta}{c_t D} = 0.17331$. The composition profiles, calculated using equation (88), are shown in Figure 22a. For this solution set I, the dimensionless rate of entropy production is

$$\frac{\sigma\delta^2}{c_t \text{Đ} R} = \left[J_1 \frac{(y_{10} - y_{1\delta})}{(y_{10} + y_{1\delta})/2} + J_2 \frac{(y_{20} - y_{2\delta})}{(y_{20} + y_{2\delta})/2} + J_3 \frac{(y_{30} - y_{3\delta})}{(y_{30} + y_{3\delta})/2} \right] \left(\frac{\delta}{c_t \text{Đ}} \right) = 0.6476 .$$

For Solution set II: $y_{1\delta}$ = 0.6555 and $y_{2\delta}$ = 0.0669, $\frac{N_1\delta}{c_t D} = 0.22078$. The composition profiles, calculated using equation (88), are shown in Figure 22b. For this solution set II, the dimensionless rate of entropy production is

$$\frac{\sigma\delta^2}{c_t \text{Đ} R} = \left[J_1 \frac{(y_{10} - y_{1\delta})}{(y_{10} + y_{1\delta})/2} + J_2 \frac{(y_{20} - y_{2\delta})}{(y_{20} + y_{2\delta})/2} + J_3 \frac{(y_{30} - y_{3\delta})}{(y_{30} + y_{3\delta})/2} \right] \left(\frac{\delta}{c_t \text{Đ}} \right) = 1.052 .$$

Our contention is that the stable, physically realizable, steady-state corresponds to the one that produces entropy at the minimum rate; this implies the realizable solution is Solution set I: $y_{1\delta}$ = 0.6414 and $y_{2\delta}$ = 0.1514, $\frac{N_1\delta}{c_t D} = 0.17331$. Löwe and Bubb[40] present a detailed stability analysis to reach the same conclusion that Solution set I is the stable steady-state; see Figure 4 of their paper. The use of the Prigogine principle of minimum entropy production obviates the need for performing detailed stability analysis to determine the stable steady-state.

32. Notation

c_t	total molar concentration of mixture, mol m^{-3}
$[B]$	inverse diffusivity matrix, m^{-2} s^{1}
d_p	diameter of pore, m
$Đ_{ij}$	M-S binary pair diffusivity, m^2 s^{-1}
$D_{i,Kn}$	Knudsen diffusivity of species *i*, m^2 s^{-1}
$[D]$	Fick diffusivity matrix, m^2 s^{-1}
$[I]$	Identity matrix, dimensionless
J_i	molar diffusion flux of species *i* with respect to u, mol m^{-2} s^{-1}
n	number of species in the mixture, dimensionless
M_i	molar mass of species *i*, kg mol^{-1}
N_i	molar flux of species *i*, mol m^{-2} s^{-1}
p_i	partial pressure, Pa
p_t	total pressure, Pa
P_i^0	vapor pressure, Pa
$[Q]$	matrix quantifying fractional departure from equilibrium, dimensionless
R	gas constant, 8.314 J mol^{-1} K^{-1}
t	time, s
T	absolute temperature, K
x_i	mole fraction of component *i* in liquid phase, dimensionless
y_i	mole fraction of component *i* in vapor phase, dimensionless
u_i	velocity of component *i*, m s^{-1}
u	molar average mixture velocity, m s^{-1}
z	direction coordinate, m

Greek letters

$[\beta]$	bootstrap matrix, dimensionless
γ_i	activity coefficient of component *i*, dimensionless
δ	film thickness, m
δ_{ij}	Kronecker delta, dimensionless
η	dimensionless distance in diffusion layer, dimensionless
λ_i	eigenvalues of $[\Phi]$, dimensionless
μ_i	molar chemical potential of component *i*, J mol^{-1}
ν_i	stoichiometric reaction coefficient, dimensionless
σ	rate of entropy production, J m^{-3} s^{-1} K^{-1}
Φ_{ij}	dimensionless mass transfer rate factors, dimensionless
ϕ_i	dimensionless mass transfer rate factors, dimensionless

Subscript

0	Referring to starting compositions, $t = 0$
0	Referring to position, $z = 0$
δ	Referring to position, $z = \delta$
1	Component 1
2	Component 2
3	Component 3
i	Component index
j	Component index
eq	Referring to final equilibrated compositions, $t \to \infty$

Table 1. Values of the molar heats of vaporization of some typical molecules, determined at their respective normal boiling points:

Compound	Normal boiling point T_b / K	Molar heat of vaporization, λ / kJ mol^{-1}
water	373.1	40.7
ethanol	351.8	38.8
methanol	337.7	35.4
acetone	329.2	29.6
chloroform	334.3	29.3
benzene	353.2	30.8
toluene	383.8	33.2
cyclohexane	353.9	29.9
2-pentane	301.0	24.7
n-hexane	341.9	28.7
acetic acid	391.0	23.5
formic acid	373.9	22.8
monomethylamine	266.8	26.1
triethylamine	276.0	23.0
tri-ethylene glycol	558	70.0

Table 2. NRTL parameters for 2-propanol(1)/water (2) mixture. These parameters are from the DECHEMA Dortmund data bank, and are used along with $G_{ij} = \exp\left(-\alpha_{ij}\tau_{ij}\right)$.

Component 1	Component 2	τ_{12}	τ_{21}	α_{12}
2-propanol(1)	water (2)	$\tau_{12} = \frac{70.6619}{T}$	$\tau_{21} = \frac{729.2208}{T}$	0.288

Table 3. NRTL parameters for ethanol(1)/water (2) mixture. These parameters are from the DECHEMA Dortmund data bank, and are used along with $G_{ij} = \exp\left(-\alpha_{ij}\tau_{ij}\right)$.

Component 1	Component 2	τ_{12}	τ_{21}	α_{12}
ethanol(1)	water (2)	$\tau_{12} = -\frac{29.169}{T}$	$\tau_{21} = \frac{624.9174}{T}$	0.2937

Table 4. NRTL parameters for acetone(1)/methanol (2) mixture. These parameters are from the Kurihara et al.[43], and are used along with $G_{ij} = \exp\left(-\alpha_{ij}\tau_{ij}\right)$.

Component 1	Component 2	τ_{12}	τ_{21}	α_{12}
Acetone (1)	methanol (2)	$\tau_{12} = \frac{770.15}{RT}$	$\tau_{21} = \frac{1023.18}{RT}$	0.1099

33. References

(1) PTC MathCad 15.0. http://www.ptc.com/, PTC Corporate Headquarters, Needham, 3 November 2015.

(2) Maxwell, J. C. On the dynamical theory of gases. *Phil. Trans. Roy. Soc.* **1866**, *157*, 49-88.

(3) Stefan, J. Über das Gleichgewicht und die Bewegung insbesondere die Diffusion von Gasgemengen. *Sitzber. Akad. Wiss. Wien.* **1871**, *63*, 63-124.

(4) Taylor, R.; Krishna, R. *Multicomponent mass transfer*; John Wiley: New York, 1993.

(5) Krishna, R. Uphill Diffusion in Multicomponent Mixtures. *Chem. Soc. Rev.* **2015**, *44*, 2812-2836.

(6) Fuller, E. N.; Schettler, P. D.; Giddings, J. C. A New Method for Prediction of Binary Gas-phase Diffusion Coefficients. *Ind. Eng. Chem.* **1966**, *58*, 19-27.

(7) Reid, R.C.; Prausnitz, J. M.; Poling, B. E. *The Properties of Gases and Liquids*; 4th Edition, McGraw-Hill: New York, 1986.

(8) Krishna, R.; Standart, G. L. A multicomponent film model incorporating a general matrix method of solution to the Maxwell-Stefan equations. *A.I.Ch.E.J.* **1976**, *22*, 383-389.

(9) Krishna, R. A film model analysis of nonequimolar distillation of multicomponent mixtures. *Chem. Eng. Sci.* **1977**, *32*, 1197-1203.

(10) Sundmacher, K.; Hoffman, U. Multicomponent Mass and Energy Transport on Different Length Scales in a Packed Reactive Distillation Column For Heterogeneously Catalyzed Fuel Ether Production. *Chem. Eng. Sci.* **1994**, *49*, 4443-4464.

(11) Krishna, R.; Martinez, H. F.; Sreedhar, R.; Standart, G. L. Murphree point efficiencies in multicomponent systems. *Trans. Inst. Chem. Eng.* **1977**, *55*, 178-183.

(12) Krishna, R.; Standart, G. L. Mass and energy transfer in multicomponent systems. *Chem. Eng. Commun.* **1979**, *3*, 201-275.

(13) Springer, P. A. M.; Baur, R.; Krishna, R. Influence of interphase mass transfer on the composition trajectories and crossing of boundaries in ternary azeotropic distillation. *Sep. Purif. Technol.* **2002**, *29*, 1-13.

(14) Springer, P. A. M.; Baur, R.; Krishna, R. Composition trajectories for heterogeneous azeotropic distillation in a bubble-cap tray column: Influence of mass transfer. *Chem. Eng. Res. Des.* **2003**, *81*, 413-426.

(15) Springer, P. A. M.; Buttinger, B.; Baur, R.; Krishna, R. Crossing of the distillation boundary in homogeneous azeotropic distillation: Influence of interphase mass transfer. *Ind. Eng. Chem. Res.* **2002**, *41*, 1621-1631.

(16) Springer, P. A. M.; Krishna, R. Crossing of boundaries in ternary azeotropic distillation: Influence of interphase mass transfer. *Int. Commun. Heat Mass Transf.* **2001**, *28*, 347-356.

(17) Springer, P. A. M.; van der Molen, S.; Baur, R.; Krishna, R. Experimental verification of the necessity to use the Maxwell-Stefan formulation in describing trajectories during azeotropic distillation. *Chem. Eng. Res. Des.* **2002**, *80*, 654-666.

(18) Springer, P. A. M.; van der Molen, S.; Krishna, R. The need for using rigorous rate-based models for simulations of ternary azeotropic distillation. *Comput. Chem. Eng.* **2002**, *26*, 1265-1279.

(19) Baur, R.; Taylor, R.; Krishna, R.; Copati, J. A. Influence of mass transfer in distillation of mixtures with a distillation boundary. *Trans. Inst. Chem. Eng.* **1999**, *77, Part A*, 561-565.

(20) Toor, H. L. Diffusion in Three-Component Gas Mixtures. *A.I.Ch.E.J.* **1957**, *3*, 198-207.

(21) Toor, H. L. Solution of the Linearised Equations of Multi-component Mass Transfer: II. Matrix Methods. *A.I.Ch.E.J.* **1964**, *10*, 460-465.

(22) Sherwood, T. K. *Absorption and Extraction*; 1st Edition, McGraw-Hil: New York, 1937.
(23) Bröcker, S.; Schulze, W. A New Method of Calculating Ternary Mass Transfer with a Non Transferring Species based on the Gilliland's Parameter Solution of the Maxwell-Stefan Equations for the Film Model. *Chem. Eng. Commun.* **1991**, *107*, 163-172.
(24) Krishna, R. An alternative linearized theory of multicomponent mass transfer. *Chem. Eng. Sci.* **1981**, *36*, 219-222.
(25) Carty, R.; Schrodt, T. Concentration Profiles in Ternary Gaseous Diffusion. *Ind. Eng. Chem. Fundamentals* **1975**, *14*, 276-278.
(26) Modine, A. D. *Ternary Mass Transfer*. Ph.D. Dissertation, Carnegie Institute of Technology, Pittsburgh, 1963.
(27) Krishna, R. Ternary mass transfer in a wetted-wall column. Significance of diffusional interactions. Part I. Stefan diffusion. *Trans. Inst. Chem. Eng.* **1981**, *59*, 35-43.
(28) Breure, B.; Peters, E. A. J. F.; Kerkhof, P. J. A. M. Separation of Azeotropic Mixtures of Alcohols and Water with FricDiff. *Sep. Purif. Technol.* **2008**, *62*, 349-362.
(29) Krishna, R. Investigating the Validity of the Knudsen Diffusivity Prescription for Mesoporous and Macroporous Materials. *Ind. Eng. Chem. Res.* **2016**, *55*, 4749-4759.
(30) Krishna, R.; van Baten, J. M. An Investigation of the Characteristics of Maxwell-Stefan Diffusivities of Binary Mixtures in Silica Nanopores. *Chem. Eng. Sci.* **2009**, *64*, 870-882.
(31) Krishna, R.; van Baten, J. M. Unified Maxwell-Stefan Description of Binary Mixture Diffusion in Micro- and Meso- Porous Materials. *Chem. Eng. Sci.* **2009**, *64*, 3159-3178.
(32) Krishna, R. Describing the Diffusion of Guest Molecules inside Porous Structures. *J. Phys. Chem. C* **2009**, *113*, 19756-19781.
(33) Krishna, R. Diffusion in Porous Crystalline Materials. *Chem. Soc. Rev.* **2012**, *41*, 3099-3118.
(34) Krishna, R.; van Baten, J. M. Influence of Adsorption on the Diffusion Selectivity for Mixture Permeation across Mesoporous Membranes. *J. Membr. Sci.* **2011**, *369*, 545-549.
(35) Mason, E. A.; Malinauskas, A. P. *Gas Transport in Porous Media: The Dusty-Gas Model*; Elsevier: Amsterdam, 1983.
(36) Krishna, R.; Wesselingh, J. A. The Maxwell-Stefan Approach to Mass Transfer. *Chem. Eng. Sci.* **1997**, *52*, 861-911.
(37) Krishna, R. Multicomponent gaseous diffusion in porous media in the transition region. A matrix method for calculation of steady-state transport rates. *Ind. Eng. Chem., Fundam.* **1977**, *16*, 228-232.
(38) Krishna, R. A Simplified Procedure for the Solution of the Dusty Gas Model Equations for Steady-State Transport in Non-Reacting Systems. *Chem. Eng. J.* **1987**, *35*, 75-81.
(39) Singh, N.; Prasad, R. Experimental studies on the effect of inert gases on diffusion distillation of ethanol–water mixtures. *J. Chem. Technol. Biotechnol.* **2011**, *86*, 1495-1500.
(40) Löwe, A.; Bub, G. Multiple Steady States for Isothermal Catalytic Gas-Solid Reactions with a Positive Reaction Order. *Chem. Eng. Sci.* **1976**, *31*, 175-178.
(41) Kuijlaars, K. J.; Kleijn, C. R.; Van Den Akker, H. E. A. Multi-component Diffusion Phenomena in Multiple-Wafer Chemical Vapor Deposition Reactors. *Chem. Eng. J.* **1995**, *57*, 127-136.
(42) Uppal, A.; Ray, W. H. On the Steady-State and Dynamic Behaviour of Permeable, Isothermal Catalysts. *Chem. Eng. Sci.* **1977**, *32*, 649-657.
(43) Kurihara, K.; Hori, H.; Kojima, K. Vapor-Liquid Equilibrium Data for Acetone + Methanol + Benzene, Chloroform + Methanol + Benzene, and Constituent Binary Systems at 101.3 KPa. *J. Chem. Eng. Data* **1998**, *43*, 264-268.

34. Caption for Figures

Figure 1. A force balance on a control volume containing an ideal gas mixture.

Figure 2. The force acting on each of the species in the diffusing binary mixture of species 1 and 2 is balanced by friction between the species 1 and 2.

Figure 3. Transfer resistances in vapor/liquid contacting on a distillation tray.

Figure 4. Vapor phase composition profiles in Stefan tube for acetone(1)/methanol(2)/air(3). The experimental data of Carty and Schrodt[25] are compared with the composition profiles calculated by the Krishna-Standart model.

Figure 5. Schematic for liquid/vapor transfer for ethanol (1)/ water (2)/nitrogen (3) at steady state across a film of thickness δ.

Figure 6. Comparison of ratio of steady-state fluxes $\frac{N_2}{N_1}$ for diffusional evaporation of 2-propanol (1)/water (2) into vapor phase containing inert gas. The flux ratios are obtained using six different inert

gases as component 3: helium, nitrogen, air, argon, CO_2, and xenon as inert gas. The *x*-axis is the square root of the molecular weight of the inert gas $\sqrt{M_3}$.

Figure 7. Comparison of ratio of steady-state fluxes $\frac{N_2}{N_1}$ for diffusional evaporation of ethanol (1)/water (2) into vapor phase containing inert gas. The flux ratios are obtained using six different inert gases as component 3: helium, nitrogen, air, argon, CO_2, and xenon as inert gas. The *x*-axis is the square root of the molecular weight of the inert gas $\sqrt{M_3}$.

Figure 8. Schematic showing vapor/liquid transfer across an inert porous barrier.

Figure 9. (a) Comparison of ratio of quasi-stationary fluxes $\frac{N_2}{N_1}$ for 2-propanol (1)/water (2)/inert gas (3), plotted as a function of pore diameter, d_p, of the barrier interposed between the vapor and liquid phases. (b) Influence of the inclusion of the porous barrier on the ratio of quasi-stationary fluxes $\frac{N_2}{N_1}$ for 2-propanol (1)/water (2)/CO_2 (3).

Figure 10. Influence of the inclusion of the porous barrier on the ratio of quasi-stationary fluxes $\frac{N_2}{N_1}$ for ethanol (1)/water (2)/CO_2 (3).

Figure 11. Influence of the inclusion of the porous barrier on the ratio of quasi-stationary fluxes $\frac{N_2}{N_1}$ for acetone (1)/methanol (2)/CO_2 (3).

Figure 12. Schematic for transient diffusion of ethanol/water into slab of half-thickness δ.

Figure 13. Transient diffusional evaporation of 2-propanol (1)/water (2) into vapor phase containing inert gas. The total pressure is 101.3 kPa, and the temperature is 313.15 K. The composition of the vapor in equilibrium with the liquid is y_{10} = 0.09836, y_{20} = 0.05963, y_{30} = 0.84201. The initial composition of the vapor slab is $y_{1\delta}$ = 0.0, $y_{2\,\delta}$ = 0.0, $y_{3\,\delta}$ = 1.0. The phase equilibrium is calculated using the NRTL parameters provided in Table 2. (a) The mole fractions of 2-propanol (1) and water (2) plotted as a function of time, *t*. (b) Ratio of the mole fraction of water (2) to that of 2-propanol (1) in the vapor phase as a function of time, *t*. (c) Comparisons of the ratios of the mole fraction of water (2) to that of 2-propanol (1) in the vapor phase as a function of time, *t* using helium, nitrogen, argon, CO_2, and xenon as inert gas. (d) Plot of $\frac{y_2}{y_1}$ during the initial transience as a function of $\sqrt{M_3}$.

Figure 14. Comparison of ratio of quasi-stationary fluxes $\frac{N_2}{N_1}$, with $\frac{y_2}{y_1}$ at initial transience for 2-propanol (1)/water (2)/inert gas (3), plotted as a function of $\sqrt{M_3}$.

Figure 15. Transient diffusional evaporation of ethanol (1)/water (2) into vapor phase containing inert. The total pressure is 101.3 kPa, and the temperature is 3143.15 K. The initial composition of the vapor slab is $y_{1\delta} = 0.0$, $y_{2\,\delta} = 0.0$, $y_{3\,\delta} = 1.0$. The composition of the vapor in equilibrium with the binary liquid mixture is $y_{1,eq} = 0.09859$, $y_{2,eq} = 0.02278$, $y_{3.eq} = 0.82455$. The phase equilibrium is calculated using the NRTL parameters provided in Table 3. (a) The mole fractions of ethanol (1) and water (2) plotted as a function of time, *t*. (b) Ratio of the mole fraction of water (2) to that of ethanol (1) in the vapor phase as a function of time, *t*. (c) Comparisons of the ratios of the mole fraction of water (2) to that of ethanol (1) in the vapor phase as a function of time, *t* using helium, nitrogen, argon, CO_2, and xenon as inert gas.. (d) Plot of $\frac{y_2}{y_1}$ during the initial transience as a function of $\sqrt{M_3}$.

Figure 16. Comparison of ratio of quasi-stationary fluxes $\frac{N_2}{N_1}$, with $\frac{y_2}{y_1}$ at initial transience for ethanol (1)/water (2)/inert gas (3), plotted as a function of $\sqrt{M_3}$.

Figure 17. Calculation of the effective diffusivities in the gaseous mixture $WF_6/H_2/HF/Ar$ at a temperature of 673 K and total pressure 100 Pa. In these calculations, the ratio of the compositions $x_2/x_1 = 3$, and the composition of Ar is held constant at $x_4 = 0.3$.

Figure 18. Calculation of the composition profiles in the gas "film" in the gaseous mixture $WF_6/H_2/HF/Ar$ at a temperature of 673 K and total pressure 100 Pa. The continuous solid lines represent the solution using the exact analytic solution of Krishna and Standart[8], taking proper account of the differences in the pair diffusivities. The dashed lines are the corresponding calculations in which all the pair diffusivities are assumed to be the same, equal to 0.03 $m^2\ s^{-1}$.

Figure 19. (a, b, c) Composition profiles in the gas film external to the catalyst surface with heterogeneous chemical reaction $H_2 + C_2H_4 \rightleftarrows C_2H_6$, corresponding to the Solution sets I, II, and III. In the calculations, we take account of differences in the M-S pair diffusivities $Đ_{12} = 2.7; \quad Đ_{13} = 2.57; \quad Đ_{23} = 0.548 \times 10^{-6}\ \mathrm{m^2 s^{-1}}$.

Figure 20. (a, b, c) Composition profiles in the gas film external to the catalyst surface with heterogeneous chemical reaction $H_2 + C_2H_4 \rightleftarrows C_2H_6$, corresponding to the Solution sets I, II, and III. In the calculations, we assume that he M-S pair diffusivities are equal to one another $Đ_{12} = Đ_{13} = Đ_{23} = 0.6 \times 10^{-6}\ \mathrm{m^2 s^{-1}}$.

Figure 21. (a, b, c) Composition profiles in the gas film external to the catalyst surface with heterogeneous chemical reaction $A + 2B \rightleftarrows C$, corresponding to the Solution sets I, II, and III for Example 1 of Löwe and Bubb.[40]

Figure 22. (a, b) Composition profiles in the gas film external to the catalyst surface with heterogeneous chemical reaction $A + 2B \rightleftarrows C$, corresponding to the Solution sets I, and II for Example 2 of Löwe and Bubb.[40]

Fig. S1

Force balance

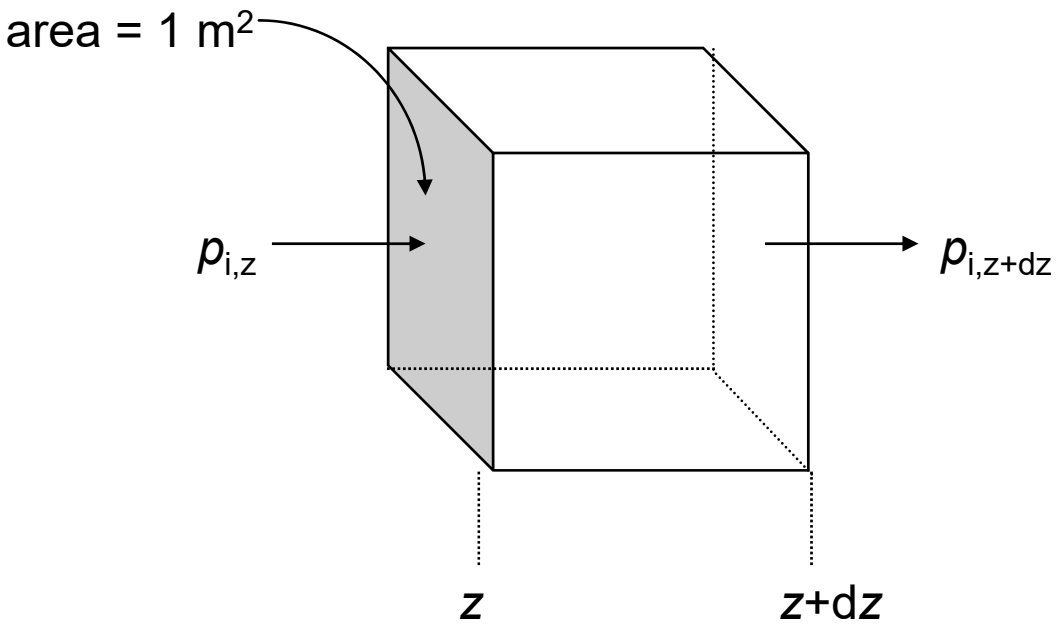

Fig. S2

Force is balanced by friction

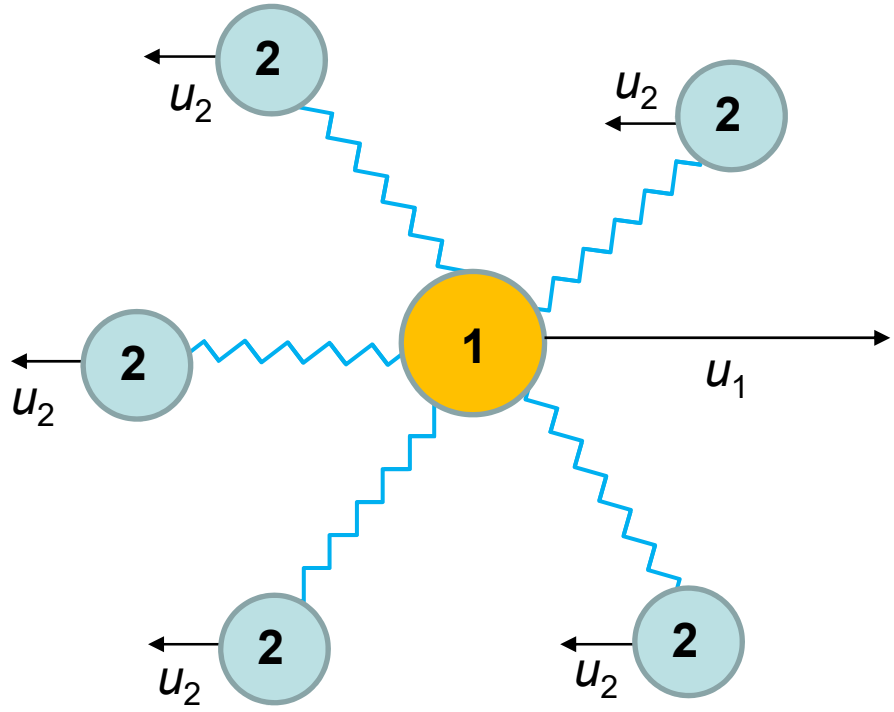

Force acting per mole of species 1

=

Friction between 1 and 2

Fig. S3

Vapor/liquid contacting on distillation tray

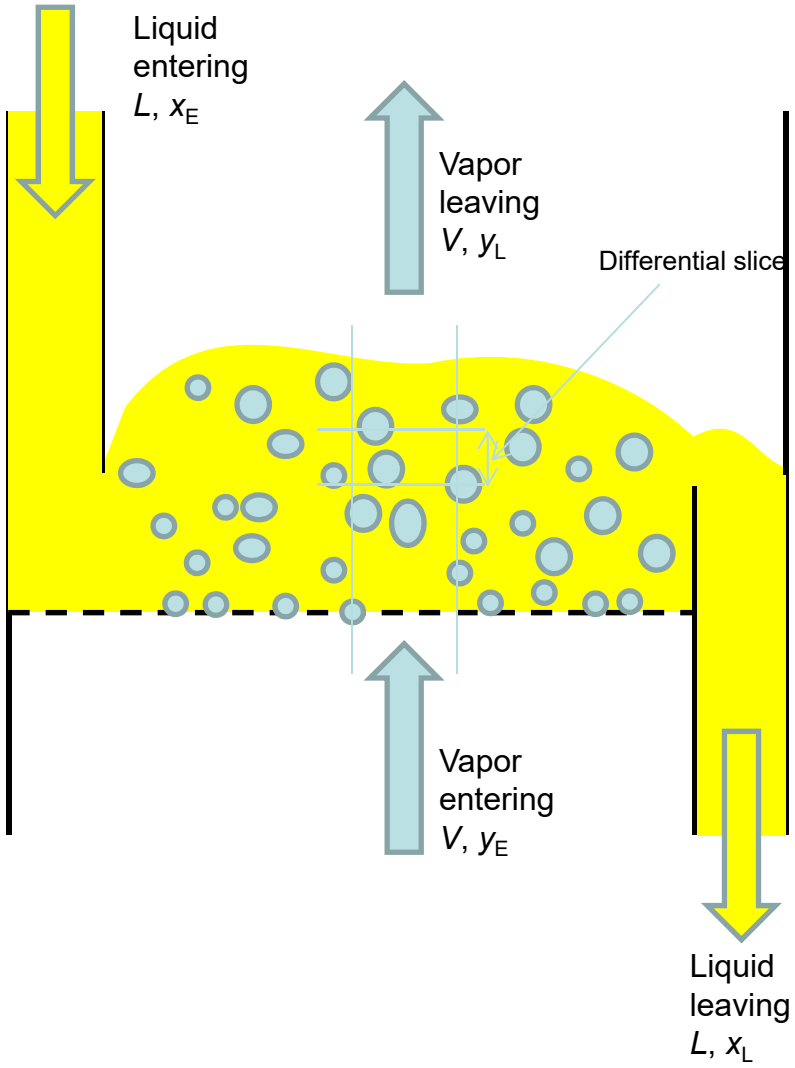

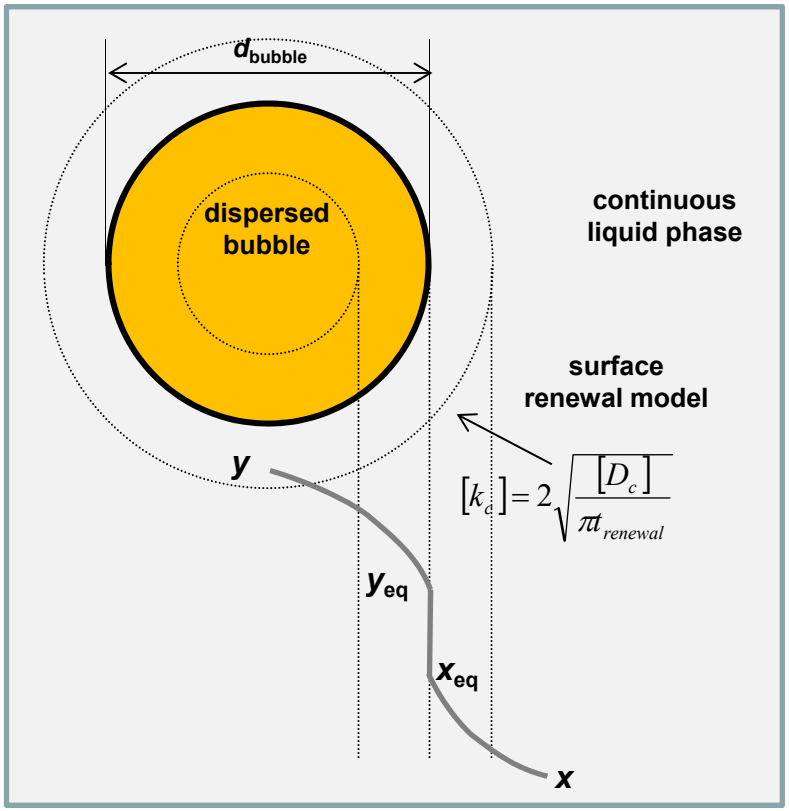

Fig. S4

Acetone/Methanol Diffusion into Air

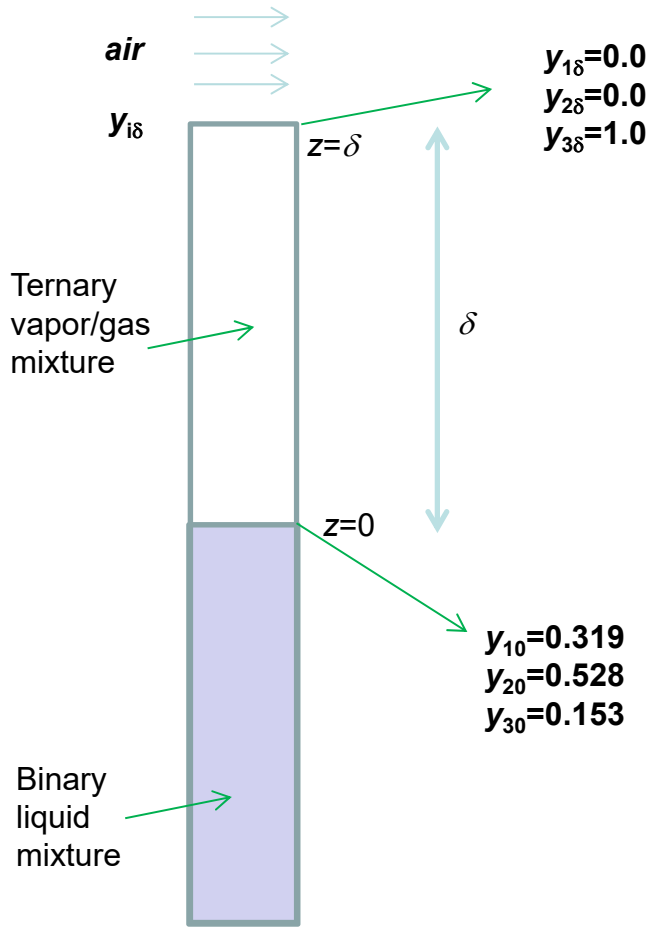

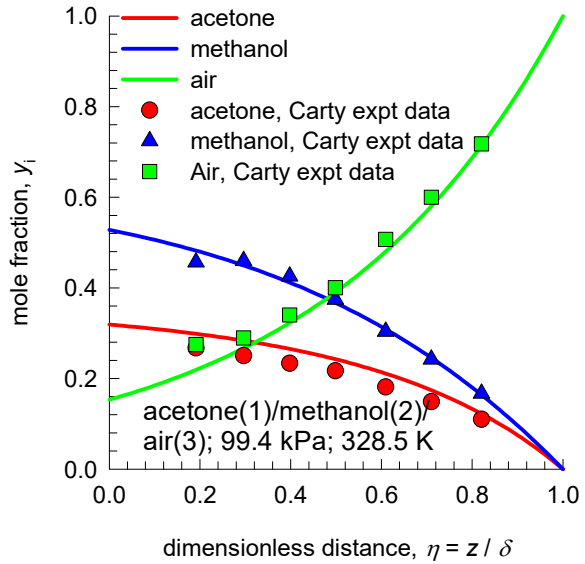

Fig. S5

Steady-state evaporation into vapor slab

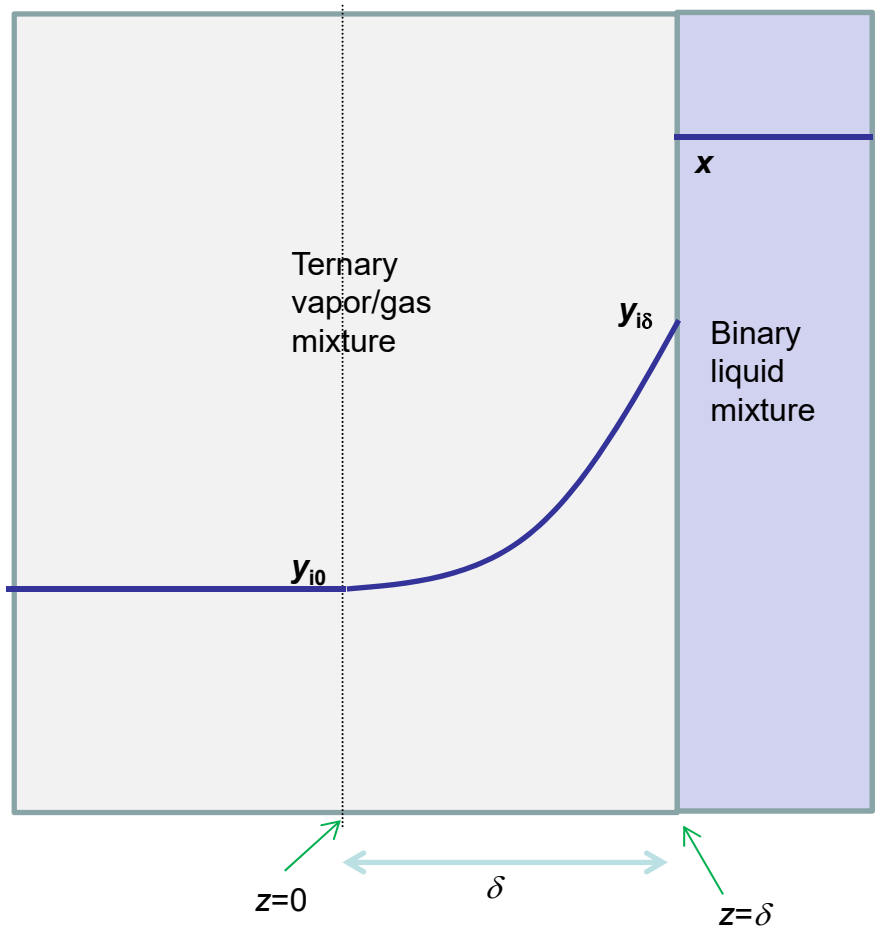

2-propanol/water/inert: diffusional evaporation

Fig. S6

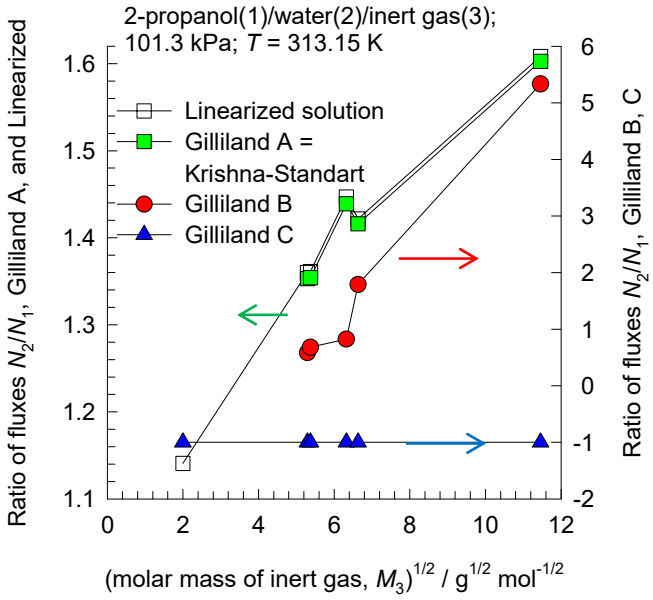

ethanol/water/inert: diffusional evaporation

Fig. S7

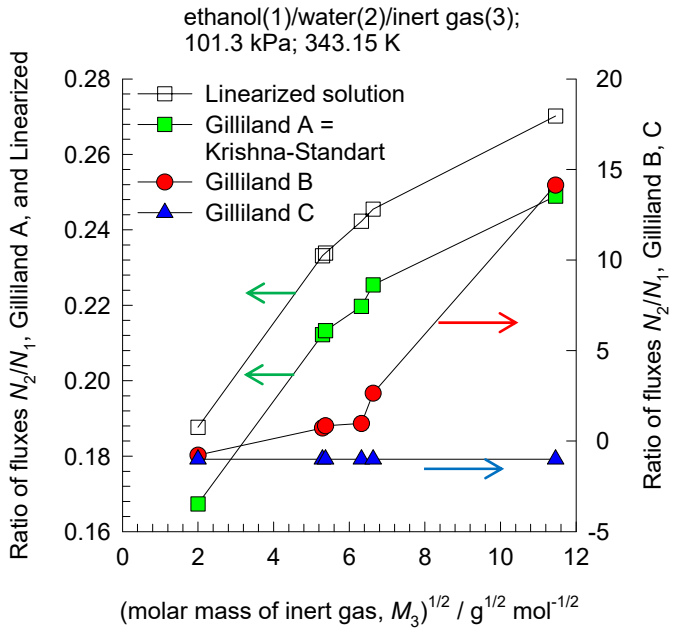

Fig. S8

Diffusion across porous barrier

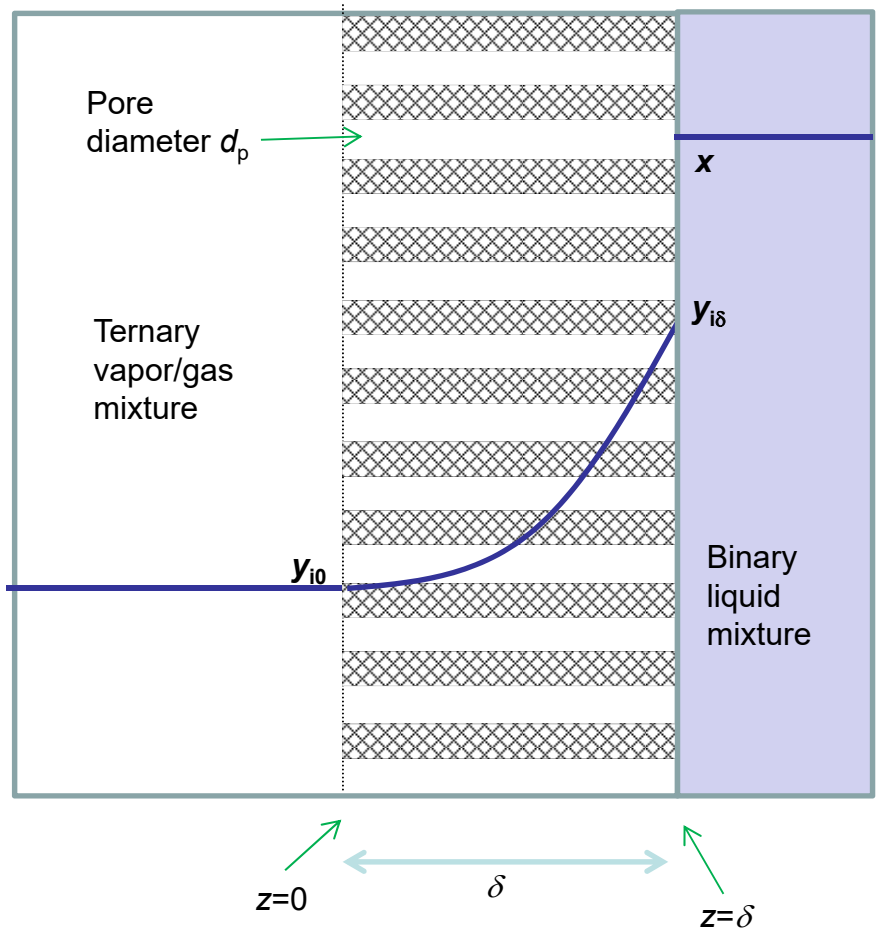

Influence of porous barrier

Fig. S9

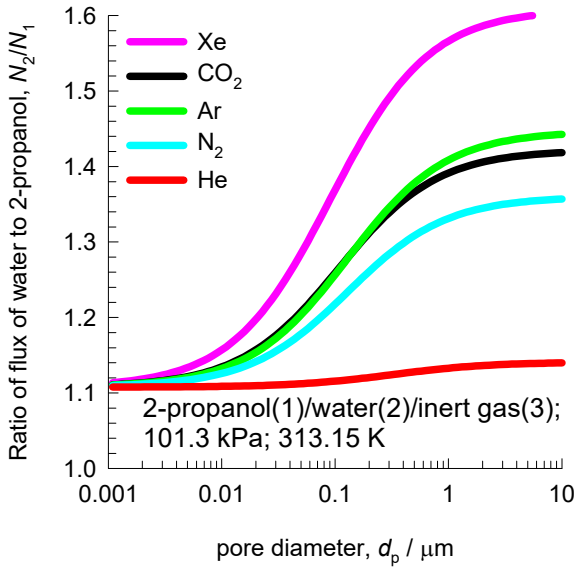

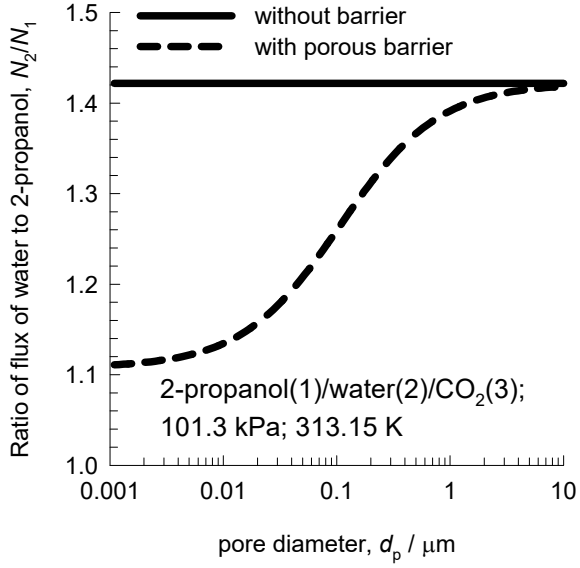

Influence of porous barrier

Fig. S10

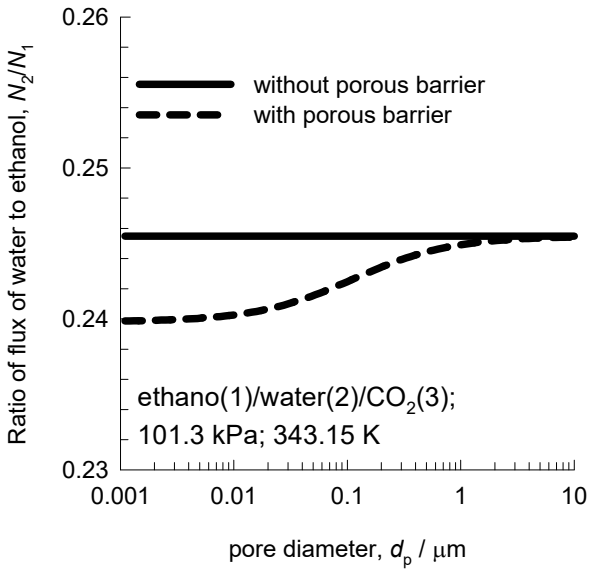

Influence of porous barrier

Fig. S11

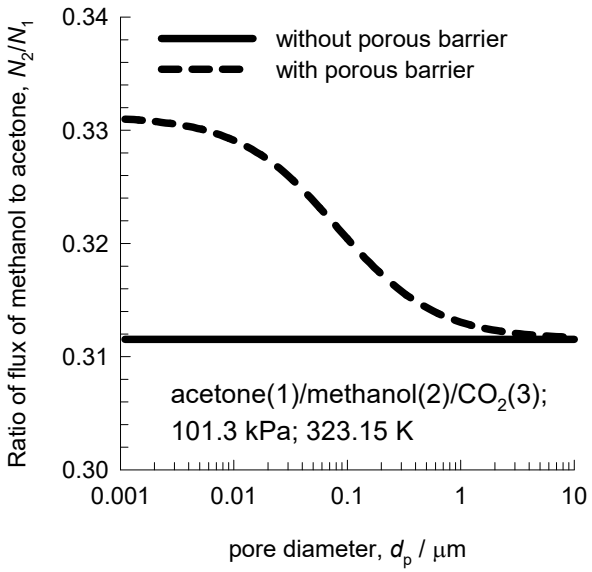

Fig. S12

Transient diffusion into vapor slab

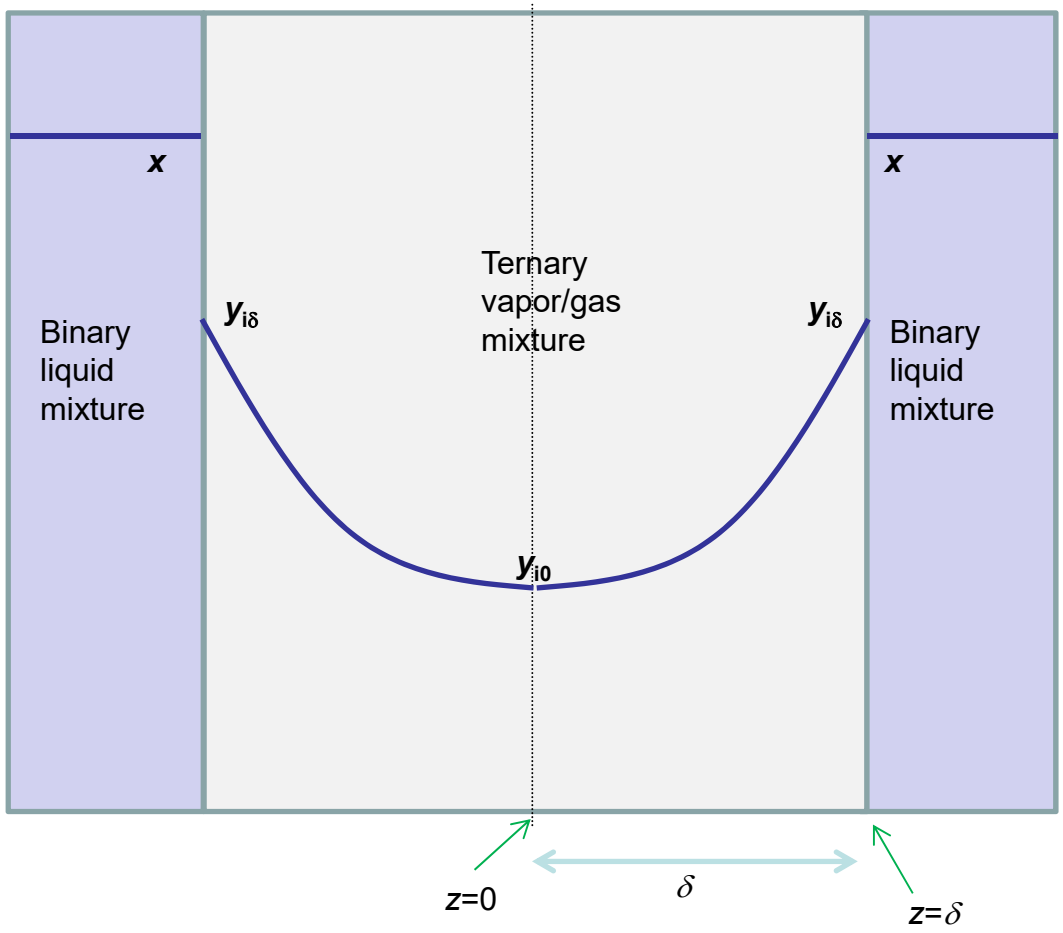

2-propanol/water/inert: diffusional evaporation

Fig. S13

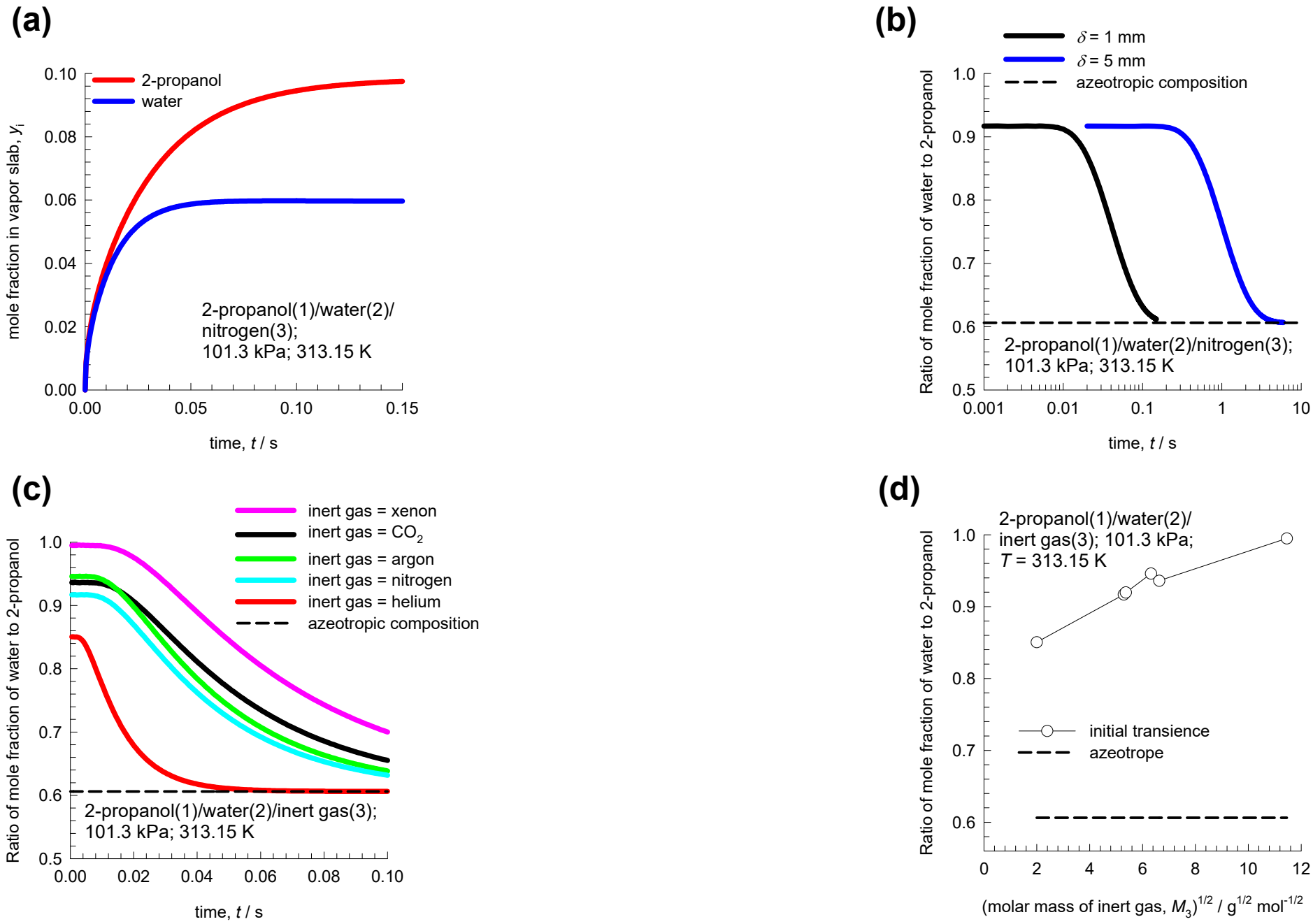

2-propanol/water/inert: diffusional evaporation

Fig. S14

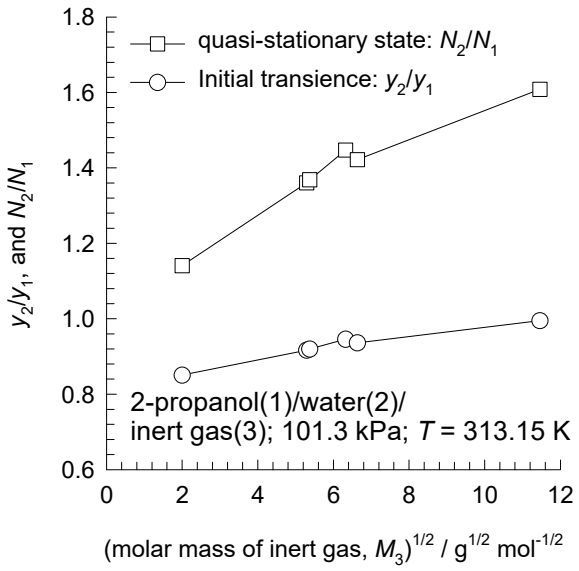

Ethanol/water/inert: diffusional evaporation

Fig. S15

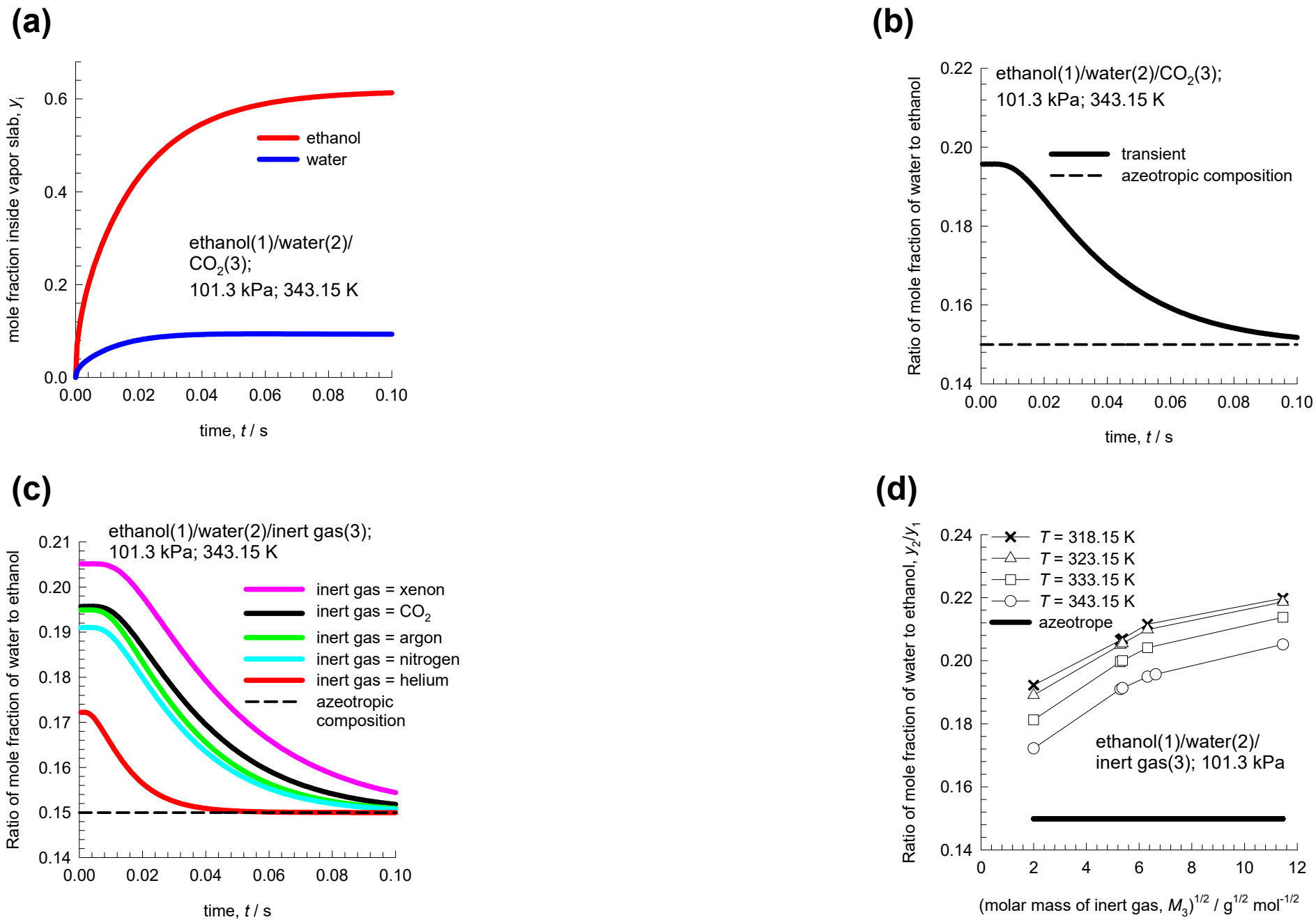

Ethanol/water/inert: diffusional evaporation

Fig. S16

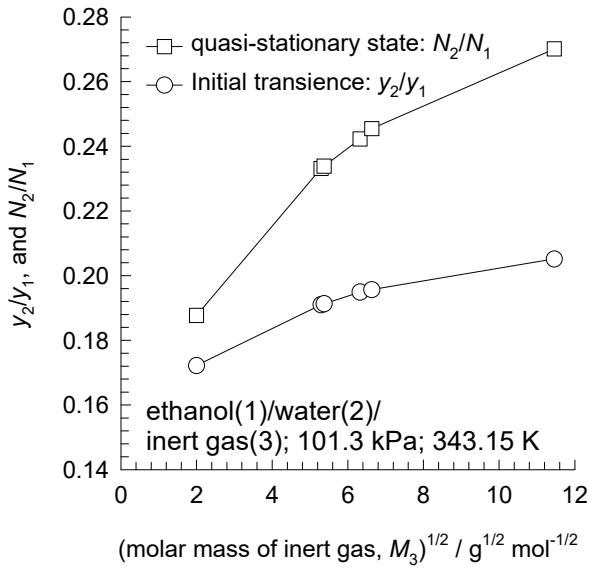

Fig. S17

Effective diffusivities in CVD reactor

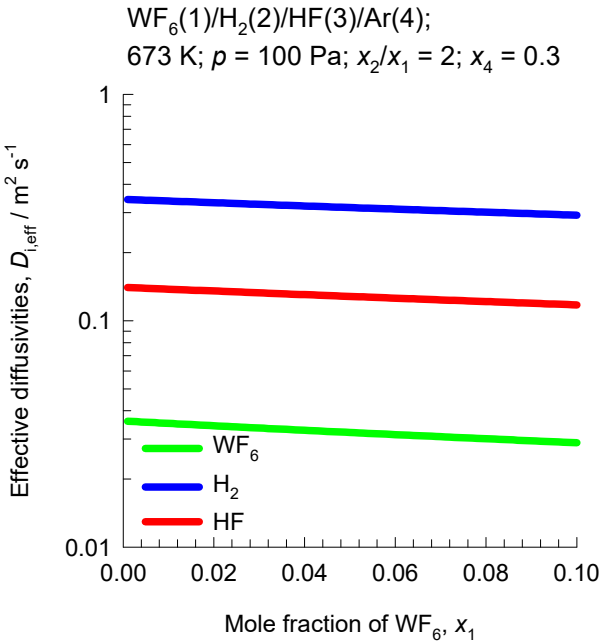

Fig. S18

Composition profiles in "Film" Of CVD reactor

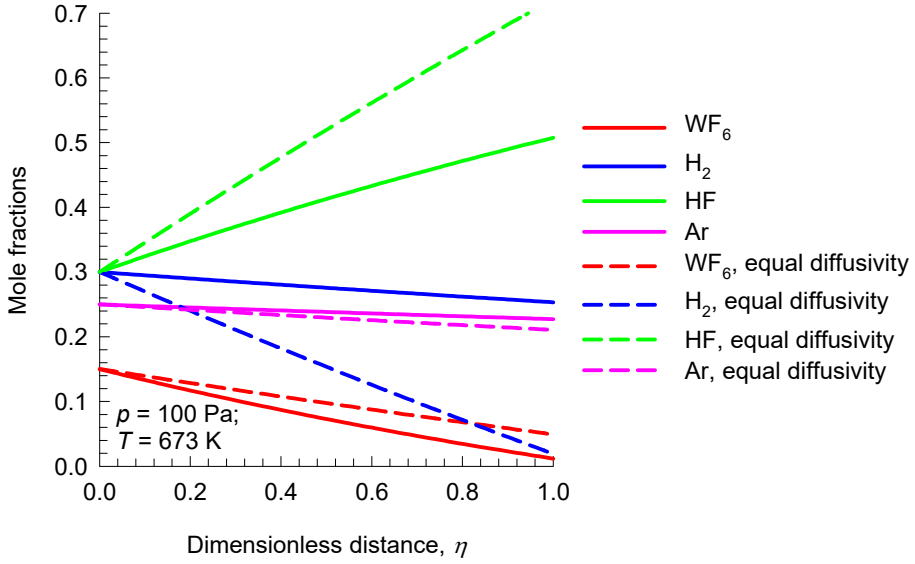

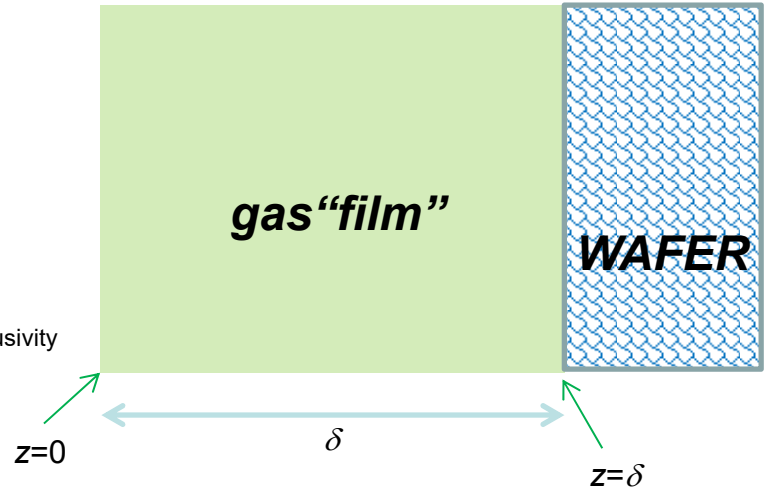

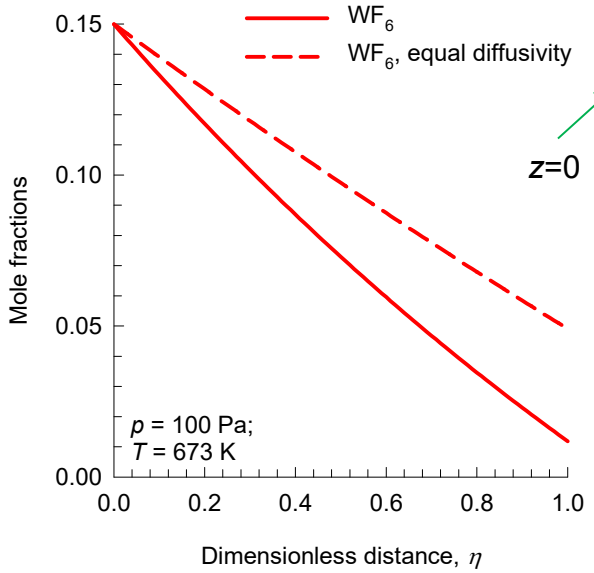

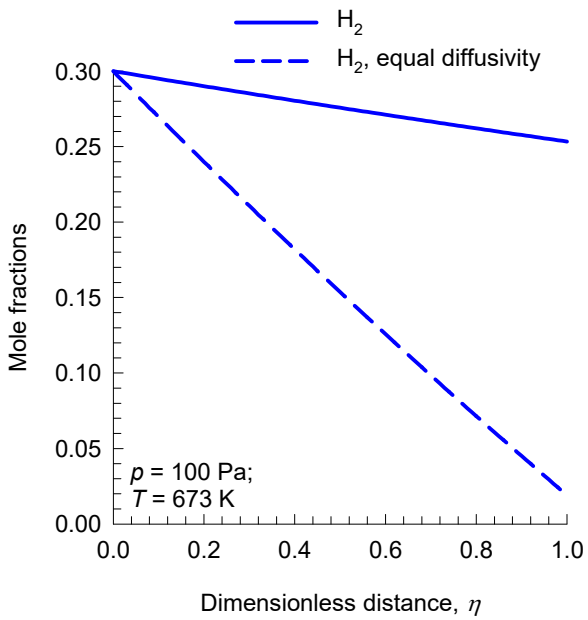

Composition profiles: Hydrogenation of Ethene

Fig. S19

$$H_2 + C_2H_4 \rightleftarrows C_2H_6$$

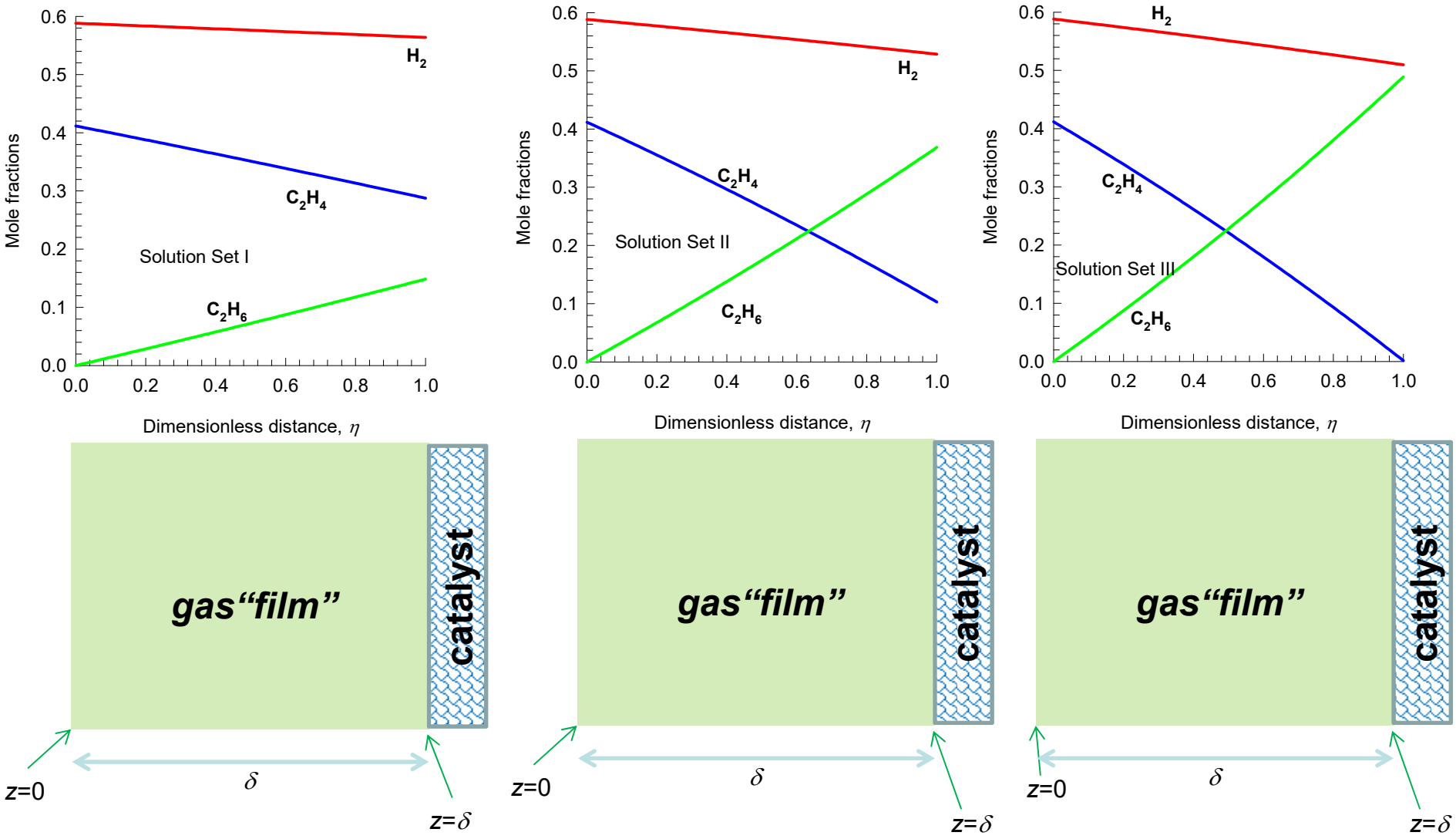

Composition profiles: Hydrogenation of Ethene

Fig. S20

$$H_2 + C_2H_4 \rightleftarrows C_2H_6$$

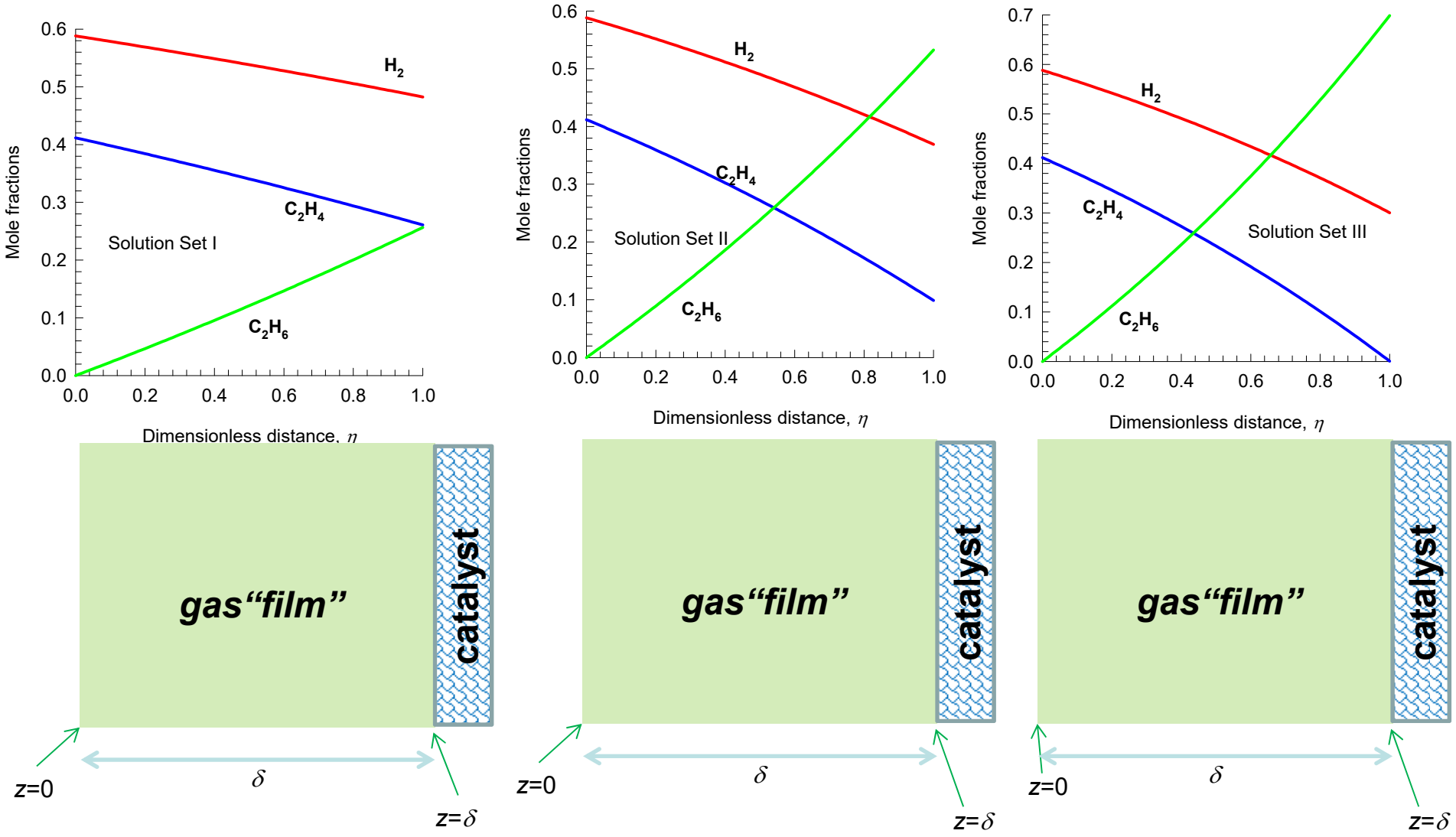

Composition profiles in Example 1

Fig. S21

$$A + 2B \rightleftarrows C$$

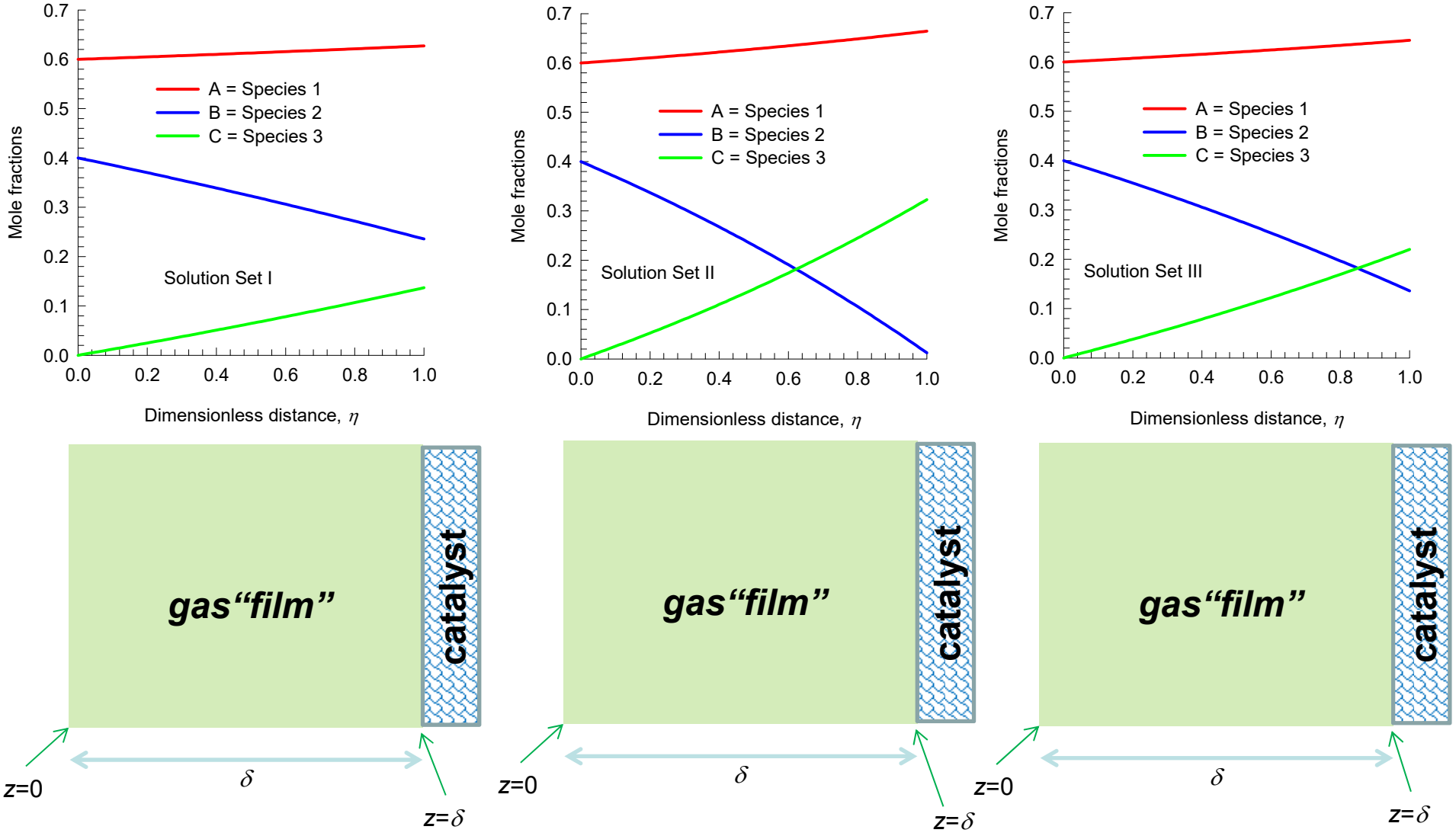

Composition profiles in Example 2

Fig. S22

$$A + 2B \rightleftarrows C$$